Identification and Characterization of Modulators of Chemotherapeutic Response in Mouse Models of Cancer

by

Jason Doles

B.A. Political Science, Biology
Brown University, 2003

MASSACHUSETTS INSTITUTE OF TECHNOLOGY
SEP 14 2010
LIBRARIES

SUBMITTED TO THE DEPARTMENT OF BIOLOGY IN
PARTIAL FULFILLMENT OF THE REQUIREMENTS FOR THE DEGREE OF

DOCTOR OF PHILOSOPHY IN BIOLOGY
AT THE
MASSACHUSETTS INSTITUTE OF TECHNOLOGY

ARCHIVES

SEPTEMBER 2010

© 2010 Massachusetts Institute of Technology. All rights reserved.

Signature of Author: _____
Department of Biology
August 10, 2010

Certified by: _____
Michael T. Hemann
Latham Family Career Development Assistant Professor of Biology
Thesis Supervisor

Accepted by: _____
Stephen P. Bell
Professor of Biology
Chairperson, Graduate Committee

Identification and Characterization of Modulators of Chemotherapeutic Response in Mouse Models of Cancer

by

Jason Doles

Submitted to the Department of Biology
on August 30, 2010 in Partial Fulfillment of the
Requirements for he Degree of Doctor of Philosophy in
Biology

ABSTRACT

Chemotherapeutic drug resistance is a major cause of cancer treatment failure. While much attention has been focused on the genetics of tumor development, less is known about the genetic determinants of therapeutic outcome. As a central focus of my graduate work, I have employed pool-based shRNA-mediated screening methodologies using the *Eμ-myc* lymphoma model to identify genes that modulate the response to front-line chemotherapeutics. In addition to identifying known mediators of chemotherapeutic response, these screens also uncovered several novel genetic targets that influenced the cellular response to selected chemotherapies.

Initial *in vitro* screening experiments identified topoisomerase 2A levels as critical determinants of doxorubicin response. Subsequent follow-up experiments – including one demonstrating doxorubicin sensitization in the presence of topoisomerase 1 shRNAs – revealed important insights into topoisomerase biology and the clinical heterogeneity associated with topoisomerase poison-based therapies. In a related screen, I also found Nek4 levels to be hitherto unappreciated determinants of the cellular response to microtubule poisons. Importantly, I went on to demonstrate that this effect on microtubule poisons was attributable, in part, to Nek4 regulation of microtubule function.

In addition to screening-based approaches, I also show that targeted shRNA-mediated knockdown strategies are useful for probing *in vivo*

chemotherapeutic response. By suppressing translesion synthesis, initially in B-cell lymphoma and later in a newly developed transplantable model of murine lung adenocarcinoma, I show that tumors are not only sensitized to clinically-relevant chemotherapeutics, but are also partially protected from drug-induced mutagenesis and acquired resistance.

Taken together, these results described in this thesis underscore the importance of both large-scale, unbiased gene discovery and target-based interrogation of genetic determinants of chemotherapeutic response.

Thesis Supervisor: Michael Hemann
Title: Latham Family Career Development Assistant Professor of Biology

Biographical Note

Jason Doles

Contact Information:
61 Winter Street Apt #1
Cambridge, MA 02141
Phone: (608) 239-4216
Email: jasondoles@gmail.com

Education:

2005-present: Ph.D. (Biology), Massachusetts Institute of Technology (MIT), Cambridge, MA, USA
Thesis: Interrogating genetic determinants of chemotherapeutic response in mouse models of cancer

1999-2003: B.A. (Political Science, Biology) Brown University, Providence, RI, USA

Research Experience:

2005-present: Graduate Student, MIT
Ph.D. Advisor: Michael T. Hemann
Selected projects: Evaluating the role of Nek4 in modulating a differential response to microtubule poisons. Sensitizing lung adenocarcinoma to cisplatin chemotherapy using Rev3 RNAi.

2003-2005: Associate Research Specialist, University of Wisconsin-Madison
PI: Wade Bushman
Project: Evaluating the significance of hedgehog signaling during mouse prostate development

Summer 2002: Research Assistant, Massachusetts General Hospital
PI: Robert Peterfreund
Project: Assisting in modeling/experimentally determining efficacy of intravenous drug delivery adaptors.

Teaching Experience:

Fall 2006: Teaching Assistant, Introductory Biology (7.012), MIT

Spring 2009: Teaching Assistant, Project Laboratory (7.16), MIT

Funding Awards:

Ludwig Center Graduate Student Fellowship (2009-2010)

Scientific Publications:

Doles J, Oliver T, Hsu G, Jacks T, Walker GC, Hemann MT. Rev3 suppression sensitizes drug-resistant lung tumors to chemotherapy. Submitted to *PNAS*.

Xie K*, **Doles J***, Hemann MT, Walker GW. Error-prone translesion synthesis mediates acquired chemoresistance. Submitted to *PNAS*.
*Equal Contributors

Doles J, Hemann MT. Nek4 status differentially alters sensitivity to distinct microtubule poisons (2010). Cancer Res. 70(3):1033-41.

Burgess DJ, **Doles J**, Zender L, Xue W, Ma B, McCombie WR, Hannon GJ, Lowe SW, Hemann MT. Topoisomerase expression levels determine chemotherapy response (2008). Proc Natl Acad Sci U S A. 105(26):9053-8.

Doles J, Cook C, Shi X, Valosky J, Lipinski R, Bushman W. Functional compensation in Hedgehog signaling during mouse prostate development (2006). Dev Biol. 295(1):13-25.

Lipinski RJ, Gipp JJ, Zhang J, **Doles JD**, Bushman W. Unique and complimentary activities of the Gli transcription factors in Hedgehog signaling (2006). Exp Cell Res. 312(11):1925-38.

Doles JD, Vezina CM, Lipinski RJ, Peterson RE, Bushman W. Growth, morphogenesis, and differentiation during mouse prostate development in situ, in renal grafts, and in vitro (2005). Prostate. 65(4):390-9.

Lovich MA, **Doles J**, Peterfreund RA. The Impact of Carrier Flow Rate and Infusion Set Dead-Volume on the Dynamics of Intravenous Drug Delivery (2005). Anesth Analg. 100(4):1048-55.

Acknowledgements

I would first like to thank my thesis advisor Dr. Michael Hemann. He has given me the intellectual freedom to pursue the research I was most interested in and inspired by over the last four years, while still helping me to become a better scientist. Thank you for your constant support.

I also thank my thesis committee members – Dr. Jackie Lees, Dr. David Housman and Dr. Graham Walker – for their advice and suggestions along the way. I continue to appreciate all of your thoughtful guidance. A special thanks also to Dr. Kevin Haigis for being so gracious with his time to serve on my thesis defense committee.

This work would not have possible without the contributions of several MIT collaborators: Dr. Tyler Jacks, Dr. Graham Walker and Dr. Paul Chang. A special thanks also to Dr. Vincent Butty and Dr. Chris Burge for bioinformatics analyses of our recent mutation sequencing data. I would also like to thank all of Dr. Hemann's former associates at Cold Spring Harbor Laboratories for laying down much of the groundwork around which this thesis is based. Additionally, I would also like to thank the fantastic CCR/Koch Institute core facilities, particularly Flow Cytometry, Histology, Microscopy, Biopolymers & Proteomics and Animal Care. Their support and dedication to quality has been instrumental to obtaining the results presented in this thesis.

To my supportive and knowledgeable colleagues in the Hemann lab (this includes you Megan): you have all been incredibly influential in this research and I am truly in your debt. Despite the often blurry line separating work and play, we always managed to get things done when it mattered most (making sure to enjoy ourselves along the way, of course). You will all be missed.

Lastly, and most importantly, I want to express my deep appreciation to my family, without whom this work would not have been possible. I would like to thank my parents, my brother Christian and sister Kara, whose love and encouragement has given me the confidence to pursue my passions. To my extended family, your continued support means the world to me. Finally, to my girls, Mali and Kadin: your endless understanding, patience, and love have been my lifeblood. I love you both so much. This thesis is dedicated to you (especially since you'd both rather me be home right now instead of here at work writing away....)

Table of Contents

Chapter 1

Introduction

1.1 Opening remarks

Chemotherapeutic intervention is a mainstay therapy for the treatment of cancer, the roots of which trace back many decades to observations of the effects of nitrogen mustards on soldiers returning from World War I (1-4). Since then, many advances – particularly the recognition of the importance of tumor genetics on chemotherapeutic response – are transforming what was once a largely observation-based practice into one driven by genetically-informed experimentation (5-7). Despite these breakthroughs, however, cancer mortality is still a leading cause of death worldwide (8) – a fact rooted in the complex reality of tumor heterogeneity as well as in our incomplete understanding of chemotherapeutic drugs themselves. A cursory look through the existing literature provides ample evidence of our continued struggle with clinical chemotherapeutic resistance and highlights the need for a deeper understanding of drug mechanism in order to overcome this obstacle. In the following section, I will introduce several key mechanisms of chemotherapeutic response in an attempt to frame my graduate work within the greater body of literature pertaining to drug resistance. I will further discuss specific efforts to define mechanisms of chemotherapeutic response in a variety of experimental settings. Lastly, as much of my graduate work focused on the development of experimental tools to identify novel mediators of chemotherapeutic response, I will briefly describe

several of the key advances using our experimental models that have helped shape the landscape upon which my graduate work was founded.

1.2 Mechanisms of chemotherapeutic response

1.2.1 Common (multi-drug) mechanisms of chemoresistance

1.2.1a Drug transport: Multiple drug resistance 1 (*mdr1*)/P-glycoprotein (Pgp)

One of the most widely studied drug resistance mechanisms involves altered expression of *mdr1* and its protein product P-glycoprotein (Pgp). (9-18). Pgp, encoded by the *mdr1* gene, is a member of the adenosine triphosphate (ATP)-binding cassette (ABC) superfamily of transmembrane drug transport proteins and is thus suggested to reduce intracellular drug levels via increased ATP-driven drug transport (19). Indeed, a number of studies have shown Pgp to be involved in bidirectional drug transport, by both decreasing drug uptake as well as increasing drug efflux (20, 21). MDR substrates are known to include a host of xenobiotic compounds including microtubule poisons, topoisomerase poisons, glucocorticoids, cardiac glycosides and antiretroviral drugs such as protease and reverse transcriptase inhibitors (22-26). Consequently, evidence of Pgp-dependent MDR has been documented across a range of pathologically distinct tumor types involving many structurally dissimilar chemotherapeutic agents (27-33).

1.2.1b Drug metabolism: Glutathione (GSH) linked drug detoxification

Glutathione-linked enzyme biology is perhaps best known for its roles in balancing cellular redox states and protecting cells against free radical damage (34, 35). This system – which includes GSH, glutathione-S-transferase (GST), as well as GSH complex transporters (GS-X pumps) – functions to conjugate reduced GSH to a wide set of substrates, effectively neutralizing their reactive properties that pose a threat to proper cell homeostasis. As a prototypical antioxidant, reduced GSH is known to neutralize harmful free radicals via hydrogen atom donation, in the process becoming reactive itself. Reactive glutathione can subsequently interact with another reactive glutathione forming glutathione disulfide (GSSH), an intermediate that can then be converted back into GSH through the action of glutathione reductases (36).

Importantly, glutathione biology also significantly influences chemotherapeutic response (37-40) by several distinct mechanisms including 1) detoxification of free radicals (eg. H_2O_2, superoxide, hydroxyl radicals) produced by redox active drugs (eg. bleomycin, doxorubicin, neocarzinostatin) (41), 2) nucleophillic (non-catalyzed) binding of GSH to drug (42), and 3) glutathione-S-transferase (GST)-catalyzed GSH/drug binding (43-45). These reactions have been implicated in the cellular response to a number of hydrophilic chemotherapeutics – including platinum-based compounds, alkylating agents such as cyclophosphamide, chlorambucil, and nitrogen mustards, cross-linking chloroethylnitrosoureas, and the topoisomerase II-poison doxorubicin (46-48). To date, many studies have shown quantitative alterations in cellular GSH or

GST content to be significantly associated with active drug detoxification, and presumably, chemotherapeutic outcome (49-51). While this would suggest that GSH/GST expression levels could be used to predict vulnerabilities to certain treatment modalities, conflicting reports remain as to the utility/practicality of such an approach (52-56).

1.2.1c Impaired apoptosis

In addition to molecular mechanisms modulating the drug/target interface, it is widely accepted that apoptosis, or programmed cell death, can be a crucial determinant of chemotherapeutic response despite effective drug/target interactions. Interestingly, many of the apoptotic genes implicated in drug resistance also have well-documented roles during tumor development. This pre-existing or 'intrinsic' drug resistance can be a significant barrier for effective tumor management as many chemotherapeutics engage the same pathways developing tumors often disable. For example, mutations in the tumor suppressor gene *p53* as well as in a host of *Bcl-2*-family members have long been associated with poor therapeutic outcome (57-63). Interestingly, many drug-refractory tumors that harbor defects in p53-dependent apoptosis are preferentially vulnerable to stimulation of the extrinsic apoptotic pathway (64). Indeed, this unique feature of many cancer cells has, for example, led to the emergence of agonistic antibodies against the TRAIL death receptor as well as soluble versions of TRAIL as promising chemotherapeutic agents (65, 66).

1.2.1d DNA damage repair

Considering that many conventional chemotherapies act to damage cellular DNA, it follows that enhanced activity of systems or pathways that exist to repair this damage can also lead to therapeutic drug resistance. As DNA repair is vital to cell survival, normal cells employ several mechanisms of repair to fix damaged DNA, including homologous recombination (HR), non-homologous end joining (NHEJ) and mismatch repair (MMR). Increased expression of several DNA repair proteins, such as ERCC1 and XPE-BF, for example, have been found to be associated with the development of resistance to chemotherapy (67, 68). Interestingly, recent experimental evidence suggests that tumors with defects in one of these repair pathways often become overly dependent upon other DNA repair mechanisms. Thus, they display exquisite sensitivity to inhibition of these compensatory pathways. Such therapeutic approaches, exemplified by the use of PARP inhibitors for tumors harboring BRCA1/2 mutations, are currently under intense investigation (69-71). Furthermore, in a recent genome-wide small-interfering RNA (siRNA) screen looking for enhancers of cisplatin treatment in p53-/- HeLa cells, Bartz and colleagues revealed dramatic enrichment for siRNAs targeting genes with annotated functions in DNA damage repair, including several (Rev1, Rev3) involved translesion repair (72). Thus, defects in repair processes are of significant therapeutic value, particularly in the context of other tumor-intrinsic mutations (ie. p53) that may impact chemotherapeutic response.

1.2.2 Drug-specific mechanisms of chemoresistance

As opposed to genetic aberrations that confer resistance to a wide range of diverse chemotherapeutics, a number of clinically encountered mutations include those that act in a more drug-specific manner. Naturally, a large proportion of these mutations affect drug-target interactions – an intuitive observation considering the commonality of many downstream DNA damage response pathways, which if improperly regulated, would have more far-reaching consequences. For the remainder of this section, I will touch upon a few of these drug-specific alterations to both demonstrate the remarkably diverse array of cellular drug targets, as well as to illustrate the educational ability of drug-specific mutations to improve our understanding of individual drug mechanism of action.

1.2.2a DNA damaging agents

Doxorubicin, a commonly used anthracycline, is known to damage DNA, leading to the induction of cell death/apoptosis pathways. The main cellular target of doxorubicin is the DNA binding protein Topoisomerase IIa, an ATP-dependent enzyme that catalyzes the topological passing of two double-stranded DNA segments by introducing a transient enzyme-linked double strand break in one of the passing strands (73). Doxorubicin functions to stabilize the reaction intermediate called the cleavable complex, resulting in the generation of unresolved double-strand breaks that fail to be re-ligated by the topoisomerase

machinery (74). Consequently, mutations in *topoisomerase II* have been found that confer specific resistance to topoIIa poisons such as doxorubicin (75-78).

In addition to its role as a topoisomerase poison, doxorubicin is also known to directly bind DNA to form toxic doxorubicin-DNA adducts (79). This could, in part, help to explain how defects in mismatch repair (MMR) not only confer resistance to the classically adduct-forming drugs cisplatin and cyclophosphamide, but also to doxorubicin (80-82). Along similar lines, many of the known mechanisms of specific resistance to drugs like cisplatin and cyclophosphamide involve specialized DNA repair mechanisms, such as the above-mentioned MMR as well as nucleotide excision repair (NER) (83-86). Clinically, these resistance mechanisms are often defined by aberrant expression of critical DNA repair genes in resistant cells, and are primarily associated with drug-induced acquired resistance (87, 88). Interestingly, recent evidence also implicates specialized transporters (eg. copper transporters) in the development of specific resistance to platinum compounds and suggests therapeutic strategies targeting these vulnerabilities (89-92).

1.2.2b Microtubule-interacting drugs

In contrast to agents directly targeting cellular DNA, chemotherapeutics belonging to a class of drugs broadly defined as microtubule poisons primarily target tubulin and associated microtubule polymers. Drugs falling into this

category can be loosely divided into two subgroups: those that have a microtubule (MT) hyperstability phenotype (eg. taxanes) or those that function to destabilize microtubule polymers (eg. *vinca* alkaloids) (93). Like other chemotherapeutics, drug resistance is a major problem limiting their clinical success. Many known resistance mechanisms function to directly alter microtubule stability and include tubulin mutations (94), isotype selection (95) and post-translational modification (96). Additionally, misregulation of regulatory microtubule-associated proteins (MAPs) can also contribute to MT-poison resistance (97). Despite this complexity, however, years of research probing cellular resistance to MT-targeting agents have culminated in the generation of extremely promising next-generation chemotherapeutics. For example, a new class of MT-stabilizing drug – the epothilones – has demonstrated antitumor activity in cells known to be resistant to both taxanes and *vinca* alkaloids (98-100). Unfortunately, drug resistance to these newer agents has already been documented (101), highlighting a need for continued research into basic mechanisms of chemotherapeutic response.

1.3 Experimental modeling

1.3.1 Modeling therapeutic response *in vitro*

Much of what we currently know about anti-cancer drugs comes from *in vitro* analyses of drug action. Controlled treatment of cells with drugs *ex vivo*, while admittedly a gross oversimplification of what tissues are exposed to *in vivo*, offers much opportunity to explore fundamental cell-drug interactions that would be comparatively difficult, if not impossible, to perform in the context of a living organism. In the following section, I will highlight a few of the early advances in *in vitro* modeling of chemotherapeutic response and briefly discuss how similar approaches are still utilized to this day.

In a 1978 *New England Journal of Medicine* article, Salmon and Hamburger presented data from 32 clinical trials showing a correlation between data collected from *in vitro* tumor colony assays with actual *in vivo* tumor response (102). Since then, countless studies have been published using similar assays describing varying degrees of correlation between *in vitro* chemotherapeutic testing and eventual *in vivo* efficacy (103-105). Despite these results, extensive analyses performed by several groups have revealed a number of technical (and conceptual) weaknesses including highly variable tumor cloning abilities and a limited ability to predict *in vivo* drug sensitivity (103). Interestingly, *in vitro* prediction of *in vivo* resistance was often highly correlated (103), an observation most likely attributable to a greater propensity for

aggressive, drug resistant tumors to grow out as clones *in vitro*. This can in part be explained by the characteristics tumor cells are known to acquire over their developmental course, which include apoptosis evasion, an inability to respond to growth-inhibitory signals, and limitless replicative potential (106). Additionally, differential chemotherapeutic response (*in vitro* vs *in vivo*) has also been suggested to result from fundamental changes in cellular state upon establishment *in vitro*, a phenomenon commonly referred to as "culture shock". Technical considerations aside, differences in drug pharmacology in a culture dish vs. a patient have proven to be a fundamental concern hampering widespread use of similar assays for investigations into mechanisms of drug response *in vivo*.

More recently, many refinements have been made to *in vitro* drug testing and include standard cell cytotoxicity assays such as those that measure vital dye exclusion, metabolic changes, or incorporation of labeled precursors into DNA, RNA or protein, as well as newer versions of the original *in vitro* clonogenic assay to test for *in vivo* drug resistance. Importantly, technological advances have made many of these assays fully automated, allowing for high-throughput screening of thousands of potentially novel drugs with minimal human effort. Thus, considering the wealth of genetic information available about the input cells themselves, *in vitro* assays clearly have much present-day value as a component of drug discovery and testing programs.

1.3.2 Modeling therapeutic response *in vivo*

As I mentioned in the previous section, much of what limits successful *in vitro* prediction of *in vivo* drug action are fundamental differences between tumor cells growing in tissue culture as opposed to growth in a live organism. These differences include (but are by no means limited to) tumor microenvironment influences and bioavailability issues, the former being of particular importance given the contribution of local and systemic factors to cellular life and death decision-making processes. With respect to chemotherapeutic drug response, the mouse quickly emerged as an excellent model organism largely due to its 1) genetic tractability, and 2) mammalian origins. In the early phases of clinical drug development, murine leukemias and lymphomas took center stage as experimental models given their sensitivities to a wide range of chemotherapeutics and ease of manipulation and monitoring (107). Not surprisingly, it was with these models that many key principles of chemotherapeutic response were established (108-114), solidifying their use as reliable pre-clinical tools to dissect drug mechanism of action (115-117).

In addition to the above mentioned models featuring the murine hematopoietic system, xenotransplantation of human tumor material into mice for the purpose of probing mechanisms of chemotherapeutic response dates back over thirty years (118-122). A landmark report by Shorthouse and colleagues in

a 1980 *British Journal of Surgery* article outlined one of the first major efforts to compare chemotherapeutic response of cancer patients with the response of their xenografts established in immune-suppressed mice (123). Using bronchial carcinoma patients as their source of tumor material, the authors were first able to demonstrate that tumor xenografts maintained proper human morphology and functional behavior. They then presented data showing concordance between clinical and xenograft response in a significant fraction of patients. Specifically, they found that xenografts derived from patients responded (as determined using tumor growth measurements) similarly to their autocthonous counterparts when administered chemotherapy (123). Interestingly, as was the often the case with the culture-based assays mentioned in the previous section, these xenograft-based studies were significantly better at predicting clinical resistance as opposed to sensitivity (123) – a fact likely rooted in the selective pressure exerted on tumor cells during their establishment *ex vivo* prior to engraftment.

As an alternative to xenotransplantation approaches, a host of genetically defined mouse models also serve as platforms from which to interrogate chemotherapeutic response. Importantly, unlike xenografts, which still rely on ectopic tranplantation of culture-adapted primary cells or established cell lines into immunocompromised mice, transgenic cancer models form primary malignancies in a physiologically relevant and immunocompetent environment. Indeed, there is now abundant literature using transgenic mice as preclinical drug models in a range of experimental settings (124). Of these, models of leukemia

and lymphoma, such as the *Eμ-myc* mouse, have been particularly useful for studying fundamental mechanisms of chemotherapeutic response. Several key attributes of these systems include 1) the ease and rapidity with which primary tumors can be generated, treated and monitored, and 2) transplantability into syngeneic, immunocompetent recipient mice generating a disease closely resembling the original tumor. These (and other) features make the *Eμ-myc* mouse particularly amenable to modern practices of genetic manipulation – qualities that I will discuss in greater detail later in this thesis.

Indeed, we are at the cusp of a convergence of traditionally high-throughput, discovery-based *in vitro* profiling and screening methodologies with traditionally low-throughput, "one gene, one mouse" *in vivo* platforms. While significant challenges remain, work from several groups highlight recent progress made towards fully realizing that potential. For example, pool-based RNAi-mediated screening approaches now allow for large-scale reverse genetic screens to be performed within the context of a living organism (125-127). In the following section, this experimental 'convergence' will hopefully become increasingly apparent as I outline recent efforts to identify mediators of chemotherapeutic response.

1.4 Identifying novel mediators of chemotherapeutic response

1.4.1 Tumor profiling

Early observations of histologically similar tumors exhibiting radically different responses to similar therapies led many to suspect a critical role for tumor genetics in dictating drug response. While research into this hypothesis quickly revealed the genetically complex nature of cancer itself, it also opened the door to the idea of personalized medicine – in other words, tailor-made therapeutic regimens informed in large part by the genetic makeup of the tumor to be treated. As an early strategy to begin sorting out these genetic puzzles, researchers turned to the cDNA microarray with the notion that gene expression patterns may reflect underlying defects in genomic DNA (128-131). Gene expression analyses of primary vs. refractory tumors and cancer cell lines with known resistance profiles have since generated and refined much of what we currently know about chemoresistance in cancer (131). A publication by Kudoh and colleagues in 2000 serves as an early example of the types of analyses that were made possible using microarray-based tumor profiling. In this study, the authors utilized cDNA microarrays to monitor gene expression profiles of MCF-7 breast cancer cells that were either transiently treated with doxorubicin or selected for resistance to doxorubicin. During the course of their analysis of

genes they found to be up- or down-regulated in response to doxorubicin, the authors identified a distinct set of genes that were altered as a consequence of long-term doxorubicin selection as well as in response to transient drug exposure (132). Calling this gene list a candidate "signature/molecular profile" and "fingerprint" of doxorubicin resistance, the authors were able to focus subsequent investigation into mechanisms of doxorubicin resistance to genes (and pathways) first identified using gene expression profiling. Importantly, the authors noted that this approach was particularly useful for identifying and defining genetic pathways involved in chemotherapeutic response – observations not likely to be made without global tumor profiling (132).

While the cDNA microarray certainly influenced the way researchers approached complex biological problems, other forms of global tumor profiling have also made significant contributions to our understanding of chemotherapeutic response. Single nucleotide polymorphism (SNP)-genotyping, for example, has served as a starting point for many groups interested in identifying genomic loci associated with chemotherapeutic response (133-135). In one instance, Ooyama and colleagues developed an algorithm to calculate DNA copy number using the Affymetrix 10K array, in order to perform a genome-wide correlation analysis between DNA copy number and therapeutic efficacy of 5-fluorouracil (5-FU)-based drugs. Using an experimental cohort of 27 human cancer xenografts, the authors identified several cytogenetic regions (18p, 17p13.2, 17p12, 11q14.1, 11q11 and 11p11.12) showing significant associations

with drug sensitivity. Importantly, strong association with 18p11.32 at the location of the thymidylate synthase gene (TYMS) led to further functional characterization of TYMS status – work that not only confirmed the validity of the algorithm itself, but also highlighted the potential utility of comprehensive DNA copy number analysis to aid in the search for genetic markers of drug sensitivity (134).

In another example of SNP profiling and genome-wide association, a recent (2010) report from Gamazon et al. attempted to evaluate whether SNPs associated with chemotherapeutic agent-induced cytotoxicity for six different anticancer agents were disproportionately likely to be within a functional class such as coding (eg. missense, nonsense, or frameshift polymorphisms), noncoding (such as those in 3'UTRs or splice sites), or expression quantitative trait loci (eQTLs; indicating that a particular SNP is associated with the transcript abundance level of a gene). In brief, the authors found that chemotherapeutic drug susceptibility-associated SNPs are significantly more likely to be eQTLs than would be expected using random SNP sets. As such, their observations will likely serve as a prospective (and retrospective) guide for the functional characterization of poorly defined SNPs emerging from genome-wide association studies (136).

1.4.2 Reverse genetic screens to identify novel mediators of chemotherapeutic response

Genetic screening in mice is another approach long used for the identification of novel determinants of chemotherapeutic response. For example, forward-genetic screening using viral- or transposon-mediated insertional mutagenesis has been instrumental in identifying key cancer genes and advancing our current understanding of chemotherapeutic response (137-139). More recently, however, reverse-genetic screening has emerged as an effective tool for novel gene discovery. An interesting and illustrative example comes from a 2007 *Cancer Research* article by Xia and colleagues where they screened a collection of Saccharomyces cerevisiae haploid gene deletion mutants and found 71 deletion strains displaying varying degrees of doxorubicin hypersensitivity. Interestingly, they found many of those implicated genes to be involved in multiple pathways including DNA repair, RNA metabolism, chromatin remodeling, amino acid metabolism, and heat shock response. Importantly, most of the genes identified in their study were found to have mammalian homologues participating in conserved pathways. Thus, while not a classically-used system to study chemotherapeutic response, the authors proposed future use of *Saccharomyces cerevisiae* deletion collections insofar as probing fundamental mechanisms of drug response (140).

In contrast to the use of targeted deletion strain collections, gene silencing is another technique frequently employed to investigate gene function. The widespread use of RNA interference (RNAi), in particular, has revolutionized the way scientists approach loss-of-function genetics in higher organisms. Current methodologies allow researchers to rapidly interrogate the function of individual genes without having to generate germline mutant knockout mice – a process that typically requires a substantial commitment of time and resources. Furthermore, the generation of shRNA-based RNAi libraries has enabled the design and execution of high-throughput loss-of-function screens in a diverse range of experimental settings (141). Indeed, many groups have utilized variations of this approach to study resistance to chemotherapy (72, 142-149).

Early screening efforts from Brummelkamp et al. and Bartz et al. are two examples using RNAi-mediated screening to elucidate novel mechanisms of chemotherapeutic response. In the former study, the authors designed a short hairpin RNA (shRNA) barcode screen to gain insight in the mechanism of action of nutlin-3, a small-molecule inhibitor of MDM2, which activates the p53 pathway. Their work resulted in the identification of the DNA damage response protein 53BP1 as a critical mediator of nutlin-3-induced cytotoxicity. Thus, the authors speculated that perhaps nutlin-3 was acting to exploit hyperactive/defective DNA damage signaling in cancer cells, a vulnerability that would certainly help to explain nutlin-3's strong antitumor effects (with extremely limited side toxicity) in mice.

In the second study, Bartz and colleagues used RNAi technology to identify novel drug targets that enhanced the cytotoxicity of established anticancer chemotherapeutics. Significantly, they found a number of shRNAs with known relevance to BRCA1/2 biology to enhance cisplatin toxicity in p53-deficient HeLa cells. Interestingly, follow-up experiments showed BRCA1/2 or BRCA1/2-associated gene knockdown to enhance cisplatin cytotoxicity approximately 4- to 7-fold more in the absence of p53 than in matched wild-type controls. Thus, these screens revealed a potentially useful genetic vulnerability, one that has significant clinical implications with respect to personalized treatment (72).

1.5 Overall thesis objectives

In an effort to better understand the genetic factors contributing to chemotherapeutic response, the goal of my research has been to explore novel strategies and settings in which to employ shRNA-screening methodologies. In particular, my initial objective was to evaluate the potential of pooled shRNA screening techniques using B-lymphoma cells derived from the *Eμ-myc* mouse – with the ultimate goal being the development of RNAi-mediated genetic screening approaches that were sufficiently tractable for *in vivo* use. Concurrent with those efforts, my second objective was to adapt technology designed for use with the lymphoma model to investigate the potential of performing similarly rapid and transplant-based therapy studies in a mouse model of epithelial cancer.

1.6 Our experimental models

1.6.1 *Eμ-myc* B-lymphoma

Given the limitations of tissue culture- and xenograft-based model systems, I initially chose to study chemotherapeutic response in a clinically relevant model of human Burkitt's lymphoma, the *Eμ-myc* mouse. This particular mouse is prone to B-cell lymphoma and leukemia due to constitutive expression of the c-*myc* oncogene under control of the Eμ immunoglobulin enhancer (150, 151). Importantly, tumor onset and response to treatment can easily be monitored by palpation of enlarged lymph nodes, peripheral blood smears, or more recently, *in vivo* imaging platforms. While initially used primarily to study lymphoma disease progression (139, 152, 153), the *Eμ-myc* mouse has since been exploited by a number of groups to study mechanisms of chemotherapeutic response (154-160). An early example using this model to study drug action comes from a 1999 *Genes and Development* article where Schmitt and colleagues cross the *Eμ-myc* mouse to mice lacking $p19^{arf}$, Rb, or p53 to evaluate the impact of these loci on tumor development and treatment response. In short, they found lymphomas formed in the presence of impaired p53 signaling

– either by mutation of *p53* or *p19^{arf}* – to be highly invasive, characterized by numerous apoptotic defects, and consequently resistant to cyclophosphamide compared to lymphomas with functional p53 signaling (161). As I will describe below, work from this paper (and many since then) highlights the many advantages of using the *Eμ-myc* mouse to study chemotherapeutic response *in vivo*.

1.6.1a *Eμ-myc* lymphoma is transplantable

A major strength of the *Eμ-myc* system is its transplantability. Primary lymphoma cells isolated from transgenic mice can be easily maintained in cell culture, particularly those isolated from mice harboring aggressive disease (ie. crossed to *p19^{arf}-/-* or *p53-/-* mice). Furthermore, isolated cells can be subsequently transplanted into syngeneic, nontransgenic recipient mice by tail vein injection. These immunocompetent recipients rapidly (~2 weeks) develop a disease histopathologically indistinguishable from the original tumor-bearing *Eμ-myc* transgenic mice. Importantly, the transplanted disease localizes to sites mirroring the primary malignancy – a critical observation given the known importance of tumor microenvironment in mediating drug action. Additionally, the act of transplantation itself does not seem to alter therapeutic response as the response profile of an individual lymphoma can be recapitulated in multiple recipient mice (162, 163). This is in contrast to primary tumors that display a heterogeneous response to chemotherapy – presumably a result of secondary mutations in the transgenic B-cell compartment – a phenomenon paralleling the clinical reality of Burkitt's patients (162, 163).

1.6.1b *Eμ-myc* lymphoma is amenable to genetic modification

A similarly powerful advantage of the *Eμ-myc* system is the ability to genetically manipulate cells using retroviral transduction. Coupled with the above-mentioned transplantation technique, this allows for the rapid evaluation of secondary genetic lesions without generating germ line transgenic mice. For example, primary lymphoma cells can be isolated form *Eμ-myc* transgenic mice, transduced with a retroviral construct expressing green florescent protein (GFP) and transplanted into syngeneic recipient animals. Importantly, this process does not seem to affect therapeutic outcome as primary cells subjected to or withheld from GFP transduction behave identically when treated as transplants *in vivo* (164).

1.6.1c *In vivo* chemotherapeutic response can be readily evaluated using genetically-altered *Eμ-myc* lymphomas

In addition to GFP overexpression, retroviral manipulation of primary lymphoma cells allows the systematic evaluation of any gene of interest in a controlled, yet clinically relevant environment. This can be accomplished by simply coexpressing a gene along with GFP and subsequently comparing response profiles to GFP-only cells (164). Retroviral overexpression of the anti-apoptotic protein *Bcl-2*, for example, has been shown to greatly reduce therapeutic efficacy – an observation consistent with work using germ line

transgenic mice as well as with patients overexpressing *Bcl-2* treated with chemotherapy (162, 165, 166).

1.6.2 *KrasG12D; p53-/-* lung adenocarcinoma

Epithelial cancers represent the majority of human malignancies. Additionally, they are typically less susceptible to chemotherapeutic intervention compared to malignancies of hematopoietic origin. Studying the genetics of drug resistance in epithelial cancer models might, therefore, provide insight into resistance mechanisms uniquely employed by these tumor types. A major limitation hampering their development, however, is the relatively inaccessible, non-systemic nature of the disease itself – qualities that lend poorly to disease progress and therapeutic response monitoring.

Interestingly, recent work from the laboratory of Tyler Jacks has described micro-computed tomography (microCT)-based imaging of $Kras^{G12D}$*; p53-/-* lung adenocarcinoma as a useful tool for tracking disease progress *in vivo* (167, 168). Additionally, preliminary work from their lab indicates that cell lines derived from autochthonous $Kras^{G12D}$*; p53-/-* lung adenocarcinoma can be transplanted into syngeneic recipient mice generating a disease similar to the original tumor (Trudy Oliver, Monte Winslow; personal communication). Thus, while clearly in the early stages of development, the prospect of using transplantable lung carcinoma as a platform for studying mechanisms of chemotherapeutic response remains

intriguing and will be the focus of several projects described towards the end of this thesis.

1.7 References

1. Berenblum R-S. The modifying influence of dichloroethyl sulphide on the induction of tumours in mice by tar. J Pathol Bacteriol 1929;32:424-34.

2. Adair FE, Bagg HJ. Experimental And Clinical Studies On The Treatment Of Cancer By Dichlorethylsulphide (Mustard Gas. Ann Surg 1931;93(1):190-9.

3. Krumbhaar EB, Krumbhaar HD. The Blood and Bone Marrow in Yelloe Cross Gas (Mustard Gas) Poisoning: Changes produced in the Bone Marrow of Fatal Cases. J Med Res 1919;40(3):497-508 3.

4. Berenblum R-S. Experimental inhibition of tumour induction by mustard gas and other compounds. J Pathol Bacteriol 1935;40:549-58.

5. Czuczman MS, Grillo-Lopez AJ, White CA, et al. Treatment of patients with low-grade B-cell lymphoma with the combination of chimeric anti-CD20 monoclonal antibody and CHOP chemotherapy. J Clin Oncol 1999;17(1):268-76.

6. Druker BJ, Talpaz M, Resta DJ, et al. Efficacy and safety of a specific inhibitor of the BCR-ABL tyrosine kinase in chronic myeloid leukemia. N Engl J Med 2001;344(14):1031-7.

7. Papac RJ. Origins of cancer therapy. Yale J Biol Med 2001;74(6):391-8.

8. American Cancer Society. Cancer facts & figures. In. Atlanta, GA: http://www.cancer.org. p. v.

9. Gerlach JH, Bell DR, Karakousis C, et al. P-glycoprotein in human sarcoma: evidence for multidrug resistance. J Clin Oncol 1987;5(9):1452-60.

10. Gerlach JH, Kartner N, Bell DR, Ling V. Multidrug resistance. Cancer Surv 1986;5(1):25-46.

11. Germann UA. P-glycoprotein--a mediator of multidrug resistance in tumour cells. Eur J Cancer 1996;32A(6):927-44.

12. Germann UA, Chambers TC. Molecular analysis of the multidrug transporter, P-glycoprotein. Cytotechnology 1998;27(1-3):31-60.

13. Juliano RL, Ling V. A surface glycoprotein modulating drug permeability in Chinese hamster ovary cell mutants. Biochim Biophys Acta 1976;455(1):152-62.

14. Kartner N, Riordan JR, Ling V. Cell surface P-glycoprotein associated with multidrug resistance in mammalian cell lines. Science 1983;221(4617):1285-8.

15. Modok S, Mellor HR, Callaghan R. Modulation of multidrug resistance efflux pump activity to overcome chemoresistance in cancer. Curr Opin Pharmacol 2006;6(4):350-4.

16. Riordan JR, Deuchars K, Kartner N, Alon N, Trent J, Ling V. Amplification of P-glycoprotein genes in multidrug-resistant mammalian cell lines. Nature 1985;316(6031):817-9.

17. Riordan JR, Ling V. Purification of P-glycoprotein from plasma membrane vesicles of Chinese hamster ovary cell mutants with reduced colchicine permeability. J Biol Chem 1979;254(24):12701-5.

18. Shoemaker R, Wolpert-DeFilippes M, Plowman J, et al. Pleiotropic resistance and drug development. Prog Clin Biol Res 1986;223:143-9.

19. Higgins CF. ABC transporters: physiology, structure and mechanism--an overview. Res Microbiol 2001;152(3-4):205-10.

20. Gill DR, Hyde SC, Higgins CF, Valverde MA, Mintenig GM, Sepulveda FV. Separation of drug transport and chloride channel functions of the human multidrug resistance P-glycoprotein. Cell 1992;71(1):23-32.

21. Higgins CF. Multiple molecular mechanisms for multidrug resistance transporters. Nature 2007;446(7137):749-57.

22. Breier A, Barancik M, Sulova Z, Uhrik B. P-glycoprotein--implications of metabolism of neoplastic cells and cancer therapy. Curr Cancer Drug Targets 2005;5(6):457-68.

23. Brinkmann U. Functional polymorphisms of the human multidrug resistance (MDR1) gene: correlation with P glycoprotein expression and activity in vivo. Novartis Found Symp 2002;243:207-10; discussion 10-2, 31-5.

24. Karssen AM, Meijer OC, van der Sandt IC, De Boer AG, De Lange EC, De Kloet ER. The role of the efflux transporter P-glycoprotein in brain penetration of prednisolone. J Endocrinol 2002;175(1):251-60.

25. Turriziani O, Scagnolari C, Bellomi F, Solimeo I, Focher F, Antonelli G. Cellular issues relating to the resistance of HIV to antiretroviral agents. Scand J Infect Dis Suppl 2003;106:45-8.

26. Webster JI, Carlstedt-Duke J. Involvement of multidrug resistance proteins (MDR) in the modulation of glucocorticoid response. J Steroid Biochem Mol Biol 2002;82(4-5):277-88.

27. Bourhis J, Goldstein LJ, Riou G, Pastan I, Gottesman MM, Benard J. Expression of a human multidrug resistance gene in ovarian carcinomas. Cancer Res 1989;49(18):5062-5.

28. Chan HS, Haddad G, Thorner PS, et al. P-glycoprotein expression as a predictor of the outcome of therapy for neuroblastoma. N Engl J Med 1991;325(23):1608-14.

29. Goldstein LJ, Gottesman MM, Pastan I. Expression of the MDR1 gene in human cancers. Cancer Treat Res 1991;57:101-19.

30. Goldstein LJ, Pastan I, Gottesman MM. Multidrug resistance in human cancer. Crit Rev Oncol Hematol 1992;12(3):243-53.

31. Lai SL, Goldstein LJ, Gottesman MM, et al. MDR1 gene expression in lung cancer. J Natl Cancer Inst 1989;81(15):1144-50.

32. Pirker R, Goldstein LJ, Ludwig H, et al. Expression of a multidrug resistance gene in blast crisis of chronic myelogenous leukemia. Cancer Commun 1989;1(2):141-4.

33. Sato H, Gottesman MM, Goldstein LJ, et al. Expression of the multidrug resistance gene in myeloid leukemias. Leuk Res 1990;14(1):11-21.

34. Jones DP. Extracellular redox state: refining the definition of oxidative stress in aging. Rejuvenation Res 2006;9(2):169-81.

35. Jones DP. Radical-free biology of oxidative stress. Am J Physiol Cell Physiol 2008;295(4):C849-68.

36. Pompella A, Visvikis A, Paolicchi A, De Tata V, Casini AF. The changing faces of glutathione, a cellular protagonist. Biochem Pharmacol 2003;66(8):1499-503.

37. Jedlitschky G, Leier I, Buchholz U, Center M, Keppler D. ATP-dependent transport of glutathione S-conjugates by the multidrug resistance-associated protein. Cancer Res 1994;54(18):4833-6.

38. Morrow CS, Cowan KH. Glutathione S-transferases and drug resistance. Cancer Cells 1990;2(1):15-22.

39. Muller M, Meijer C, Zaman GJ, et al. Overexpression of the gene encoding the multidrug resistance-associated protein results in increased ATP-dependent glutathione S-conjugate transport. Proc Natl Acad Sci U S A 1994;91(26):13033-7.

40. Tew KD. Glutathione-associated enzymes in anticancer drug resistance. Cancer Res 1994;54(16):4313-20.

41. Sies H, Brigelius R, Wefers H, Muller A, Cadenas E. Cellular redox changes and response to drugs and toxic agents. Fundam Appl Toxicol 1983;3(4):200-8.

42. Taylor YC, Evans JW, Brown JM. Mechanism of sensitization of Chinese hamster ovary cells to melphalan by hypoxic treatment with misonidazole. Cancer Res 1983;43(7):3175-81.

43. Carmichael J, Adams DJ, Ansell J, Wolf CR. Glutathione and glutathione transferase levels in mouse granulocytes following cyclophosphamide administration. Cancer Res 1986;46(2):735-9.

44. Carmichael J, Friedman N, Tochner Z, et al. Inhibition of the protective effect of cyclophosphamide by pre-treatment with buthionine sulfoximine. Int J Radiat Oncol Biol Phys 1986;12(7):1191-3.

45. Wolf CR, Lewis AD, Carmichael J, Adams DJ, Allan SG, Ansell DJ. The role of glutathione in determining the response of normal and tumor cells to anticancer drugs. Biochem Soc Trans 1987;15(4):728-30.

46. Colvin OM, Friedman HS, Gamcsik MP, Fenselau C, Hilton J. Role of glutathione in cellular resistance to alkylating agents. Adv Enzyme Regul 1993;33:19-26.

47. O'Brien ML, Tew KD. Glutathione and related enzymes in multidrug resistance. Eur J Cancer 1996;32A(6):967-78.

48. Tew KD, O'Brien M, Laing NM, Shen H. Coordinate changes in expression of protective genes in drug-resistant cells. Chem Biol Interact 1998;111-112:199-211.

49. Evans CG, Bodell WJ, Tokuda K, Doane-Setzer P, Smith MT. Glutathione and related enzymes in rat brain tumor cell resistance to 1,3-bis(2-chloroethyl)-1-nitrosourea and nitrogen mustard. Cancer Res 1987;47(10):2525-30.

50. Funke S, Timofeeva M, Risch A, et al. Genetic polymorphisms in GST genes and survival of colorectal cancer patients treated with chemotherapy. Pharmacogenomics;11(1):33-41.

51. Martinez V, Kennedy S, Doolan P, et al. Drug metabolism-related genes as potential biomarkers: analysis of expression in normal and tumour breast tissue. Breast Cancer Res Treat 2008;110(3):521-30.

52. D'Incalci M, Bonfanti M, Pifferi A, et al. The antitumour activity of alkylating agents is not correlated with the levels of glutathione, glutathione transferase and O6-alkylguanine-DNA-alkyltransferase of human tumour xenografts. EORTC SPG and PAMM Groups. Eur J Cancer 1998;34(11):1749-55.

53. Schipper DL, Wagenmans MJ, Peters WH, Wils JA, Wagener DJ. Glutathione S-transferases and iododeoxyuridine labelling index during chemotherapy of gastric cancer. Anticancer Res 2000;20(3A):1705-10.

54. Vallbohmer D, Iqbal S, Yang DY, et al. Molecular determinants of irinotecan efficacy. Int J Cancer 2006;119(10):2435-42.

55. Cabelguenne A, Loriot MA, Stucker I, et al. Glutathione-associated enzymes in head and neck squamous cell carcinoma and response to cisplatin-based neoadjuvant chemotherapy. Int J Cancer 2001;93(5):725-30.

56. Ferrandina G, Scambia G, Damia G, et al. Glutathione S-transferase activity in epithelial ovarian cancer: association with response to chemotherapy and disease outcome. Ann Oncol 1997;8(4):343-50.

57. el Rouby S, Thomas A, Costin D, et al. p53 gene mutation in B-cell chronic lymphocytic leukemia is associated with drug resistance and is independent of MDR1/MDR3 gene expression. Blood 1993;82(11):3452-9.

58. Fan S, el-Deiry WS, Bae I, et al. p53 gene mutations are associated with decreased sensitivity of human lymphoma cells to DNA damaging agents. Cancer Res 1994;54(22):5824-30.

59. Lowe SW, Bodis S, Bardeesy N, et al. Apoptosis and the prognostic significance of p53 mutation. Cold Spring Harb Symp Quant Biol 1994;59:419-26.

60. Lowe SW, Bodis S, McClatchey A, et al. p53 status and the efficacy of cancer therapy in vivo. Science 1994;266(5186):807-10.

61. Lowe SW, Ruley HE, Jacks T, Housman DE. p53-dependent apoptosis modulates the cytotoxicity of anticancer agents. Cell 1993;74(6):957-67.

62. Gasparini G, Barbareschi M, Doglioni C, et al. Expression of bcl-2 protein predicts efficacy of adjuvant treatments in operable node-positive breast cancer. Clin Cancer Res 1995;1(2):189-98.

63. Reed JC. Bcl-2: prevention of apoptosis as a mechanism of drug resistance. Hematol Oncol Clin North Am 1995;9(2):451-73.

64. Almasan A, Ashkenazi A. Apo2L/TRAIL: apoptosis signaling, biology, and potential for cancer therapy. Cytokine Growth Factor Rev 2003;14(3-4):337-48.

65. Fox NL, Humphreys R, Luster TA, Klein J, Gallant G. Tumor Necrosis Factor-related apoptosis-inducing ligand (TRAIL) Receptor-1 and Receptor-2 agonists for cancer therapy. Expert Opin Biol Ther;10(1):1-18.

66. Luster TA, Carrell JA, McCormick K, Sun D, Humphreys R. Mapatumumab and lexatumumab induce apoptosis in TRAIL-R1 and TRAIL-R2 antibody-resistant NSCLC cell lines when treated in combination with bortezomib. Mol Cancer Ther 2009;8(2):292-302.

67. Chu G. Cellular responses to cisplatin. The roles of DNA-binding proteins and DNA repair. J Biol Chem 1994;269(2):787-90.

68. Rosell R, Taron M, Ariza A, et al. Molecular predictors of response to chemotherapy in lung cancer. Semin Oncol 2004;31(1 Suppl 1):20-7.

69. Fong PC, Boss DS, Yap TA, et al. Inhibition of poly(ADP-ribose) polymerase in tumors from BRCA mutation carriers. N Engl J Med 2009;361(2):123-34.

70. Fong PC, Yap TA, Boss DS, et al. Poly(ADP)-ribose polymerase inhibition: frequent durable responses in BRCA carrier ovarian cancer correlating with platinum-free interval. J Clin Oncol;28(15):2512-9.

71. Jones P, Altamura S, Boueres J, et al. Discovery of 2-{4-[(3S)-piperidin-3-yl]phenyl}-2H-indazole-7-carboxamide (MK-4827): a novel oral poly(ADP-ribose)polymerase (PARP) inhibitor efficacious in BRCA-1 and -2 mutant tumors. J Med Chem 2009;52(22):7170-85.

72. Bartz SR, Zhang Z, Burchard J, et al. Small interfering RNA screens reveal enhanced cisplatin cytotoxicity in tumor cells having both BRCA network and TP53 disruptions. Mol Cell Biol 2006;26(24):9377-86.

73. Tewey KM, Rowe TC, Yang L, Halligan BD, Liu LF. Adriamycin-induced DNA damage mediated by mammalian DNA topoisomerase II. Science 1984;226(4673):466-8.

74. Cummings J, Smyth JF. DNA topoisomerase I and II as targets for rational design of new anticancer drugs. Ann Oncol 1993;4(7):533-43.

75. Kruczynski A, Barret JM, Van Hille B, et al. Decreased nucleotide excision repair activity and alterations of topoisomerase IIalpha are associated with the in vivo resistance of a P388 leukemia subline to F11782, a novel catalytic inhibitor of topoisomerases I and II. Clin Cancer Res 2004;10(9):3156-68.

76. Leontiou C, Lakey JH, Lightowlers R, Turnbull RM, Austin CA. Mutation P732L in human DNA topoisomerase IIbeta abolishes DNA cleavage in the

presence of calcium and confers drug resistance. Mol Pharmacol 2006;69(1):130-9.

77. Mao Y, Yu C, Hsieh TS, et al. Mutations of human topoisomerase II alpha affecting multidrug resistance and sensitivity. Biochemistry 1999;38(33):10793-800.

78. Okada Y, Tosaka A, Nimura Y, Kikuchi A, Yoshida S, Suzuki M. Atypical multidrug resistance may be associated with catalytically active mutants of human DNA topoisomerase II alpha. Gene 2001;272(1-2):141-8.

79. Coldwell KE, Cutts SM, Ognibene TJ, Henderson PT, Phillips DR. Detection of Adriamycin-DNA adducts by accelerator mass spectrometry at clinically relevant Adriamycin concentrations. Nucleic Acids Res 2008;36(16):e100.

80. Fedier A, Schwarz VA, Walt H, Carpini RD, Haller U, Fink D. Resistance to topoisomerase poisons due to loss of DNA mismatch repair. Int J Cancer 2001;93(4):571-6.

81. Lage H, Dietel M. Involvement of the DNA mismatch repair system in antineoplastic drug resistance. J Cancer Res Clin Oncol 1999;125(3-4):156-65.

82. Swift LP, Rephaeli A, Nudelman A, Phillips DR, Cutts SM. Doxorubicin-DNA adducts induce a non-topoisomerase II-mediated form of cell death. Cancer Res 2006;66(9):4863-71.

83. Furuta T, Ueda T, Aune G, Sarasin A, Kraemer KH, Pommier Y. Transcription-coupled nucleotide excision repair as a determinant of cisplatin sensitivity of human cells. Cancer Res 2002;62(17):4899-902.

84. Martin LP, Hamilton TC, Schilder RJ. Platinum resistance: the role of DNA repair pathways. Clin Cancer Res 2008;14(5):1291-5.

85. Massey A, Offman J, Macpherson P, Karran P. DNA mismatch repair and acquired cisplatin resistance in E. coli and human ovarian carcinoma cells. DNA Repair (Amst) 2003;2(1):73-89.

86. Rosell R, Taron M, Barnadas A, Scagliotti G, Sarries C, Roig B. Nucleotide excision repair pathways involved in Cisplatin resistance in non-small-cell lung cancer. Cancer Control 2003;10(4):297-305.

87. Helleman J, van Staveren IL, Dinjens WN, et al. Mismatch repair and treatment resistance in ovarian cancer. BMC Cancer 2006;6:201.

88. Yu JJ, Bicher A, Ma YK, Bostick-Bruton F, Reed E. Absence of evidence for allelic loss or allelic gain for ERCC1 or for XPD in human ovarian cancer cells and tissues. Cancer Lett 2000;151(2):127-32.

89. Choi MK, Kim DD. Platinum transporters and drug resistance. Arch Pharm Res 2006;29(12):1067-73.

90. Ishida S, Lee J, Thiele DJ, Herskowitz I. Uptake of the anticancer drug cisplatin mediated by the copper transporter Ctr1 in yeast and mammals. Proc Natl Acad Sci U S A 2002;99(22):14298-302.

91. Safaei R. Role of copper transporters in the uptake and efflux of platinum containing drugs. Cancer Lett 2006;234(1):34-9.

92. Safaei R, Katano K, Samimi G, et al. Cross-resistance to cisplatin in cells with acquired resistance to copper. Cancer Chemother Pharmacol 2004;53(3):239-46.

93. Zhou J, Giannakakou P. Targeting microtubules for cancer chemotherapy. Curr Med Chem Anticancer Agents 2005;5(1):65-71.

94. Cabral F, Abraham I, Gottesman MM. Isolation of a taxol-resistant Chinese hamster ovary cell mutant that has an alteration in alpha-tubulin. Proc Natl Acad Sci U S A 1981;78(7):4388-91.

95. Jaffrezou JP, Dumontet C, Derry WB, et al. Novel mechanism of resistance to paclitaxel (Taxol) in human K562 leukemia cells by combined selection with PSC 833. Oncol Res 1995;7(10-11):517-27.

96. Kavallaris M, Tait AS, Walsh BJ, et al. Multiple microtubule alterations are associated with Vinca alkaloid resistance in human leukemia cells. Cancer Res 2001;61(15):5803-9.

97. Martello LA, Verdier-Pinard P, Shen HJ, et al. Elevated levels of microtubule destabilizing factors in a Taxol-resistant/dependent A549 cell line with an alpha-tubulin mutation. Cancer Res 2003;63(6):1207-13.

98. Chou TC, Zhang XG, Harris CR, et al. Desoxyepothilone B is curative against human tumor xenografts that are refractory to paclitaxel. Proc Natl Acad Sci U S A 1998;95(26):15798-802.

99. Kavallaris M, Verrills NM, Hill BT. Anticancer therapy with novel tubulin-interacting drugs. Drug Resist Updat 2001;4(6):392-401.

100. Kowalski RJ, Giannakakou P, Hamel E. Activities of the microtubule-stabilizing agents epothilones A and B with purified tubulin and in cells resistant to paclitaxel (Taxol(R)). J Biol Chem 1997;272(4):2534-41.

101. Yang CP, Verdier-Pinard P, Wang F, et al. A highly epothilone B-resistant A549 cell line with mutations in tubulin that confer drug dependence. Mol Cancer Ther 2005;4(6):987-95.

102. Salmon SE, Hamburger AW, Soehnlen B, Durie BG, Alberts DS, Moon TE. Quantitation of differential sensitivity of human-tumor stem cells to anticancer drugs. N Engl J Med 1978;298(24):1321-7.

103. Bertelsen CA, Sondak VK, Mann BD, Korn EL, Kern DH. Chemosensitivity testing of human solid tumors. A review of 1582 assays with 258 clinical correlations. Cancer 1984;53(6):1240-5.

104. Parker RL, Jr., Welander CE, Homesley HD, Jobson VW, Kawamoto EH. Use of the human tumor stem cell assay to study chemotherapy sensitivity in cancer of the cervix. Obstet Gynecol 1984;64(3):412-6.

105. Teicher BA. In vivo/ex vivo and in situ assays used in cancer research: a brief review. Toxicol Pathol 2009;37(1):114-22.

106. Hanahan D, Weinberg RA. The hallmarks of cancer. Cell 2000;100(1):57-70.

107. Keating MJ. Leukemia: A model for drug development. Clin Cancer Res 1997;3(12 Pt 2):2598-604.

108. Skipper HE, Schabel FM, Jr., Bell M, Thomson JR, Johnson S. On the curability of experimental neoplasms. I. Amethopterin and mouse leukemias. Cancer Res 1957;17(7):717-26.

109. Skipper HE, Schabel FM, Jr., Wilcox WS. Experimental Evaluation Of Potential Anticancer Agents. Xiii. On The Criteria And Kinetics Associated With "Curability" Of Experimental Leukemia. Cancer Chemother Rep 1964;35:1-111.

110. Bruce WR. The action of chemotherapeutic agents at the cellular level and the effects of these agents on hematopoietic and lymphomatous tissue. Proc Can Cancer Conf 1967;7:53-64.

111. Bruce WR. A model system for examining the action of anti-cancer agents at the cellular level in vivo. Natl Cancer Inst Monogr 1967;24:249-56.

112. Bruce WR, Meeker BE. Dissemination And Growth Of Transplanted Isologous Murine Lymphoma Cells. J Natl Cancer Inst 1964;32:1145-59.

113. Bruce WR, Meeker BE, Valeriote FA. Comparison of the sensitivity of normal hematopoietic and transplanted lymphoma colony-forming cells to chemotherapeutic agents administered in vivo. J Natl Cancer Inst 1966;37(2):233-45.

114. Valeriote FA, Bruce WR, Meeker BE. A model for the action of vinblastine in vivo. Biophys J 1966;6(2):145-52.

115. Black PC, Dinney CP. Bladder cancer angiogenesis and metastasis--translation from murine model to clinical trial. Cancer Metastasis Rev 2007;26(3-4):623-34.

116. Klein S, Levitzki A. Targeted cancer therapy: promise and reality. Adv Cancer Res 2007;97:295-319.

117. Kumar S, Anderson KC. Drug insight: thalidomide as a treatment for multiple myeloma. Nat Clin Pract Oncol 2005;2(5):262-70.

118. Berenbaum MC, Sheard CE, Reittie JR, Bundick RV. The growth of human tumours in immunosuppressed mice and their response to chemotherapy. Br J Cancer 1974;30(1):13-32.

119. Davies AJ. Chemotherapy of tumours in immuno-deprived mice. Recent Results Cancer Res 1977(62):13-6.

120. Kopper L, Steel GG. The therapeutic response of three human tumor lines maintained in immune-suppressed mice. Cancer Res 1975;35(10):2704-13.

121. Mitchley BC, Clarke SA, Connors TA, Neville AM. Hexamethylmelamine-induced regression of human lung tumors growing in immune deprived mice. Cancer Res 1975;35(4):1099-102.

122. Povlsen CO, Jacobsen GK. Chemotherapy of a human malignant melanoma transplanted in the nude mouse. Cancer Res 1975;35(10):2790-6.

123. Shorthouse AJ, Smyth JF, Steel GG, Ellison M, Mills J, Peckham MJ. The human tumour xenograft--a valid model in experimental chemotherapy? Br J Surg 1980;67(10):715-22.

124. Rottenberg S, Jonkers J. Modeling therapy resistance in genetically engineered mouse cancer models. Drug Resist Updat 2008;11(1-2):51-60.

125. Bric A, Miething C, Bialucha CU, et al. Functional identification of tumor-suppressor genes through an in vivo RNA interference screen in a mouse lymphoma model. Cancer Cell 2009;16(4):324-35.

126. Meacham CE, Ho EE, Dubrovsky E, Gertler FB, Hemann MT. In vivo RNAi screening identifies regulators of actin dynamics as key determinants of lymphoma progression. Nat Genet 2009;41(10):1133-7.

127. Zender L, Xue W, Zuber J, et al. An oncogenomics-based in vivo RNAi screen identifies tumor suppressors in liver cancer. Cell 2008;135(5):852-64.

128. Kunz M. Genomic signatures for individualized treatment of malignant tumors. Curr Drug Discov Technol 2008;5(1):9-14.

129. Mariadason JM, Arango D, Augenlicht LH. Customizing chemotherapy for colon cancer: the potential of gene expression profiling. Drug Resist Updat 2004;7(3):209-18.

130. McHugh SM, O'Donnell J, Gillen P. Genomic and oncoproteomic advances in detection and treatment of colorectal cancer. World J Surg Oncol 2009;7:36.

131. Quintieri L, Fantin M, Vizler C. Identification of molecular determinants of tumor sensitivity and resistance to anticancer drugs. Adv Exp Med Biol 2007;593:95-104.

132. Kudoh K, Ramanna M, Ravatn R, et al. Monitoring the expression profiles of doxorubicin-induced and doxorubicin-resistant cancer cells by cDNA microarray. Cancer Res 2000;60(15):4161-6.

133. Efferth T, Volm M. Pharmacogenetics for individualized cancer chemotherapy. Pharmacol Ther 2005;107(2):155-76.

134. Ooyama A, Okayama Y, Takechi T, Sugimoto Y, Oka T, Fukushima M. Genome-wide screening of loci associated with drug resistance to 5-fluorouracil-based drugs. Cancer Sci 2007;98(4):577-83.

135. Voisey J, Morris CP. SNP technologies for drug discovery: a current review. Curr Drug Discov Technol 2008;5(3):230-5.

136. Gamazon ER, Huang RS, Cox NJ, Dolan ME. Chemotherapeutic drug susceptibility associated SNPs are enriched in expression quantitative trait loci. Proc Natl Acad Sci U S A;107(20):9287-92.

137. Collier LS, Carlson CM, Ravimohan S, Dupuy AJ, Largaespada DA. Cancer gene discovery in solid tumours using transposon-based somatic mutagenesis in the mouse. Nature 2005;436(7048):272-6.

138. Jonkers J, Berns A. Retroviral insertional mutagenesis as a strategy to identify cancer genes. Biochim Biophys Acta 1996;1287(1):29-57.

139. van Lohuizen M, Verbeek S, Scheijen B, Wientjens E, van der Gulden H, Berns A. Identification of cooperating oncogenes in E mu-myc transgenic mice by provirus tagging. Cell 1991;65(5):737-52.

140. Xia L, Jaafar L, Cashikar A, Flores-Rozas H. Identification of genes required for protection from doxorubicin by a genome-wide screen in Saccharomyces cerevisiae. Cancer Res 2007;67(23):11411-8.

141. Chang K, Elledge SJ, Hannon GJ. Lessons from Nature: microRNA-based shRNA libraries. Nat Methods 2006;3(9):707-14.

142. Azorsa DO, Gonzales IM, Basu GD, et al. Synthetic lethal RNAi screening identifies sensitizing targets for gemcitabine therapy in pancreatic cancer. J Transl Med 2009;7:43.

143. Bauer JA, Ye F, Marshall CB, et al. RNA interference (RNAi) screening approach identifies agents that enhance paclitaxel activity in breast cancer cells. Breast Cancer Res;12(3):R41.

144. Brummelkamp TR, Fabius AW, Mullenders J, et al. An shRNA barcode screen provides insight into cancer cell vulnerability to MDM2 inhibitors. Nat Chem Biol 2006;2(4):202-6.

145. Juul N, Szallasi Z, Eklund AC, et al. Assessment of an RNA interference screen-derived mitotic and ceramide pathway metagene as a predictor of

response to neoadjuvant paclitaxel for primary triple-negative breast cancer: a retrospective analysis of five clinical trials. Lancet Oncol;11(4):358-65.

146. Lam LT, Davis RE, Ngo VN, et al. Compensatory IKKalpha activation of classical NF-kappaB signaling during IKKbeta inhibition identified by an RNA interference sensitization screen. Proc Natl Acad Sci U S A 2008;105(52):20798-803.

147. Lord CJ, Iorns E, Ashworth A. Dissecting resistance to endocrine therapy in breast cancer. Cell Cycle 2008;7(13):1895-8.

148. Mullenders J, von der Saal W, van Dongen MM, et al. Candidate biomarkers of response to an experimental cancer drug identified through a large-scale RNA interference genetic screen. Clin Cancer Res 2009;15(18):5811-9.

149. Whitehurst AW, Bodemann BO, Cardenas J, et al. Synthetic lethal screen identification of chemosensitizer loci in cancer cells. Nature 2007;446(7137):815-9.

150. Adams JM, Harris AW, Pinkert CA, et al. The c-myc oncogene driven by immunoglobulin enhancers induces lymphoid malignancy in transgenic mice. Nature 1985;318(6046):533-8.

151. Harris AW, Pinkert CA, Crawford M, Langdon WY, Brinster RL, Adams JM. The E mu-myc transgenic mouse. A model for high-incidence spontaneous lymphoma and leukemia of early B cells. J Exp Med 1988;167(2):353-71.

152. Adams JM, Harris AW, Langdon WY, et al. c-myc-induced lymphomagenesis in transgenic mice and the role of the Pvt-1 locus in lymphoid neoplasia. Curr Top Microbiol Immunol 1986;132:1-8.

153. Langdon WY, Harris AW, Cory S. Growth of E mu-myc transgenic B-lymphoid cells in vitro and their evolution toward autonomy. Oncogene Res 1988;3(3):271-9.

154. Amaravadi RK, Yu D, Lum JJ, et al. Autophagy inhibition enhances therapy-induced apoptosis in a Myc-induced model of lymphoma. J Clin Invest 2007;117(2):326-36.

155. Bordeleau ME, Robert F, Gerard B, et al. Therapeutic suppression of translation initiation modulates chemosensitivity in a mouse lymphoma model. J Clin Invest 2008;118(7):2651-60.

156. Lindemann RK, Newbold A, Whitecross KF, et al. Analysis of the apoptotic and therapeutic activities of histone deacetylase inhibitors by using a mouse model of B cell lymphoma. Proc Natl Acad Sci U S A 2007;104(19):8071-6.

157. Mason KD, Vandenberg CJ, Scott CL, et al. In vivo efficacy of the Bcl-2 antagonist ABT-737 against aggressive Myc-driven lymphomas. Proc Natl Acad Sci U S A 2008;105(46):17961-6.

158. Newbold A, Lindemann RK, Cluse LA, Whitecross KF, Dear AE, Johnstone RW. Characterisation of the novel apoptotic and therapeutic activities of the histone deacetylase inhibitor romidepsin. Mol Cancer Ther 2008;7(5):1066-79.

159. Schmitt CA, Lowe SW. Apoptosis and chemoresistance in transgenic cancer models. J Mol Med 2002;80(3):137-46.

160. Wendel HG, Malina A, Zhao Z, et al. Determinants of sensitivity and resistance to rapamycin-chemotherapy drug combinations in vivo. Cancer Res 2006;66(15):7639-46.

161. Schmitt CA, McCurrach ME, de Stanchina E, Wallace-Brodeur RR, Lowe SW. INK4a/ARF mutations accelerate lymphomagenesis and promote chemoresistance by disabling p53. Genes Dev 1999;13(20):2670-7.

162. Schmitt CA, Lowe SW. Bcl-2 mediates chemoresistance in matched pairs of primary E(mu)-myc lymphomas in vivo. Blood Cells Mol Dis 2001;27(1):206-16.

163. Schmitt CA, Wallace-Brodeur RR, Rosenthal CT, McCurrach ME, Lowe SW. DNA damage responses and chemosensitivity in the E mu-myc mouse lymphoma model. Cold Spring Harb Symp Quant Biol 2000;65:499-510.

164. Schmitt CA, Rosenthal CT, Lowe SW. Genetic analysis of chemoresistance in primary murine lymphomas. Nat Med 2000;6(9):1029-35.

165. Ilyas M, Kendall M, Jalal H, Linton C, Rooney N. Changes in Bcl-2 and p53 expression in recurrent B-cell lymphomas. J Pathol 1996;180(3):249-53.

166. Strasser A, Harris AW, Jacks T, Cory S. DNA damage can induce apoptosis in proliferating lymphoid cells via p53-independent mechanisms inhibitable by Bcl-2. Cell 1994;79(2):329-39.

167. Meylan E, Dooley AL, Feldser DM, et al. Requirement for NF-kappaB signalling in a mouse model of lung adenocarcinoma. Nature 2009;462(7269):104-7.

168. Oliver TG, Mercer KL, Sayles LC, et al. Chronic cisplatin treatment promotes enhanced damage repair and tumor progression in a mouse model of lung cancer. Genes Dev;24(8):837-52.

Chapter 2

Pooled shRNA screening identifies genetic mediators of doxorubicin response[1]

2.1 Abstract

Topoisomerase poisons are chemotherapeutic agents that are used extensively for treating human malignancies. These drugs can be highly effective, yet tumors are frequently refractory to treatment or become resistant upon tumor relapse. Using a pool-based RNAi screening approach and a well-characterized mouse model of lymphoma, we explored the genetic basis for heterogeneous responses to topoisomerase poisons *in vitro* and *in vivo*. These experiments identified Top2A expression levels as major determinants of response to the topoisomerase 2 poison doxorubicin and showed that suppression of Top2A produces resistance to doxorubicin *in vitro* and *in vivo*. Analogously, using a targeted RNAi approach, we demonstrated that suppression of Top1 produces resistance to the topoisomerase 1 poison camptothecin yet hypersensitizes cancer cells to doxorubicin. Importantly, lymphomas relapsing after treatment display spontaneous changes in topoisomerase levels as predicted by in vitro gene knockdown studies. These results highlight the utility of pooled shRNA screens for identifying genetic determinants of chemotherapy response and suggest strategies for improving the effectiveness of topoisomerase poisons in the clinic.

Contributions:

Drs. Hemann, Burgess and Lowe designed and wrote the manuscript as it appears in the *Proceedings of the National Academy of Sciences.* I contributed to the design, generation and analysis of selected experiments, namely the serial enrichment screen and several of the Top2A and Top1 *in vivo* experiments. Figures and data that I have not personally contributed to are clearly noted and properly recognized in the figure legends.

[1]Significant sections of this chapter have been previously published in:

Burgess DJ, Doles J, Zender L, Xue W, Ma B, McCombie WR, Hannon GJ, Lowe SW, Hemann MT. Topoisomerase levels determine chemotherapy response *in vitro* and *in vivo*. *Proc Natl Acad Sci U S A.* 2008 Jul 1;105(26):9053-8. Epub 2008 Jun 23. PMID: 18574145

2.2 Introduction

A myriad of genetic factors influence the efficacy of cancer chemotherapy, including both somatic changes in the tumor itself as well as genetic polymorphisms present in the patient. These factors include increased expression of detoxification pumps that prevent access of the drug to its target (1), point mutations that disrupt the drug–target interaction (2, 3), and mutations in stress response pathways [e.g., *p53* loss (4)]. To tailor treatment successfully to the individual patient, a more complete understanding of the genetic determinants of therapy response is necessary.

RNA interference (RNAi) exploits a mechanism of gene regulation whereby double-stranded RNAs are processed by a conserved cellular machinery to suppress the expression of genes containing homologous sequences (5). Importantly, libraries of DNA-based vectors encoding short hairpin RNAs (shRNAs) capable of targeting most genes in the human and mouse genomes have been produced and enable forward genetic screens to be performed in mammalian cells. Indeed, by using human tumor-derived cell lines treated *in vitro*, RNAi has been used to evaluate potential drug targets (6) or to investigate mechanisms of drug action and drug resistance by screening for new molecules that modulate the response of tumor-derived cell lines to a given chemotherapeutic agent (7-10).

Here, we evaluate the suitability of combining mouse models and RNAi to identify genetic modifiers of drug action in tumors in their natural site. Initially, we

chose to investigate resistance to doxorubicin in the *E*μ-*Myc* mouse lymphoma system. Doxorubicin (Adriamycin) is an anthracycline DNA-damaging agent that exerts its effects primarily by targeting of the topoisomerase 2 activity and DNA intercalation (11). Along with etoposide and the camptothecin derivatives, doxorubicin is one of several topoisomerase-targeted drugs currently used as front-line therapies for a wide variety of cancers. Here, we demonstrate that the *E*μ-*Myc* system can successfully identify crucial mediators of the response to topoisomerase poisons. These genes validate for relevance *in vivo*, suggesting strategies for improved clinical use of these drugs.

2.3 Results

2.3.1 RNAi screens identify shRNAs mediating doxorubicin resistance

Because *in vivo* studies of drug sensitivity and resistance require stable gene knockdown, we performed our initial *in vitro* screens using retrovirally encoded shRNAs based on the MiR-30 microRNA (12). Importantly, these shRNAs can stably and efficiently knockdown target genes when expressed at single copy in the genome (13). We chose to survey shRNAs targeting the "cancer 1000," a set of known or putative cancer-relevant genes compiled by manual curation, microarray expression data, and literature mining (14). To improve gene knockdown and facilitate *in vivo* experiments (13), all of the existing murine shRNAs targeting the cancer 1000 set (≈2,300 shRNAs, two to three shRNAs per gene) were cloned into a murine stem cell virus (MSCV)-based vector that coexpressed green fluorescent protein.

Our initial screen for shRNAs capable of conferring doxorubicin resistance used Eμ-*Myc; p19* $^{arf-/-}$ lymphoma cells, which retain the *p53* tumor suppressor and an intact DNA damage response (15, 16). Pools of ~50 shRNAs were introduced into lymphoma cells by retroviral transduction, and infected cultures were treated with doxorubicin at doses that typically would kill 70–95% of cells in 24 h. Standard DNA sequencing of amplified provirus shRNAs was used to identify constituent shRNAs and to determine their relative representation in the treated and untreated cell populations. Deconvolution of enriched shRNA pools was prioritized based on whether a given pool exhibited drug-induced GFP

enrichment (indicating that at least one shRNA in that pool was itself being enriched; Figure 1). Indeed several pools showed enrichment of GFP+ cells in response to doxorubicin and were subsequently found to contain over-represented shRNAs, namely shp53, shTop2A, and shChk2 (Figure 2).

In a complementary experiment, the entire 'Cancer 1000' library was subjected to repeated rounds of doxorubicin selection in what can be described as a 'serial enrichment' screening approach (Figure 3A). Initially, the percentage of GFP+ cells remained unchanged before and after doxorubicin treatment (Figure 3B, left). However, by the third round of exposure to doxorubicin, lymphoma cells infected with the twice-selected library exhibited a robust enrichment of GFP. This suggested that library [pool] complexity was sufficiently reduced such that at least one shRNA was promoting resistance to drug (Figure 3B, right). Interestingly, and in support of the initial small pool-based screen, shRNAs targeting *p53*, *Chk2*, and *Top2A* were identified as being enriched upon doxorubicin treatment. Of these, shTop2A comprised the majority of the enriched library by the third round of selection – to the extent that its enrichment profile mirrored that of shTop2A alone in a short term GFP enrichment assay (Figure 3C).

To validate these collective screening results, we formally retested the major shRNA hits in our GFP-competition assay. Indeed, shRNAs targeting *p53*, *Chk2*, and *Top2A* successfully validated in this context as they were all dramatically enriched in cell populations within 24 h after doxorubicin treatment

(Figure 4A). Additionally, these shRNAs effectively suppressed expression of their intended target (Figure 4B).

p53 and *Chk2* are key components of DNA damage response pathways and, indeed, *p53* loss confers resistance to doxorubicin in the *E*μ-*Myc* transgenic model (13, 17). Importantly, multiple shRNAs targeting *Chk2* promoted doxorubicin resistance, suggesting that the effects of these shRNAs were "on target" (i.e. specifically due to *Chk2* gene knockdown). Although *Chk2* can sensitize cells to DNA-damaging agents in some contexts (18, 19), our results are consistent with a role for Chk2 in signaling p53-dependent apoptosis in lymphoid cells (17, 20). These results suggest we can identify relevant mediators of drug resistance using pool-based RNAi screening approaches.

2.3.2 *Top2A* shRNAs cause resistance specifically to topoisomerase 2 poisons.

shRNAs targeting Topoisomerase 2α (*Top2A*) were the most frequently recovered shRNAs from doxorubicin-treated cells, with at least two independent shRNAs isolated per screen. *Top2A* is a target of the drug doxorubicin (11) and is an essential gene in mammals (21). Unlike typical enzyme inhibitors where knockdown of the drug target would be expected to mimic drug action and promote cell death, doxorubicin is a topoisomerase poison that stabilizes the cleavable complex consisting of double-stranded DNA breaks to which the

enzyme is covalently attached. Doxorubicin therefore causes excessive double-stranded DNA breaks via unresolved cleavable complexes in a topoisomerase-dependent manner, thereby explaining how *Top2A* down-regulation might confer doxorubicin resistance (22).

Although previous work has suggested a relationship between *Top2A* levels and doxorubicin sensitivity (23), the effect has not been studied extensively or validated *in vivo*. The effects of *Top2A* knockdown were specific to topoisomerase 2 poisons: shTop2A caused resistance to another, structurally unrelated TOP2A poison, etoposide, but not to the alkylating agent maphosphamide (an active metabolite of cyclophosphamide) nor the topoisomerase 1 poison camptothecin (Figure 5A). In contrast, an shRNA targeting *p53* caused cross-resistance to these different agents (Figure 5B). The drug response-modifying effects of *Top2A* knockdown were likely "on target": four of four *Top2A* shRNAs mediated resistance specifically to topoisomerase 2 poisons (Figure 5C and Supplemental Figure S2). As expected, cells with reduced TOP2A levels displayed a diminished DNA damage signal and response, as shown by lower γ-H2AX signal, less p53 stabilization, and less apoptosis upon doxorubicin treatment (Figure 5D and Supplemental Figure S1). Accordingly, the ability of *Top2A* shRNAs to promote doxorubicin resistance was attenuated in *p53*-null *Eμ-Myc* lymphoma cells (Supplemental Figure S2), although clearly some signals downstream of chemotherapy-induced DNA damage are p53-independent (24).

2.3.3 *Top2A* shRNAs confer resistance to doxorubicin *in vivo*.

To test the role of *Top2A* in doxorubicin resistance *in vivo*, *E*μ-*Myc;p19*$^{Arf\ -/-}$ lymphoma cells were infected *in vitro* with shTop2A or a control vector and transplanted via tail vein injection into multiple syngeneic recipient mice. Tumor-bearing recipient mice were then treated with the maximum tolerated dose of doxorubicin. *Top2A* knockdown caused doxorubicin resistance *in vivo* as measured by an *in vivo* competition assay (an increase in the percentage of GFP-positive cells after drug treatment; Figure 6A) and reduced tumor-free (Figure 6B) and overall survival (data not shown). These results demonstrate that reduced *Top2A* expression is a bona fide mechanism of drug resistance *in vivo*.

2.3.4 *Top1* shRNAs confer resistance to topoisomerase 1 poisons *in vitro* and *in vivo*.

TOP2A is not the only topoisomerase targeted by front-line anticancer therapeutics. Topoisomerase 1 (TOP1) is the target of camptothecin (25, 26) and its derivatives irinotecan (Camptosar/CPT-11) and topotecan (Hycamtin). *TOP1*-deficient yeast are viable and resistant to camptothecin (27), but complete knockout of *Top1*, like *Top2A*, is lethal in mammals (28). Prompted by our studies on doxorubicin and *Top2A*, we tested whether *Top1* knockdown could induce camptothecin resistance in cancer cells. Indeed, *Top1* knockdown in *E*μ-

Myc;p19$^{Arf\,-/-}$ lymphomas caused resistance specifically to camptothecin (Figure 7A), and the effects were reproducible by using multiple independent *Top1* shRNAs (Figure 7B). Even modest *Top1* knockdown achieved this cytoprotective effect (Figure 7C).p53 induction was compromised in shTop1-expressing lymphoma cells treated with camptothecin, suggesting that these cells mounted a weaker DNA damage response (Figure 7C).

Accordingly, resistance was also attenuated in an *Eμ-Myc;p53* $^{-/-}$ background (Supplemental Figure S3). Mice harboring shTop1-expressing lymphomas displayed a reduced tumor-free survival compared with controls after treatment with irinotecan, indicating that reduced *Top1* expression promotes resistance to topoisomerase 1 poisons *in vivo* (Figure 7D). Therefore, sufficient expression of *Top2A* or *Top1* is required to achieve a potent response to chemotherapeutic agents targeting each particular topoisomerase.

2.3.5 *Top1* shRNAs enhance sensitivity to topoisomerase 2 poisons.

The drug resistance phenotypes conferred by *Top1* shRNAs were specific for topoisomerase 1 poisons. For example, *Top1* knockdown had little effect on tumor cell sensitivity to the alkylating agent maphosphamide (Figure 7A). Unexpectedly, *Top1* knockdown hypersensitized cells to the topoisomerase 2 poisons doxorubicin and etoposide (Figure 7A). Furthermore, mice harboring transplanted lymphomas expressing *Top1* shRNAs showed an improved tumor-

free survival compared with controls after irinotecan treatment (Figure 8A). Therefore, in this tumor model, suppression of *Top1* synergizes with topoisomerase 2 poisoning by chemotherapeutic agents.

2.3.6 Spontaneous changes in topoisomerase levels accompany relapse after doxorubicin therapy.

To examine the relevance of topoisomerase status to resistance mechanisms spontaneously occurring in treated lymphomas, primary tumors and post-doxorubicin treatment relapses from Figure 8A were analyzed for *Top1* and *Top2A* expression levels (Figure 8B). The relevance of *Top2A* levels to the emergence of tumor relapses was supported by the fact that half of the relapsed tumors displayed dramatically reduced *Top2A* levels (one of two control tumors and two of four shTop1-expressing tumors) without experimental manipulation via *Top2A* shRNAs. As further evidence that *Top1* knockdown can sensitize to the topoisomerase 2 poison doxorubicin, one shTop1 relapse (relapse 3) recovered expression of *Top1* to approximately wild-type levels. Relapsed tumors treated *ex vivo* showed resistance to doxorubicin, but not cisplatin, suggesting that the resistance mechanisms were topoisomerase-specific (Supplemental Figure S4). Together, these results indicate that although alterations in topoisomerase expression levels represent one of undoubtedly many therapy resistance mechanisms, these changes can play a substantial role in chemotherapy response *in vivo*.

2.4 Discussion

In this study we document the utility of combining RNAi screens with mouse cancer models to identify and characterize molecular determinants of therapeutic response that are relevant to treatment outcome *in vivo*. This approach is ideal for rapid *in vivo* validation of candidate genes and may serve as a relevant setting for conducting *in vivo* RNAi-based screens for genetic determinants of drug resistance. Such methodology is easily extendable to other chemotherapeutics and tumor systems to allow a more global view of therapy response mediators, including their context-dependence across different tumor and host genotypes.

The mechanism whereby *Top1* and *Top2A* down-regulation produces resistance to their respective poisons is probably due to a reduction in topoisomerase–DNA cleavage complexes, resulting in less DNA damage (see Figure 5D and 7C; ref. (29)). By contrast, the mechanism whereby *Top1* down-regulation hypersensitizes to topoisomerase 2 poisons remains to be precisely determined. However, this effect is not simply due to a compensatory up-regulation of *Top2A* because *Top2A* levels did not increase in response to *Top1* knockdown in our system (Figure 5D and 7C). Studies in yeast suggest that an overall amount of topoisomerase activity may be required for cell viability because topoisomerase I/II double mutants exhibit more serious defects in DNA unwinding, chromatin structure, and cell cycle progression compared with either single mutant (30, 31). If so, therapeutic poisoning of *Top2A* with simultaneous

down-regulation of *Top1* could cause cellular topoisomerase activity to fall below this crucial threshold, triggering cell death.

The relative importance of various mechanisms to clinical drug resistance is an area of active debate. In some settings efflux pump overexpression may predominate (32), whereas in other settings, blocked apoptosis or senescence may be largely responsible for resistance (15, 33). Our studies using RNAi *in vivo*, together with our observation that relapsed tumors frequently display altered topoisomerase levels compared with the parental tumor, suggest that topoisomerase expression levels are relevant determinants of therapeutic response. In fact, *TOP2A* amplification [linked to the *ERBB2* locus and thus common in human breast cancer (34)] predicts a favorable response to anthracycline therapy (35). Surprisingly, hemizygous deletion of *TOP2A* is also common in breast cancer (36), and our results suggest that patients with such deletions in *TOP2A* may be less responsive to doxorubicin therapy, a possibility that is readily testable.

Similarly, TOP1 levels may also influence the response to topoisomerase poisons and thus serve as a useful biomarker to guide the use of these agents in the clinic. The *TOP1* gene is located on chromosome 20q12, a locus that is often amplified in colon carcinoma (37). The enhanced sensitivity to these drugs predicted to arise from higher TOP1 levels may explain, in part, why topoisomerase 1 poisons are a mainstay therapy for this disease. Although more detailed functional and clinical studies remain to be performed, our results

highlight the potential of combining RNAi and *in vivo* mouse models to identify potential therapeutic targets as well as biomarkers for predicting treatment response.

2.5 Materials and Methods

2.5.1 Short Hairpin RNA Vectors

A MiR-30-based shRNA library (12) targeting the cancer 1000 gene set (≈2,300 shRNAs) was subcloned into LTR-driven MiR30 Puro-IRES-GFP (LMP) and LTR-driven MiR30 SV40-GFP (LMS) (MSCV-based vectors) (13) in pools of 96 or 48 shRNAs, respectively. Individual shRNA constructs were generated as described previously. Targeting sequences were selected based on RNAi Codex algorithms (12) or BIOPREDsi design (38) and are available upon request.

2.5.2 RNAi Screens

Lymphoma cells were cultured and infected as described previously. *E*μ-*Myc;Arf* $^{-/-}$ lymphoma cells, 2 days after infection with shRNA libraries (infected to ≈30%), were treated for 24 h with 7.8 ng/ml and 15.6 ng/ml doxorubicin for lenient and stringent selection conditions, respectively. Ninety percent of the culture was removed and replaced with fresh B cell medium on day 2 and day 5 after infection to allow recovery and proliferation of surviving cells. Final samples were taken on day 8 for GFP competition assay/shRNA representation determination. Pool-by-pool screens were performed in a 12-well format by using ≈500,000 cells per experimental condition. Serial enrichment screening was performed by infecting 1×10^7 cells with the entire cancer 1000 shRNA library to a final infection rate of ≈20%. Unsorted populations of infected cells were treated for 24 h with 7.8 ng/ml doxorubicin and then surviving cells were allowed to

regrow for 4 days in fresh medium. shRNAs from GFP-sorted surviving cells were recloned into the LMS parent vector and used to infect naïve lymphoma cells. This process was repeated until GFP enrichment was detectable acutely (at 24 h) after doxorubicin treatment. This occurred consistently after three rounds of treatment.

To identify constituent shRNAs, genomic shRNA integrants were PCR-amplified and subcloned into the LMP vector. Constituent shRNAs were identified by using the MSCV-specific 5′ primer, CCCTTGAACCTCCTCGTTCGACC.

2.5.3 Immunoblotting

Western blotting was performed as described in ref. (13). Proteins were detected by using the following antibodies: anti-p53 (clone 505, 1:500; Novacastra); anti-CHK2 (clone 151-176, in-house monoclonal, 1:100); anti-TOP1 (human scleroderma serum, 1:1,000; Topogen); anti-TOP2A (rabbit polyclonal, 1:1,000; Topogen); anti-γH2AX (monoclonal clone JBW301, 1:1000; Upstate/Millipore); and anti-tubulin (B5-1-2, 1:5,000; Sigma). Secondary antibodies were horseradish peroxidase-conjugated anti-mouse/rabbit/human IgG (GE Healthcare; 1:5,000). p53 was stabilized by using 31 ng/ml doxorubicin for 8 h (Figure 4B), 16 ng/ml doxorubicin for 8 h (Figure 5D), or 31 nM camptothecin for 8 h (Figure 7C).

2.5.4 Competition and Viability Assays

Two days after infection, lymphoma cells were split into replicate wells of ≈500,000 cells in 12-well plates. After 24-h treatments with a range of drug doses, the GFP-positive percentage was quantified in the surviving cell population by using a BD Biosciences LSRII flow cytometer. The live cell population was gated via a forward scatter (FSC) versus side scatter (SSC) plotting. For *in vivo* competition assays, lymphoma cells were infected *in vitro*, as described above. Lymphoma cells, GFP^+ FACS sorted or unsorted, as indicated, were tail vein-injected into syngeneic recipient mice. Upon tumor onset (day 0), mice were treated with doxorubicin (10 mg/kg intraperitoneal injection) or irinotecan (CPT-11, 50 mg/kg intraperitoneal injection, daily for 2 days) and monitored for overall survival and tumor-free survival. Isolation of lymphomas for the GFP competition assay was carried out as described (13, 33). For *in vitro* cell viability assays, lymphoma cells were treated in triplicate at the indicated doses of doxorubicin/camptothecin. Viability was determined after 24 h by an FSC versus SSC gate and plotted relative to untreated viability.

2.6 Figures

Figure 1

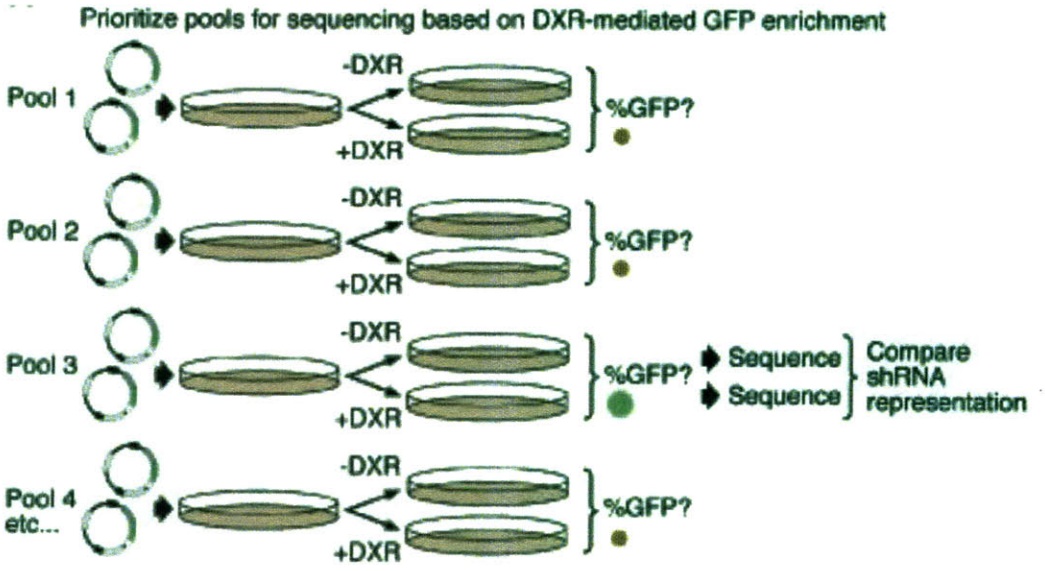

Figure 1 - Pool-based shRNA screening strategy
The 'Cancer 1000' shRNA library was subdivided into pools of ~50 shRNAs and partially infected into target lymphoma cells. All pools were then treated with doxorubicin (DXR) (8 and 16 ng/ml). Pools scoring for GFP enrichment in this GFP competition assay were prioritized for genomic PCR amplification of shRNA integrants, subcloning, and sequencing.

*** figure excerpted from published manuscript

Figure 2

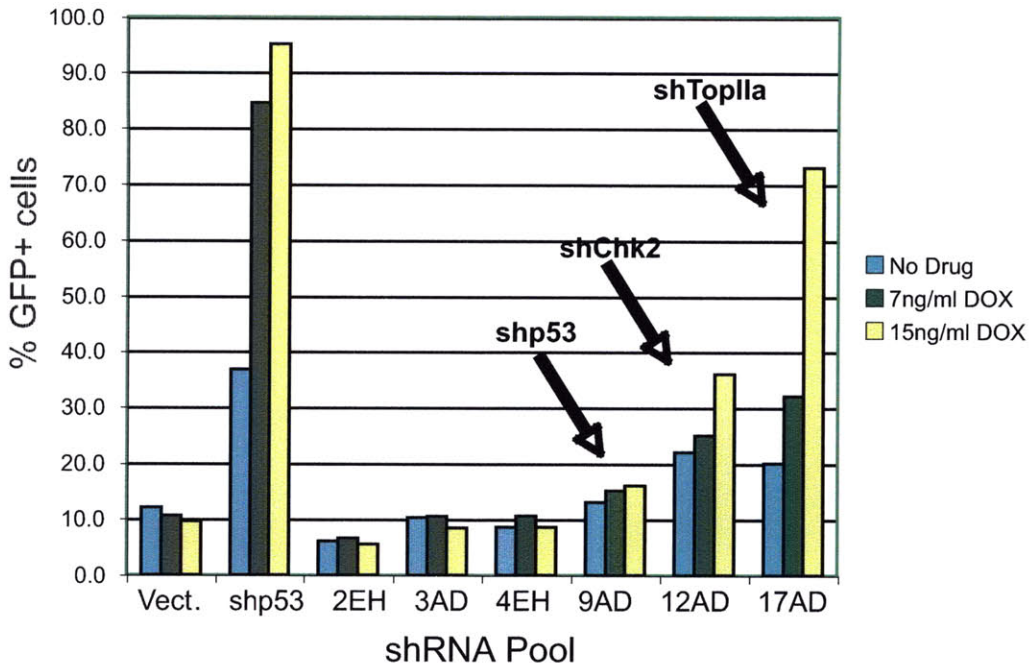

Figure 2- Representative raw data obtained from shRNA pool screen
Vector control, shp53 positive control, and selected shRNA pools (Cancer 1000, pools of 50 shRNAs) were subjected to a GFP-enrichment assay. Pools showing enrichment of GFP+ cells were subsequently sequenced to uncover the identity of the resistance-conferring shRNA(s). Sequence data obtained from pools 9AD, 12AD, and 17AD revealed an overrepresentation of shRNAs targeting p53, Chk2 and Top2A, respectively.

***Experiments performed by M.T.H and D.B.

Figure 3

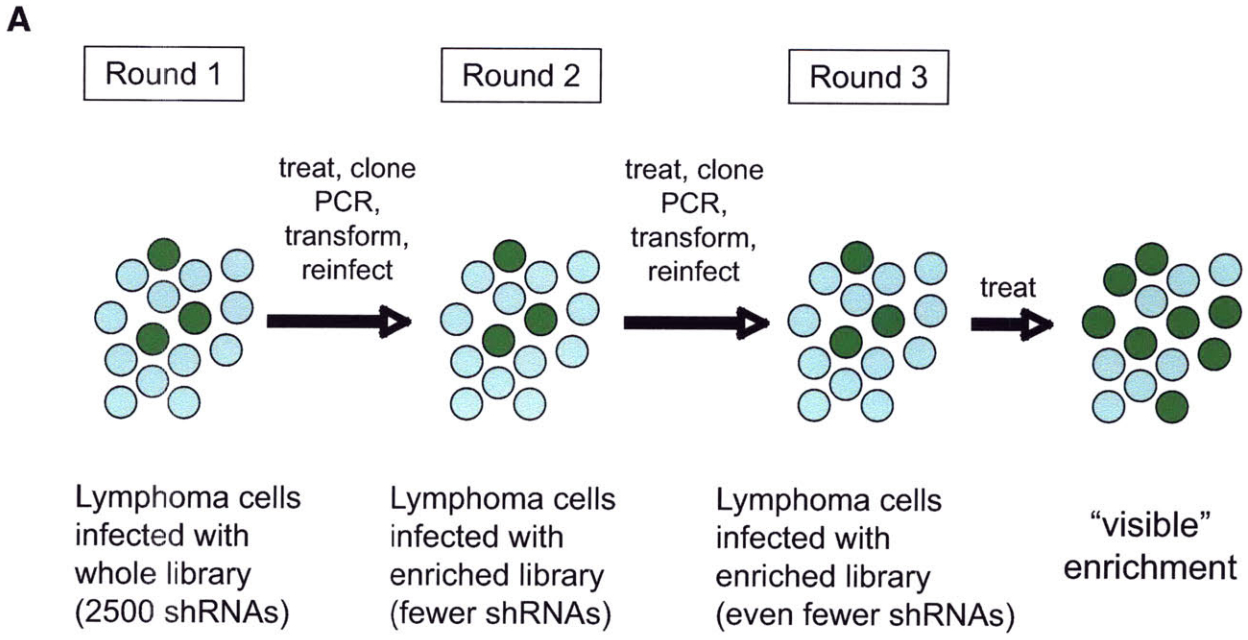
A
Round 1
Round 2
Round 3
treat, clone PCR, transform, reinfect
treat, clone PCR, transform, reinfect
treat
Lymphoma cells infected with whole library (2500 shRNAs)
Lymphoma cells infected with enriched library (fewer shRNAs)
Lymphoma cells infected with enriched library (even fewer shRNAs)
"visible" enrichment

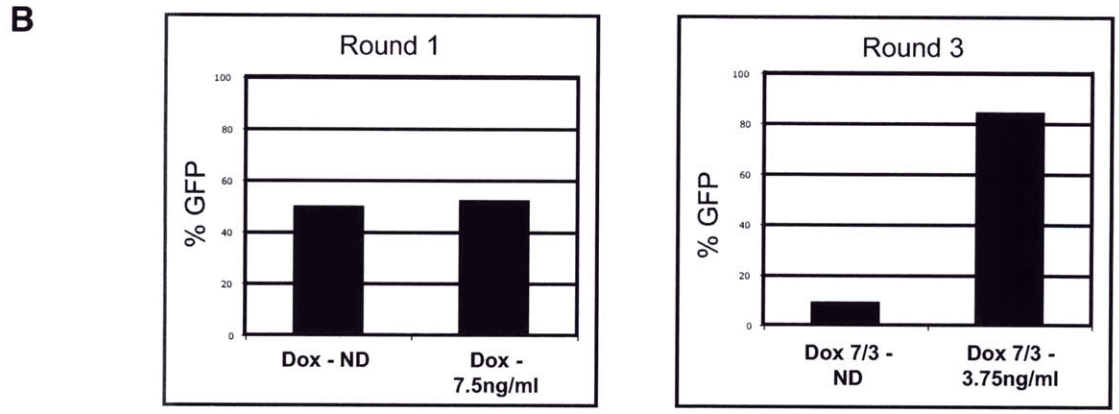
B
Round 1
% GFP
100
80
60
40
20
0
Dox - ND
Dox - 7.5ng/ml
Round 3
% GFP
Dox 7/3 - ND
Dox 7/3 - 3.75ng/ml

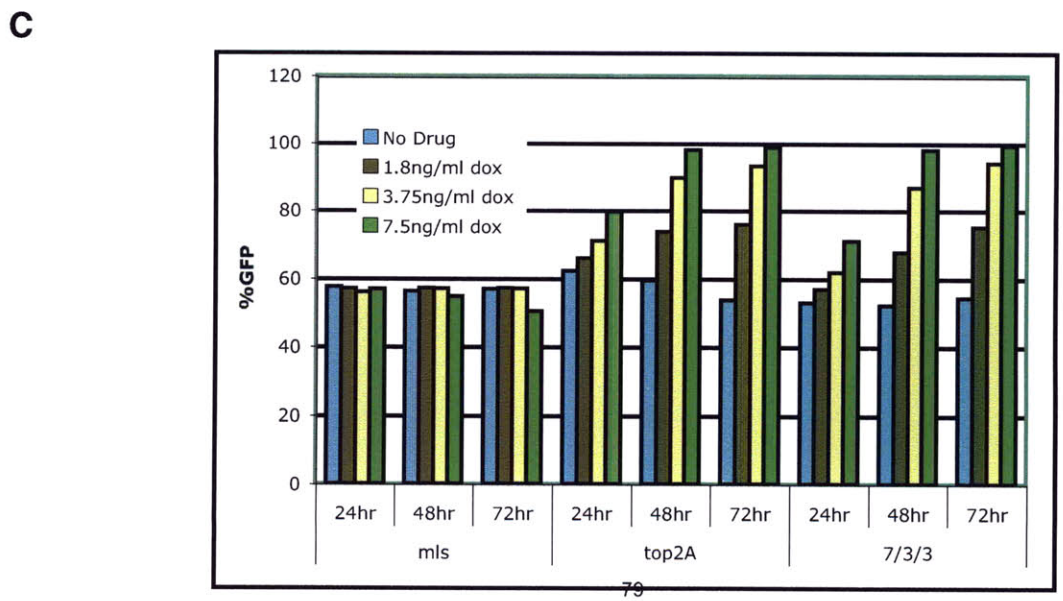
C
%GFP
120
100
80
60
40
20
0
No Drug
1.8ng/ml dox
3.75ng/ml dox
7.5ng/ml dox
24hr
48hr
72hr
mls
top2A
7/3/3

Figure 3- Serial enrichment of the 'Cancer 1000' shRNA library identifies Top2A, p53 and Chk2 as key mediators of doxorubicin response.
(A) Serial enrichment strategy. Multiple rounds of shRNA selection by treatment, bulk PCR amplification and recloning were performed until visible GFP enrichment of the selected shRNA library was achieved. (B) Graphs showing the percent of GFP+ cells before and after treatment during the first (left) and third rounds (right) of doxorubicin treatment. (C) A graph showing GFP percentages of acutely (48h) treated lymphoma cells infected with either shTop2A, the selected (three rounds) shRNA library, or a vector control.

Figure 4

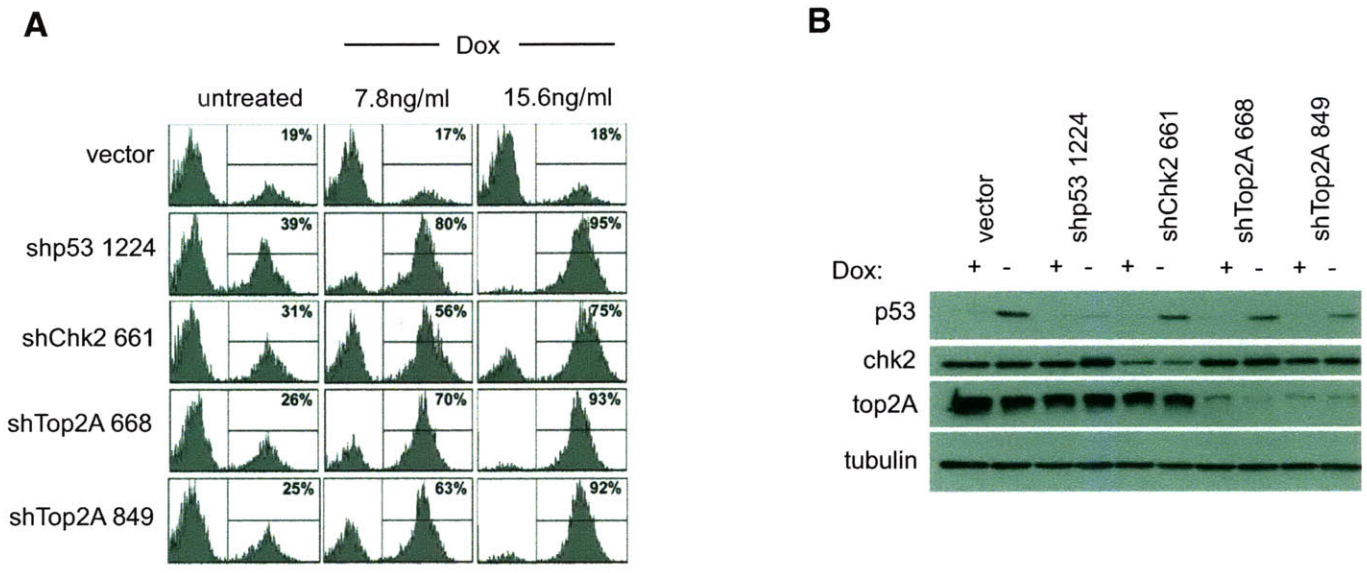

Figure 4- Validation of screening hits.
(A) GFP competition assay data from lymphoma cells infected with the indicated shRNA 'hits' either untreated or 24 h after doxorubicin (Dox) treatment at the indicated doses. (C) Immunoblotting of lysates from lymphoma cells transduced with shRNAs targeting p53, Chk2, and Top2A either untreated or treated for 8 h with 31 ng/ml doxorubicin to stabilize p53. Tubulin serves as a loading control.

***Experiments performed by M.T.H and D.B. Figure excerpted from published manuscript.

Figure 5

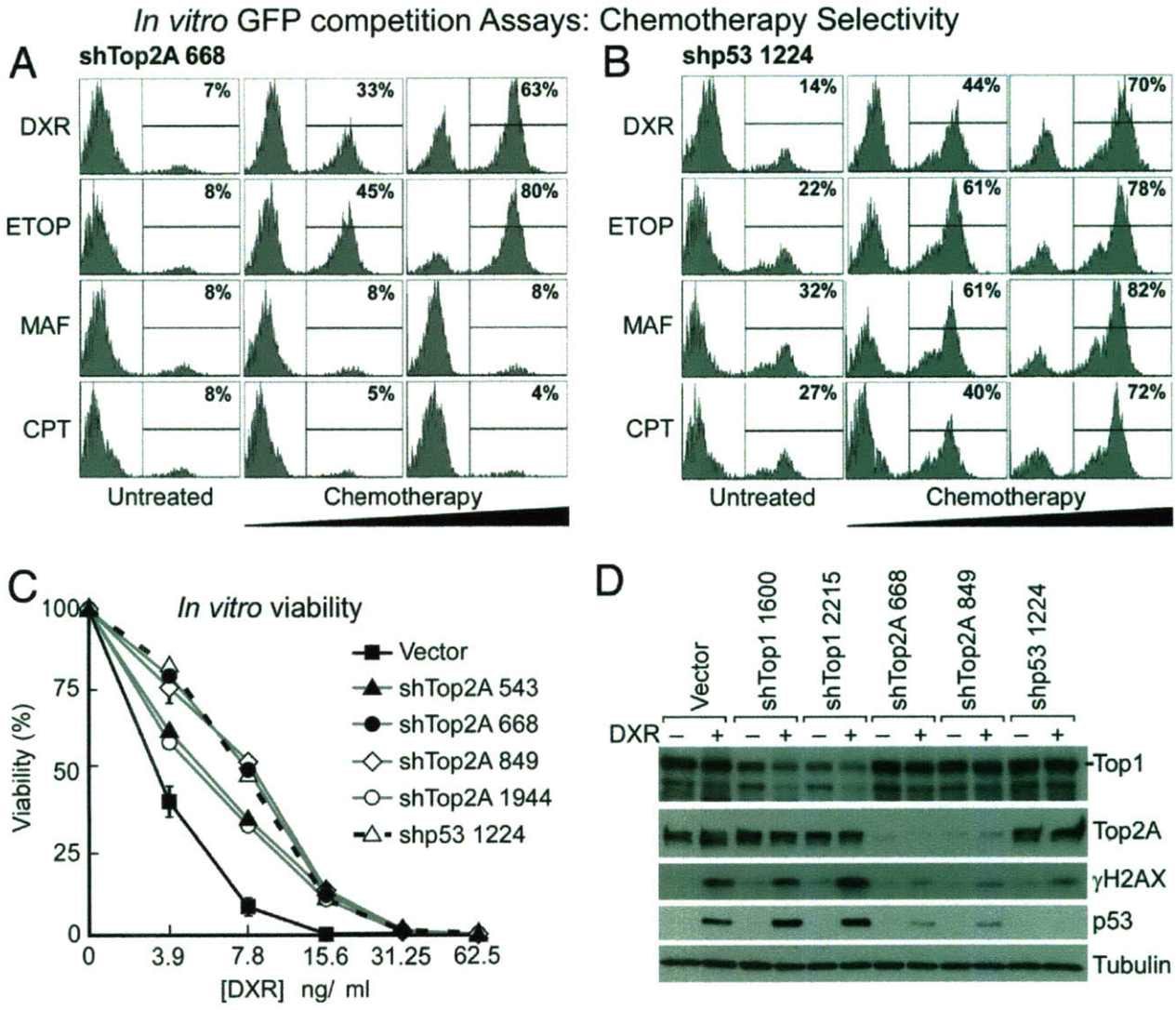

Figure 5 - Suppression of Top2A expression causes resistance to topoisomerase 2 poisons in vitro.

(A and B) Flow cytometric analyses of lymphoma cells expressing shTop2A 668 (A) or shp53 1224 (B) after 24 h of the indicated drug treatments. DXR, doxorubicin; ETOP, etoposide; MAF, maphosphamide; CPT, camptothecin. (C) Lymphoma cells, transduced singly with four independent Top2A shRNAs, were puromycin-selected and treated with doxorubicin for 24 h at the indicated doses. Viability was assayed by flow cytometry (FSC versus SSC) and plotted relative to untreated controls. Error bars are SEM from three replicates. (D) Immunoblotting of lymphoma cell lysates expressing no short hairpin (Vector) or Top1, Top2A, or p53 shRNAs in the presence or absence of doxorubicin (DXR; 15.6 ng/ml for 8 h).

***Experiments performed by D.B. and M.T.H. Figure excerpted from published manuscript.

Figure 6

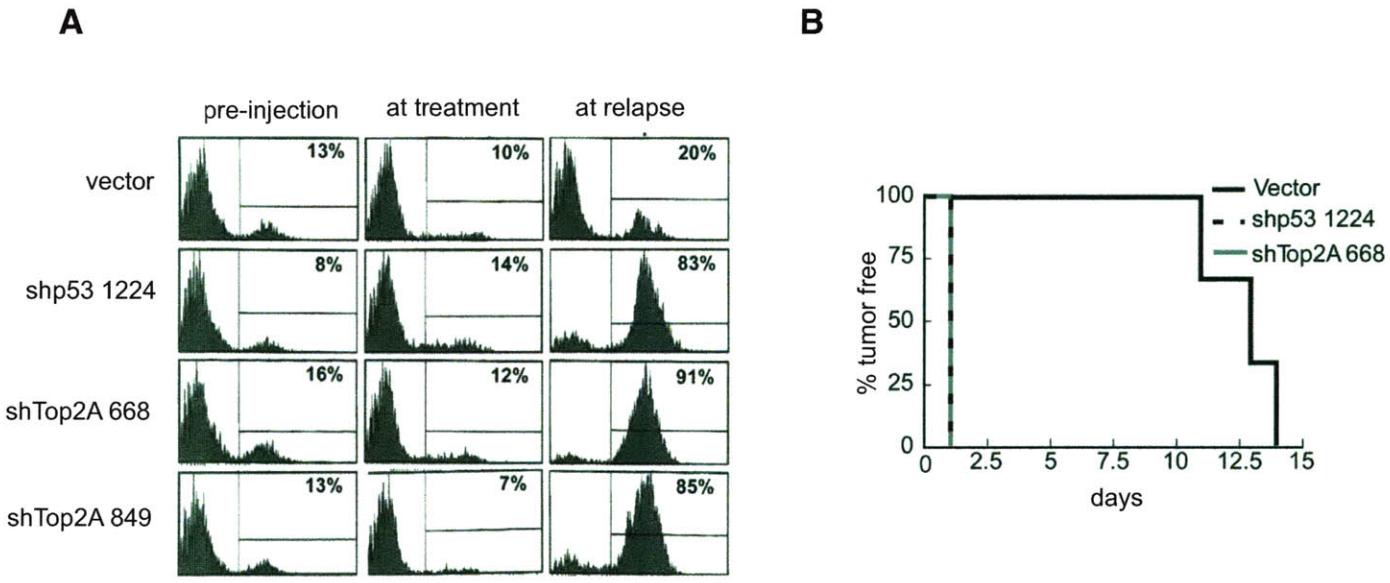

Figure 6- Top2A knockdown causes doxorubicin resistance in vivo.
(A) GFP flow cytometry plots. Lymphoma cells were infected in vitro with GFP-tagged shTop2A 668 or 849, shp53, or vector control constructs (A Left). These cells were injected into the tail vein of syngeneic recipient mice (five mice per cohort) and were monitored daily for tumors by palpation. Upon tumor onset (day 0), one mouse from each cohort was killed, and lymphoma cells were assayed for percentage GFP+ (A Middle). The remaining mice were treated with doxorubicin (10 mg/kg i.p. injection), and tumors were harvested upon relapse and assayed for percentage GFP (A Right). (B) Kaplan–Meier tumor-free survival curves. Vector, shTop2A, and shp53 tumors were FACS-sorted to 100% GFP+ before injection into recipient mice and DXR-treated as in (A) at day 0.

***Original experiments performed by M.T.H and D.B. I assisted in confirmatory replicate experiments. Figure excerpted from published manuscript.

Figure 7

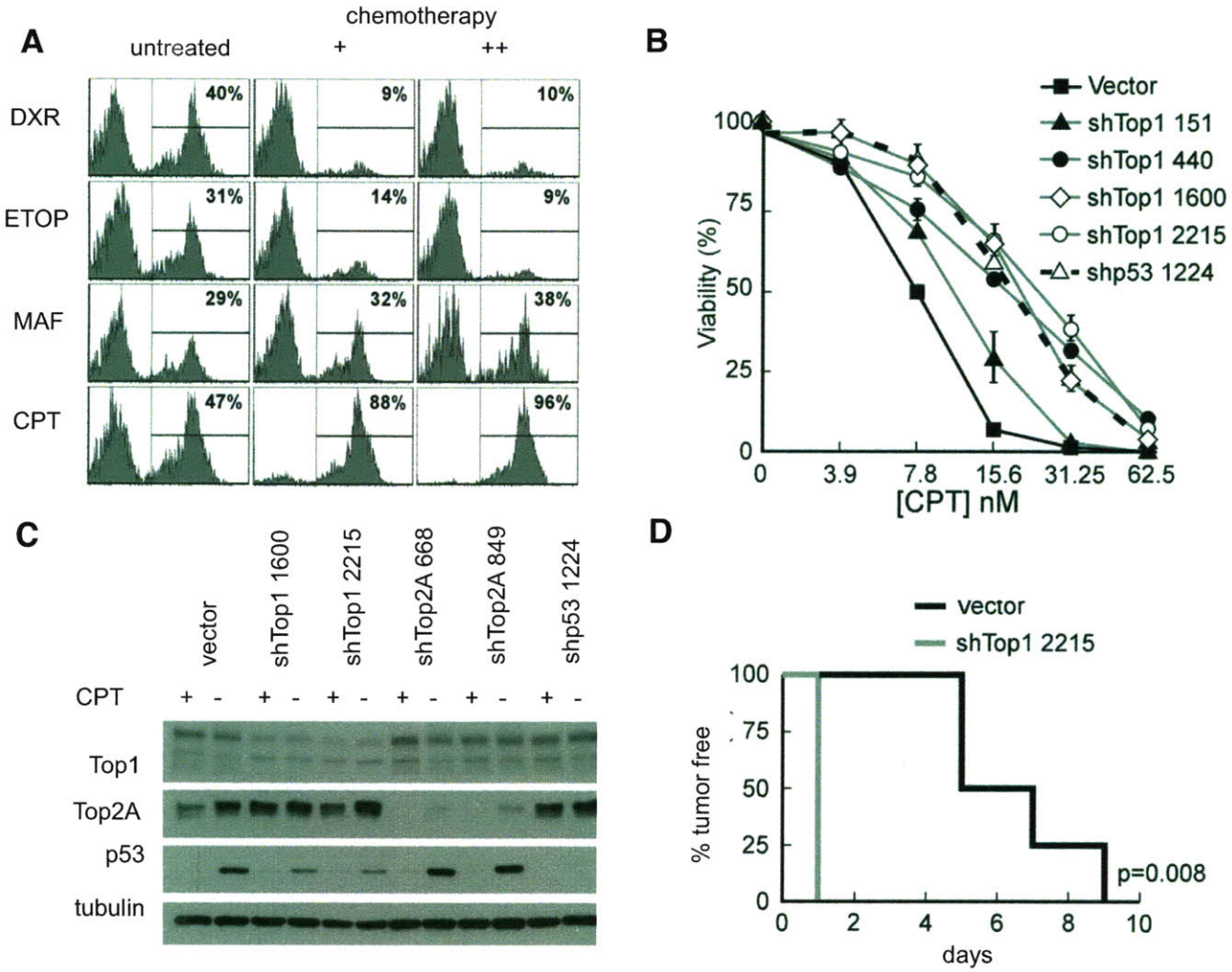

Figure 7- Top1 knockdown causes camptothecin resistance in vitro and in vivo
(A) Top1 knockdown causes resistance to camptothecin but hypersensitizes to the topoisomerase 2 poisons, doxorubicin and etoposide, as shown by a GFP competition assay 24 h after drug treatment. (B) In vitro viability assays of puromycin-selected (shRNA-containing) cells for four independent shRNAs targeting Top1, after 24-h camptothecin treatment. Error bars are ±SEM from three replicates. (C) Immunoblotting of Eμ-Myc;Arf-/- lymphoma cell lysates with or without camptothecin (31 nM CPT, 8 h). (D) Kaplan–Meier survival curve. Eμ-Myc;Arf-/- lymphomas were infected in vitro with vector control or shTop1 2215 and were FACS-sorted to 100% GFP+ before injection into recipient mice. Upon lymphoma onset (day 0) mice were treated with irinotecan (CPT-11), a clinically relevant camptothecin derivative (50 mg/kg intraperitoneal injection daily for 2 days) and monitored for survival.

***Original experiments performed by M.T.H and D.B. I assisted with the in vivo Top1 experiments. Figure excerpted from published manuscript.

Figure 8

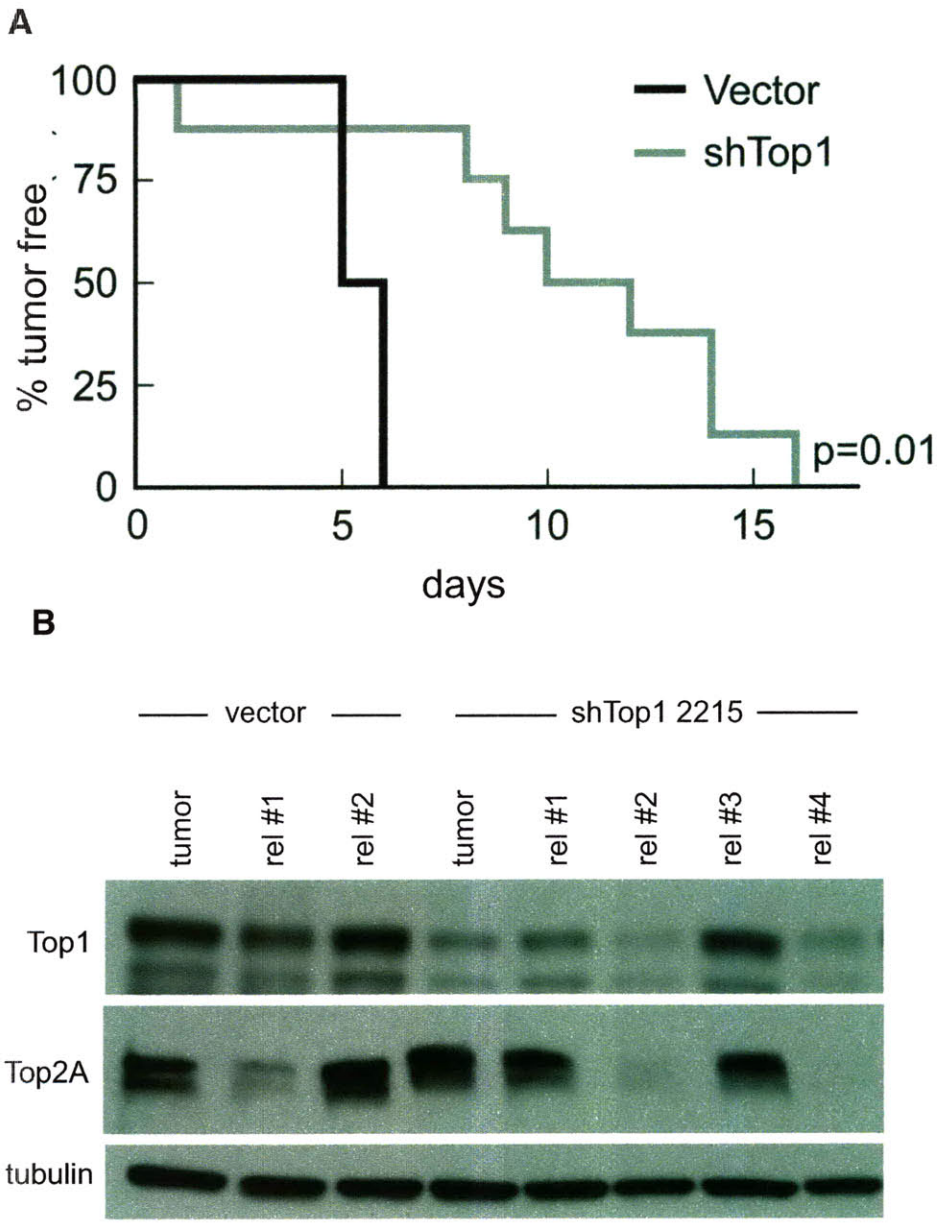

Figure 8- Top1 knockdown can sensitize to doxorubicin treatment in vivo.
(A) Top1 knockdown sensitizes Eμ-Myc;Arf-/- lymphomas to doxorubicin in vivo, as shown by an increased in vivo tumor-free survival after doxorubicin treatment (10 mg/kg, day 0). shTop1 data are pooled from four shTop1 1600 and four shTop1 2215 mice. (B) Predicted changes in topoisomerase expression levels occur spontaneously during treatment failure in vivo. Immunoblotting analysis of untreated lymphomas and postdoxorubicin-treated relapses from A.

***Experiments performed by M.T.H and D.B. I assisted with the Top1/doxorubicin sensitization experiment. Figure excerpted from published manuscript.

Supplemental Figure S1

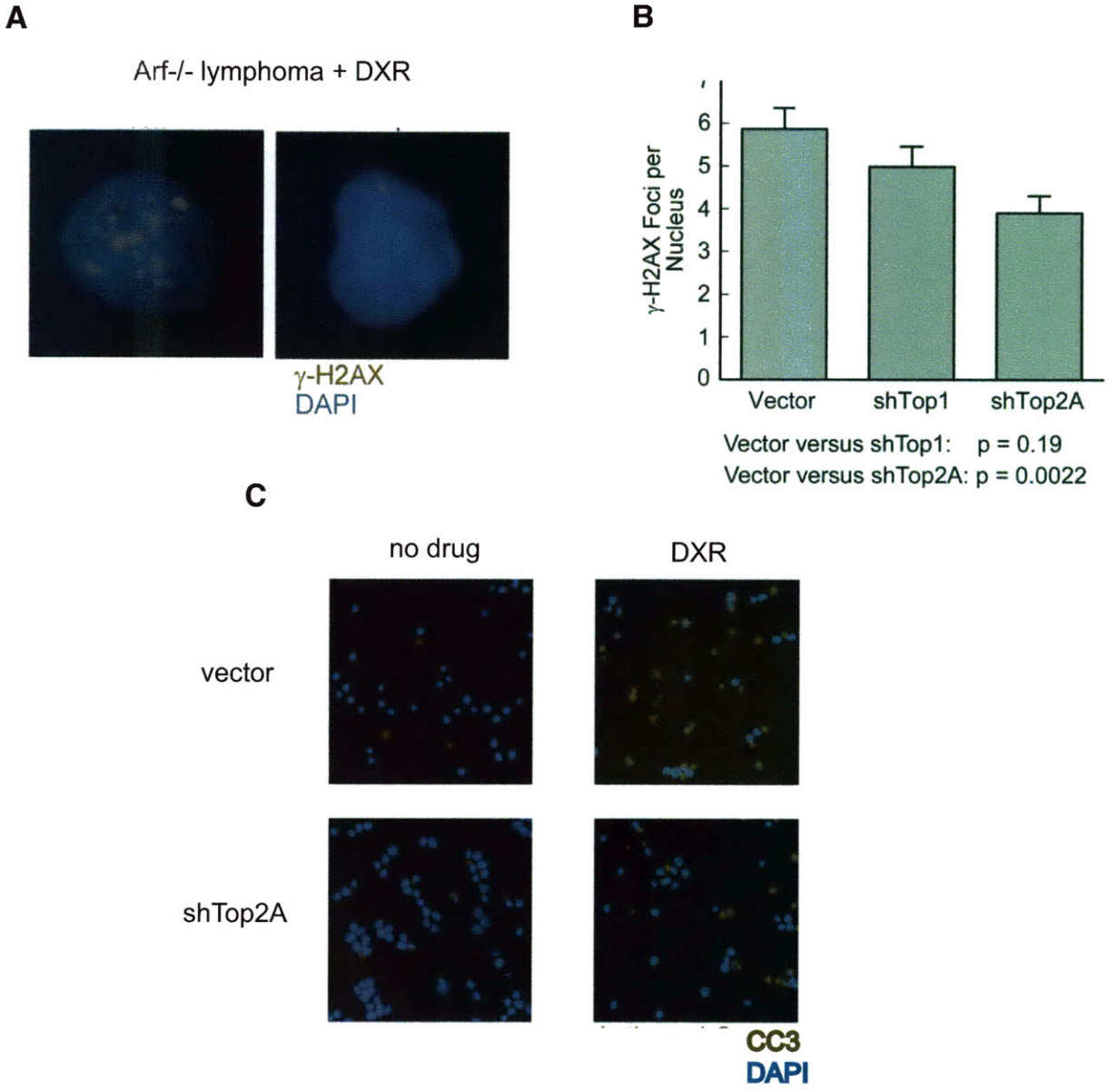

Supplemental Figure S1- Top2A knockdown results in diminished DNA damage and apoptosis upon doxorubicin treatment.
(A) Sample gamma-H2AX immunofluorescence images. (B) Quantitation of A. Mean gamma-H2AX foci per nucleus is plotted. Error bars represent SEM. Vector versus shTop2A 668 t test; P = 0.0022 (shTop1 2215 served as an additional control). (C) Activated caspase-3 immuno-fluorescence of cytospun Em-Myc;Arf/-/-lymphoma cells reveals an attenuation of doxorubicin-induced apoptosis in shTop2A cells compared with vector control cells.

***I assisted M.T.H with the H2AX experiments along with Holly Thompson. D.B. and M.T.H performed the CC3 immunostaining. Figure excerpted from published manuscript.

Supplemental Figure S2

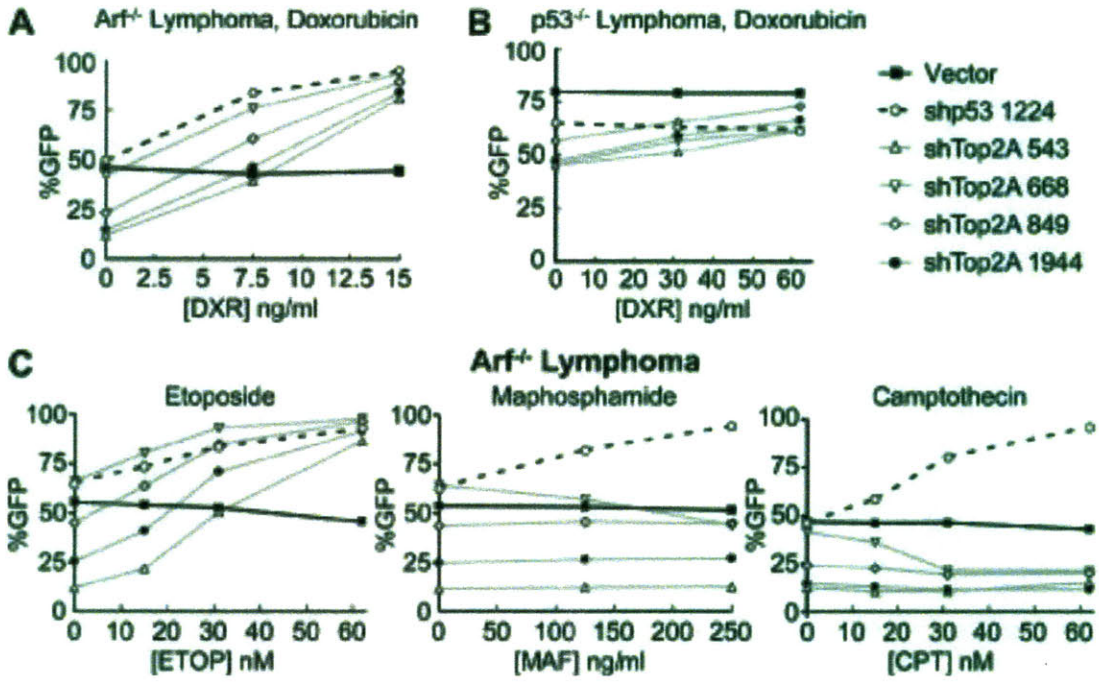

Supplemental Figure S2- Multiple Top2A shRNAs cause resistance specifically to topoisomerase 2 poisons.
(A) Top2A knockdown (via four independent Top2A shRNAs) causes doxorubicin resistance in Em-Myc;Arf-/- lymphoma cells in vitro, as shown by doxorubicin-mediated GFP enrichment in the GFP competition assay, 24 h after treatment. (B) shTop2A causes attenuated doxorubicin resistance in a p53-deficient background. GFP competition assay on Em-Myc;p53-/- lymphoma cells treated for 24 h at the indicated doxorubicin doses. (C) Top2A knockdown causes resistance specifically to topoisomerase 2 poisons. GFP competition assay in Arf-/- lymphoma cells, 24 h after treatment.

***Experiments performed by D.B. and M.T.H. Figure excerpted from published manuscript.

Supplemental Figure S3

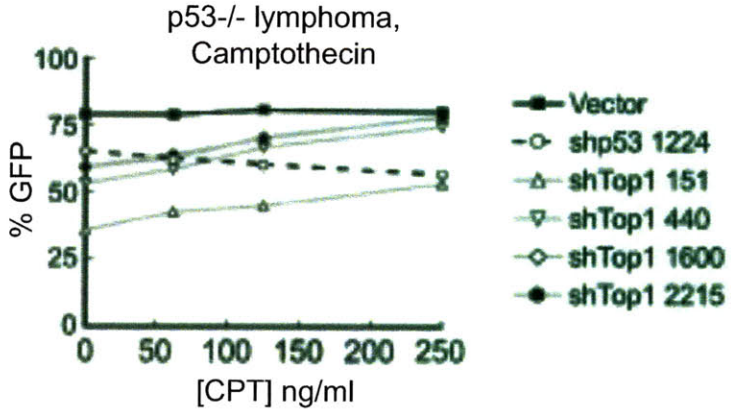

Supplemental Figure S3- shTop1 causes attenuated camptothecin resistance in Em-Myc;p53 -/- lymphoma cells as determined using a GFP competition assay 24 h after treatment.

***Experiment performed by D.B. and M.T.H. Figure excerpted from published manuscript.

Supplemental Figure S4

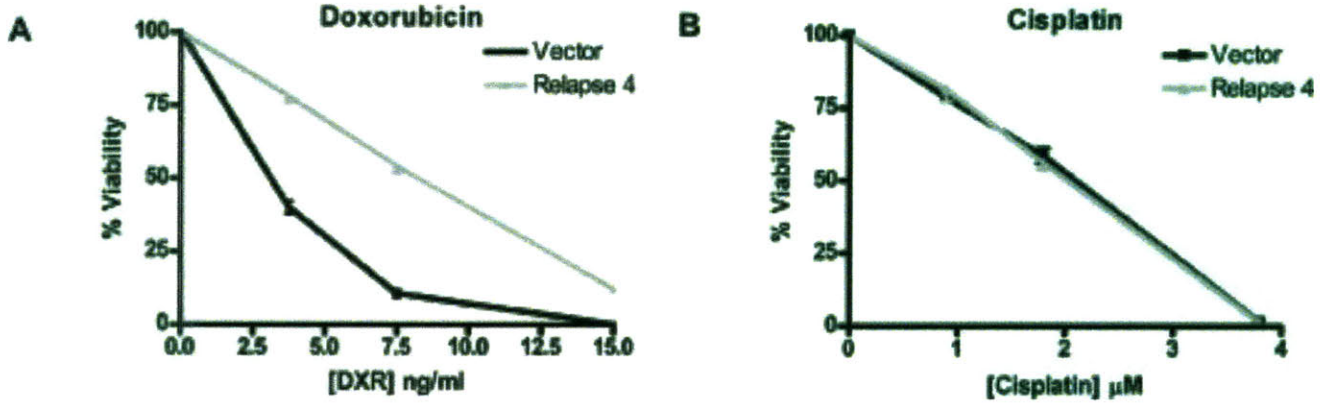

Supplemental Figure S4- Relapsed Top2A-down-regulated tumors failing doxorubicin treatment are not broadly drug-resistant.
Tumor cells from shTop1 2215 relapsed tumor no. 4 from Fig. 8 were treated ex vivo for 24 h with chemotherapy at the indicated doses. Viability, measured by propidium iodide exclusion flow cytometry, is plotted relative to untreated cells. The Top2A down-regulated relapse displays doxorubicin resistance (A) but not cross-resistance to cisplatin (B) compared to a control primary tumor. Together with the observation of striking Top2A down-regulation in relapsed tumors, these data suggest that the resistance mechanism is specific to topoisomerase 2 poisons rather than a general multidrug-resistant pump-based mechanism.

***Experiment performed by D.B. and M.T.H. Figure excerpted from published manuscript.

2.8 Acknowledgments

The authors thank Lidia Nascimento, Beth Miller, and Stephanie Muller (CSHL) for analysis of shRNA representation by DNA sequencing, Carmelita Bautista (CSHL) for Chk2 antibodies, Holly Thompson for H2AX analysis, and Luke Gilbert for help with sensitization studies. We thank Mona Spector for critical reading and editing of the manuscript and members of the Lowe and Hannon laboratories for helpful advice and discussions. D.J.B. is an Engelhorn Scholar of the Watson School of Biological Sciences (CSHL). W.X. is in the Molecular and Cellular Biology graduate program at Stony Brook University (Stony Brook, NY). This work was supported by Alan and Edith Seligson (to L.Z.), the V Foundation for Cancer Research (to M.T.H.), a Mouse Models of Human Cancer Consortium grant, a program project grant from the National Cancer Institute (to G.J.H. and S.W.L.), and the Don Monti Memorial Research Foundation.

2.9 References

1. Gros P, Ben Neriah YB, Croop JM, Housman DE. Isolation and expression of a complementary DNA that confers multidrug resistance. Nature 1986;323(6090):728-31.

2. Mao Y, Yu C, Hsieh TS, et al. Mutations of human topoisomerase II alpha affecting multidrug resistance and sensitivity. Biochemistry 1999;38(33):10793-800.

3. Shah NP, Nicoll JM, Nagar B, et al. Multiple BCR-ABL kinase domain mutations confer polyclonal resistance to the tyrosine kinase inhibitor imatinib (STI571) in chronic phase and blast crisis chronic myeloid leukemia. Cancer Cell 2002;2(2):117-25.

4. Lowe SW, Ruley HE, Jacks T, Housman DE. p53-dependent apoptosis modulates the cytotoxicity of anticancer agents. Cell 1993;74(6):957-67.

5. Hannon GJ. RNA interference. Nature 2002;418(6894):244-51.

6. Farmer H, McCabe N, Lord CJ, et al. Targeting the DNA repair defect in BRCA mutant cells as a therapeutic strategy. Nature 2005;434(7035):917-21.

7. Berns K, Horlings HM, Hennessy BT, et al. A functional genetic approach identifies the PI3K pathway as a major determinant of trastuzumab resistance in breast cancer. Cancer Cell 2007;12(4):395-402.

8. Brummelkamp TR, Fabius AW, Mullenders J, et al. An shRNA barcode screen provides insight into cancer cell vulnerability to MDM2 inhibitors. Nat Chem Biol 2006;2(4):202-6.

9. Iorns E, Lord CJ, Turner N, Ashworth A. Utilizing RNA interference to enhance cancer drug discovery. Nat Rev Drug Discov 2007;6(7):556-68.

10. Whitehurst AW, Bodemann BO, Cardenas J, et al. Synthetic lethal screen identification of chemosensitizer loci in cancer cells. Nature 2007;446(7137):815-9.

11. Fortune JM, Osheroff N. Topoisomerase II as a target for anticancer drugs: when enzymes stop being nice. Prog Nucleic Acid Res Mol Biol 2000;64:221-53.

12. Silva JM, Li MZ, Chang K, et al. Second-generation shRNA libraries covering the mouse and human genomes. Nat Genet 2005;37(11):1281-8.

13. Dickins RA, Hemann MT, Zilfou JT, et al. Probing tumor phenotypes using stable and regulated synthetic microRNA precursors. Nat Genet 2005;37(11):1289-95.

14. Witt AE, Hines LM, Collins NL, et al. Functional proteomics approach to investigate the biological activities of cDNAs implicated in breast cancer. J Proteome Res 2006;5(3):599-610.

15. Schmitt CA, Fridman JS, Yang M, et al. A senescence program controlled by p53 and p16INK4a contributes to the outcome of cancer therapy. Cell 2002;109(3):335-46.

16. Sherr CJ. The INK4a/ARF network in tumour suppression. Nat Rev Mol Cell Biol 2001;2(10):731-7.

17. Schmitt CA, McCurrach ME, de Stanchina E, Wallace-Brodeur RR, Lowe SW. INK4a/ARF mutations accelerate lymphomagenesis and promote chemoresistance by disabling p53. Genes Dev 1999;13(20):2670-7.

18. Mukhopadhyay UK, Senderowicz AM, Ferbeyre G. RNA silencing of checkpoint regulators sensitizes p53-defective prostate cancer cells to chemotherapy while sparing normal cells. Cancer Res 2005;65(7):2872-81.

19. Yu Q, Rose JH, Zhang H, Pommier Y. Antisense inhibition of Chk2/hCds1 expression attenuates DNA damage-induced S and G2 checkpoints and enhances apoptotic activity in HEK-293 cells. FEBS Lett 2001;505(1):7-12.

20. Hirao A, Cheung A, Duncan G, et al. Chk2 is a tumor suppressor that regulates apoptosis in both an ataxia telangiectasia mutated (ATM)-dependent and an ATM-independent manner. Mol Cell Biol 2002;22(18):6521-32.

21. Akimitsu N, Adachi N, Hirai H, et al. Enforced cytokinesis without complete nuclear division in embryonic cells depleting the activity of DNA topoisomerase IIalpha. Genes Cells 2003;8(4):393-402.

22. Wang JC. Cellular roles of DNA topoisomerases: a molecular perspective. Nat Rev Mol Cell Biol 2002;3(6):430-40.

23. Gudkov AV, Zelnick CR, Kazarov AR, et al. Isolation of genetic suppressor elements, inducing resistance to topoisomerase II-interactive cytotoxic drugs, from human topoisomerase II cDNA. Proc Natl Acad Sci U S A 1993;90(8):3231-5.

24. Strasser A, Harris AW, Jacks T, Cory S. DNA damage can induce apoptosis in proliferating lymphoid cells via p53-independent mechanisms inhibitable by Bcl-2. Cell 1994;79(2):329-39.

25. Hsiang YH, Hertzberg R, Hecht S, Liu LF. Camptothecin induces protein-linked DNA breaks via mammalian DNA topoisomerase I. J Biol Chem 1985;260(27):14873-8.

26. Hsiang YH, Liu LF. Identification of mammalian DNA topoisomerase I as an intracellular target of the anticancer drug camptothecin. Cancer Res 1988;48(7):1722-6.

27. Nojima K, Hochegger H, Saberi A, et al. Multiple repair pathways mediate tolerance to chemotherapeutic cross-linking agents in vertebrate cells. Cancer Res 2005;65(24):11704-11.

28. Morham SG, Kluckman KD, Voulomanos N, Smithies O. Targeted disruption of the mouse topoisomerase I gene by camptothecin selection. Mol Cell Biol 1996;16(12):6804-9.

29. Miao ZH, Rao VA, Agama K, Antony S, Kohn KW, Pommier Y. 4-nitroquinoline-1-oxide induces the formation of cellular topoisomerase I-DNA cleavage complexes. Cancer Res 2006;66(13):6540-5.

30. Trigueros S, Roca J. Failure to relax negative supercoiling of DNA is a primary cause of mitotic hyper-recombination in topoisomerase-deficient yeast cells. J Biol Chem 2002;277(40):37207-11.

31. Uemura T, Yanagida M. Isolation of type I and II DNA topoisomerase mutants from fission yeast: single and double mutants show different phenotypes in cell growth and chromatin organization. Embo J 1984;3(8):1737-44.

32. Rottenberg S, Nygren AO, Pajic M, et al. Selective induction of chemotherapy resistance of mammary tumors in a conditional mouse model for hereditary breast cancer. Proc Natl Acad Sci U S A 2007;104(29):12117-22.

33. Schmitt CA, Rosenthal CT, Lowe SW. Genetic analysis of chemoresistance in primary murine lymphomas. Nat Med 2000;6(9):1029-35.

34. Mano MS, Rosa DD, De Azambuja E, Ismael GF, Durbecq V. The 17q12-q21 amplicon: Her2 and topoisomerase-IIalpha and their importance to the biology of solid tumours. Cancer Treat Rev 2007;33(1):64-77.

35. Tanner M, Isola J, Wiklund T, et al. Topoisomerase IIalpha gene amplification predicts favorable treatment response to tailored and dose-escalated anthracycline-based adjuvant chemotherapy in HER-2/neu-amplified breast cancer: Scandinavian Breast Group Trial 9401. J Clin Oncol 2006;24(16):2428-36.

36. Jarvinen TA, Liu ET. Topoisomerase IIalpha gene (TOP2A) amplification and deletion in cancer--more common than anticipated. Cytopathology 2003;14(6):309-13.

37. Boonsong A, Marsh S, Rooney PH, Stevenson DA, Cassidy J, McLeod HL. Characterization of the topoisomerase I locus in human colorectal cancer. Cancer Genet Cytogenet 2000;121(1):56-60.

38. Huesken D, Lange J, Mickanin C, et al. Design of a genome-wide siRNA library using an artificial neural network. Nat Biotechnol 2005;23(8):995-1001.

Chapter 3

RNAi screening identifies Nek4 as a novel mediator of paclitaxel response[1]

3.1 Abstract

While microtubule poisons are commonly used for the treatment of diverse malignancies, relatively little is known about cellular factors that determine the relative efficacy of these drugs. Here, we identified the NIMA kinase, Nek4, in a genetic screen for mediators of the response to the front-line chemotherapeutic taxol. To identify the mechanism underlying taxol resistance in Nek4-deficient cells, we examined Nek4 function in mitosis and microtubule homeostasis. Notably, we found that Nek4 promotes microtubule outgrowth following transient depolymerization. Additionally, cells lacking Nek4 showed an impaired G2/M arrest following taxol treatment, as well as a decrease in mitotic-like asters, further suggesting a role for Nek4 in the regulation of microtubule synthesis. Interestingly, Nek4 suppression also *sensitized* cancer cells to vincristine, another microtubule poison with a distinct mechanism of action. Therefore, Nek4 deficiency may either antagonize or promote the effects of microtubule poisons, depending on whether an individual drug hyper- or hypo-stabilizes microtubule polymers. While this phenomenon has previously been documented for cells bearing specific tubulin mutations, these data provide yet another example of how an alteration promoting drug resistance in a particular tumor can

simultaneously enhance the efficacy of another, similar conventional chemotherapeutic. Of note, Nek4 is located in a commonly deleted genomic locus in non-small cell lung cancer. Consequently, these data also suggest a rationale for the selective use of particular microtubule poisons in specific lung cancer patients.

[1]Significant sections of this chapter have been published in:

Doles J, Hemann MT. Nek4 status differentially alters sensitivity to distinct microtubule poisons. *Cancer Res.* 2010 Feb 1;70(3):1033-41. Epub 2010 Jan 26. PMID: 20103636

3.2 Introduction

Microtubules are highly dynamic tubulin polymers crucial for the proper execution of numerous cellular processes. They play key roles in mitosis, promoting both mitotic spindle formation as well as the subsequent segregation of replicated DNA. Consequently, microtubules are an attractive anti-cancer target, as disruption of mitosis in highly proliferative cancer cells often results in cell death (1-5). Indeed, several classes of microtubule-disrupting drugs are currently used in clinical settings. Notably, the taxanes and the *vinca alkaloids* are front-line therapies in the treatment ovarian, breast, lung and certain hematopoietic malignancies. Unfortunately, acquired and intrinsic drug resistance significantly limits the efficacy of these agents (6-9).

One of the most widely studied mechanisms of tumor cell survival following chemotherapy is multi-drug resistance (MDR), a phenotype involving decreased drug accumulation resulting from increased drug efflux (10, 11). However, many tumors with inactive MDR still display resistance to microtubule poisons. Thus, multi-factorial or alternative mechanisms of resistance must exist. Indeed, a number of resistance-causing alterations at the drug-target interface have previously been described for tubulin, including genetic mutations, isotype selection, post-translational modification and altered regulation (12). Further, modifications in downstream signal transduction have also been suggested to contribute to microtubule-poison resistance (13-15). Still, major genetic factors

underlying the efficacy of microtubule-targeting drugs, as well as the rationale for using one microtubule poison versus another, remain unclear.

In an effort to better understand the genetic basis of chemotherapeutic response to specific microtubule drugs, we performed an *in vitro* RNAi-based screen for mediators of the response to taxol, a commonly used microtubule-stabilizing taxane. This screen identified Nek4, a gene with unknown function belonging to a family of mitotic kinases termed NIMA-related kinases. Functional studies involving Nek4 showed that it has a role in microtubule regulation and that altered expression of this protein not only affected chemotherapeutic response, but also conferred differential sensitivity to select microtubule-disrupting drugs. Interestingly, Nek4 is frequently deleted in lung cancer, and Nek4 levels in several human cell lines correlated with differential sensitivity to microtubule poisons.

3.3 Results

3.3.1 RNAi screen for modulators of taxol-induced cell death

We used cells from a well-established pre-clinical model of Burkitt's lymphoma, the *Eμ-myc* mouse, to screen a library of shRNAs for genes that promote the activity of the microtubule poison taxol. These shRNA-encoding vectors also expressed green fluorescent protein (GFP) to facilitate easy identification of transduced cells (16). shRNA pools were introduced into lymphoma cells by retroviral transduction, such that 20-30% of the target cells were infected, and were subsequently treated with taxol to enrich for shRNA-containing cells displaying enhanced drug resistance (Figure 1A). Using GFP-based flow cytometry to monitor the percentage of transduced (GFP-positive) lymphoma cells, we identified several pools that displayed GFP enrichment following treatment with taxol, indicating the presence of at least one resistance-conferring shRNA within each pool. Deconvolution of these enriched, post-treatment shRNA pools was performed using a previously described PCR/colony sequencing technique (17). Identification of known modulators of chemotherapeutic response (eg. p53) using our screening protocol suggested that this approach was sufficiently robust to identify contributors to the cellular response to taxol.

3.3.2 Nek4 is a modulator of microtubule poison-induced cell death

Examination of our enrichment data revealed an shRNA targeting Nek4 (shNek4) as a candidate suppressor of taxol-induced death. As an initial

validation measure, shNek4 was isolated from the library and tested for the ability to promote taxol resistance as a single construct. As in our general screening strategy, a population of lymphoma cells was partially transduced with the shNek4 construct (co-expressing GFP), treated with taxol and analyzed by flow cytometry before and after treatment for changes in overall GFP percentage. In this context, shNek4-infected cells enriched relative to cells receiving a control vector. Additional shRNA constructs were then designed and tested to confirm this initial finding and address potential issues arising from well-documented 'off-target' RNAi effects (Figure 1B and Supplemental Table S1). Importantly, quantitative PCR analysis of Nek4 mRNA levels and western blotting for Nek4 protein in knockdown cells showed a correlation between the level of taxol resistance and the extent of target suppression (Figure 1C).

To determine how Nek4 suppression might promote resistance to taxol, we first examined whether Nek4 supression conferred resistance to other, functionally distinct chemotherapeutic drugs. Here, we examined the response of shNek4-transduced cells to doxorubicin (a topoisomerase poison), cisplatin (a platinum-based DNA crosslinking agent), 5-fluorouracil (an antimetabolite) and vincristine (a microtubule destabilizer). To control for differential drug efficacy, cells were treated with drug doses that resulted in ~90% death at 48 hours. GFP-competition assays using the most potent Nek4 shRNA (shNek4-2) revealed no significant change in GFP percentage when treated with doxorubicin, cisplatin or 5-fluorouracil. Unexpectedly, Nek4 suppression *sensitized* lymphoma

cells to treatment with vincristine, as evidenced by a depletion of GFP-positive shNek4-2 transduced cells following drug treatment (Figure 1D). Given that taxol and vincristine have opposing effects on microtubule stabilization, yet activate similar downstream checkpoints (18-20), these results suggested that Nek4 might promote or inhibit drug action directly at microtubules – as opposed to acting in a signaling network emanating from microtubule disruption.

Many regulators of microtubule dynamics have observable effects on cell cycle progression. Further, many chemotherapeutic agents preferentially affect actively cycling cells. To address the possibility that Nek4 suppression promotes taxol resistance by altering cell cycle progression, we determined the population growth rate, cell cycle profile (DNA content analysis), and mitotic index of shNek4-transduced cells. All three shNek4 populations were indistinguishable from control cells in these experiments, suggesting that gross impairment of the cell cycle was not responsible for the taxol resistant phenotype (Table 1).

We next sought to determine if Nek4 status had any effect on microtubule poison-induced cell cycle profiles. For these experiments, we used a cell line derived from a previously described *LSL-Kras*^{G12D}*; p53*$^{fl/fl}$ lung adenocarcinoma (LA) mouse model (21) as these cells display a more protracted response to chemotherapy (as opposed to highly chemosensitive *Eμ-myc* lymphoma cells). Thus, we were able to more clearly define subtle changes in the intermediate events preceding cell death. Importantly, we first confirmed that these cells also

display opposing survival profiles in response to microtubule stabilizing versus destabilizing drugs (Figure 2A). Additionally, consistent with the data observed from untreated lymphoma cells, a comparison of 4N/2N DNA content ratios of untreated control versus shNek4-2 LA cells revealed little to no difference in cell cycle distribution (Figure 2B, first bar). However, in the presence of 5μM taxol, shNek4-2-transduced LA cells displayed a defective G2/M arrest relative to vector-infected controls. Conversely, vincristine treatment yielded a more pronounced accumulation of G2/M arrested cells in the absence of Nek4 (Figure 2B). Thus, the cellular status of Nek4 appears to impact the efficacy of microtubule poisons proximal to the drug/target interface.

3.3.3 Nek4 is involved in the regulation of microtubules following exposure to microtubule poisons

Exposure to taxol is known to have profound effects on microtubule organization, namely, the accumulation of mitotic-like asters and formation of abnormal microtubule bundles (22, 23). Since precise microtubule phenotypes are known to vary from cell type to cell type (24), we first examined the impact of taxol on microtubules in lung adenocarcinoma cells. After a four-hour exposure to taxol, we found evidence of both mitotic-like asters and microtubule bundles in control cells. Under these conditions, the 'aster' phenotype predominated (Figure 3A and Supplemental Figure S1). Quantification of this phenotype in taxol treated control versus shNek4-transduced cell populations revealed a significant decrease in the percentage of cells harboring these aster-like

structures: ~14% in Nek4-knockdown populations as compared to ~22% in controls (Figures 3A and 3B). Importantly, this effect was not simply dependent upon the number of cells available to form asters, as the mitotic index was not significantly different between the two cell populations - either in the absence or presence of taxol or vincristine (Figure 3b, right graph).

It has been previously reported that alterations in microtubule dynamics are associated with and can contribute to microtubule poison efficacy (25). Utilizing an established *in situ* microtubule polymerization assay, we examined whether Nek4-knockdown had any effect on microtubule repolymerization following nocodazole treatment. Cells were transiently exposed to nocodazole to depolymerize existing microtubules, washed with excess media to initiate repolymerization, and fixed, stained, and imaged at various time points to examine microtubule status. After a 30-minute incubation with nocodazole, microtubules were no longer detectable, as determined using α-tubulin immunofluorescence. While control cells showed rapid microtubule polymerization from centrosomes following nocodazole release, defects in microtubule synthesis in Nek4-knockdown cells were apparent as early as one minute following release and clearly observable at the two-minute time point (Figures 3C and D). This suggests that impaired microtubule polymerization may underlie the differential sensitivity of Nek4-knockdown cells to taxol and vincristine.

3.3.4 Nek4 knockdown modulates microtubule poison efficacy *in vivo*

A strength of the *Eμ-myc* lymphoma model as a pre-clinical system is the ability to transplant genetically altered tumor cells into syngeneic, immunocompetent recipient mice, where the resulting disease is pathologically indistinguishable from lymphomas arising in germline *Eμ-myc* mice (26). This, along with the ability to specifically silence individual genes, allows for rapid evaluation of putative regulators of chemotherapeutic response in an immunocompetent *in vivo* setting (Figure 4a). Utilizing this approach, we transplanted partially transduced control and shNek4-2 knockdown lymphomas into recipient mice and allowed palpable tumors to form (~14 days). Upon tumor presentation, mice were administered either 25mg/kg taxol or 1.5 mg/kg vincristine for 24hr, at which time tumor material was harvested for analysis by flow cytometry. In agreement with *in vitro* experiments, acute treatment of control tumors had no effect on the percentage of GFP-positive cells (not shown). In contrast, the percentage of GFP-positive shNek4-2 cells increased upon treatment with taxol, while selectively depleting when exposed to vincristine (Figure 4B). Further, mice harboring pure population (GFP sorted) shNek4-2 tumors showed an improved overall response to vincristine, with extended tumor-free and overall survival relative to their control counterparts (Figure 4c and data not shown).

3.3.5 Nek4 status modulates the relative sensitivity of human lung cancer cell lines to microtubule poisons

Microtubule poisons are front-line chemotherapies for the treatment of non-small cell lung cancer (NSCLC). Interestingly, many lung cancers harbor deletions on the short arm of chromosome 3 that include the Nek4 genomic locus. Thus, we reasoned that Nek4 status in NSCLC might contribute to the differential response of lung cancer cell lines to microtubule poisons. Given the complex constellation of mutations undoubtedly present across multiple cell lines, we limited our analysis to the relative sensitivity of cell lines to taxol versus vincristine. We tested several cell lines - one with a high level of Nek4 protein (colo669) and three (sklu1, H460, H1395) with reduced Nek4 levels. Interestingly, we found that colo669 cells had a significantly lower taxol versus vincristine (Tax/Vin) survival ratio – indicative of relative taxol sensitivity and/or vincristine resistance (Figure 5A). Importantly, shRNA-mediated knockdown of Nek4 in colo669 cells changed the response profile of these cells, promoting both taxol resistance and vincristine sensitivity (Figure 5B and Supplemental Table S2). Conversely, changes in drug sensitivity were not seen in a cell line expressing low levels of Nek4 (Sklu1). However, overexpression of human Nek4 promoted vincristine resistance and taxol sensitivity in Sklu1 cells (Figure 5C and Supplemental Figure S2). Thus, Nek4 levels in human cancers can significantly impact the relative sensitivity of these tumors to distinct microtubule poisons.

3.4 Discussion

The founding member of the NIMA kinase family was first identified in an *Aspergillus nidulans* screen for mutants that were "Never In Mitosis" (27, 28). Since then, 11 NIMA kinases have been identified by homology in mammalian cells. Four of these proteins, Nek2, Nek6, Nek7 and Nek9, have been shown to play roles in mitosis, while Nek1 and Nek8 are important for cilia function (29-31). Here, we show that Nek4 also plays a role in microtubule homeostasis. Importantly, however, this effect is only seen in the context of microtubule poisons. Multiple explanations could account for this effect. First, other proteins may compensate for Nek4 loss function during mitosis in untreated cells. Alternatively, partial Nek4 activity may be sufficient to allow for normal mitosis. While the shRNAs used in this study achieve near complete knockdown of Nek4 by western blot, it remains to be seen whether these vectors recapitulate Nek4 null phenotypes.

Interestingly, Nek4 deficiency results in resistance to taxol and sensitivity to vincristine. These data suggest that Nek4 functions at the level of microtubules, rather than on common downstream signal transduction pathways emanating from altered microtubule homeostasis. Given that at high drug doses, taxol is a microtubule-stabilizing agent and vincristine destabilizes microtubules, our data also suggests that Nek4 may play a role in promoting microtubule polymerization in the presence of drug. Consistent with this idea, Nek4

deficiency impairs microtubule re-polymerization following nocodazole treatment. That a genetic alteration can confer opposite cellular responses to vincristine and taxol is not novel (32-35). Previous efforts in generating taxol-resistant cell lines have, in some instances, yielded cells that were vincristine sensitive (33, 34, 36). These studies highlighted the ability of tubulin mutations to confer differential sensitivity to microtubule poisons. Here, loss of function screening allowed for the identification of a regulator of therapeutic response that may have been obscured in more targeted studies of the cellular response to microtubule poisons.

Interestingly, Nek4 is located in a genomic region that is commonly mutated in lung cancer. While it is unclear whether Nek4 is relevant to the pathogenesis of lung cancer, these data suggest a connection between the specific alterations that occur lung cancer development and the ultimate response of that cancer to chemotherapy. Notably, the fact that Nek4 deficiency confers sensitivity to microtubule destabilizers suggests that combination therapies can be tailored towards this deficiency. The combination of cisplatin and taxol are commonly used as a front-line therapy for lung cancer. Our data suggests that a more personalized approach to treating lung cancer, utilizing vincristine rather than taxol in tumors with 3p deletions, may result in enhanced chemotherapeutic response.

3.5 Materials and methods

3.5.1 Cell culture and chemicals

Eμ-myc mouse B-cell lymphomas were cultured in B-cell medium (45% DMEM/45% IMDM/10% FBS, supplemented with 2 mM L-glutamine and 5μM β-mercaptoethanol). Mouse and human lung adenocarcinoma cells were cultured in standard DMEM/FBS and RPMI/FBS medias, respectively. Chemotherapeutic agents were purchased from LC Laboratories (taxol) and Calbiochem (doxorubicin, vincristine, cisplatin, 5-florouracil) and used at the indicated concentrations. For *in vivo* studies, vincristine (0.9% NaCl solution) and taxol (EtOH:Cremaphor:NaCl) were dissolved immediately prior to injection.

3.5.2 Retroviral constructs

shRNA constructs were designed and cloned as previously described (37). Sequences (5'-3') targeted by shRNAs are as follows: shNek4-1 (Mm): GGAGAATCGTTGAAGTCTTAA, shNek4-2 (Mm): CACGTGGATGCCGCTGATGAA, shNEK4-1 (Hs): CAGCGTAAATATTGACATCTTA, shNEK4-4 (Hs): CTAAGGAGTAGTTGATAAATTA. Additional shRNA sequences are available upon request. Full-length human Nek4 cDNA was purchased from Open Biosystems (clone ID: 5169184) and cloned into a MSCV-based retroviral vector (pMIG). Cloning strategies and primer sequences are also available from the authors on request.

3.5.3 Western blotting, Immunofluorescence and RT-qPCR

For western blotting and RT-qPCR, protein or total RNA was isolated after retroviral infection and puromycin selection. RT-qPCR was performed using SYBR green on a BioRad thermal cycler. Primers sequences are available upon request. For western blotting, cell lysates were prepared in lysis buffer (1% sodium deoxycholine, 0.1% SDS, 1% triton-X, 10 mM Tris-HCl, pH 8.0, 140 mM NaCl) for 10 minutes, cleared for 15 minutes at 14,000 rpm, then mixed with 5x SDS sample buffer. Proteins were then run on a 10% SDS-PAGE gel, transferred to PVDF (Millipore) and detected with the following antibodies: anti-Nek4 (Hahn Lab, 1:250) and anti-GAPDH (Santa Cruz, 1:10000). Cells for immunofluorescence were grown and treated on poly-L-lysine coated coverslips, fixed with 100% methanol for 5 minutes at -20°C and stored for later use. Anti-α-tubulin [YL1/2] (Abcam, 1:2000) and anti-γ-tubulin (Sigma, 1:200) were used along with Alexa secondary antibodies (Molecular Probes) to visualize microtubules and centrosomes, respectively. Stained coverslips were imaged and analyzed using Applied Precision DeltaVision instruments and deconvolution software.

3.5.4 Flow Cytometry

All assays were performed using Becton-Dickinson FACScan or MoFlo flow cytometers. Cell death was detected by propidium iodide (PI) incorporation (0.05 mg/mL), and dead cells were excluded from GFP analysis. Live cell sorting was performed using GFP co-expression as a marker of cell transduction. For

phospho-histone H3 assays, cells were fixed in 70% EtOH, then stained using an anti-pH3 antibody (Santa Cruz, 1:2500) followed by an Alexa (488) secondary antibody. Stained cells were then co-stained in a sodium citrate/PI buffer prior to analysis.

3.5.5 GFP-competition and viability assays

For competition assays, lymphoma cells were partially transduced with the indicated shRNA constructs, treated with chemotherapeutic agents, as indicated, and monitored by flow cytometry for changes in the percentage of GFP+ cells. For viability assays, cells were plated subconfluently in 96-well plates, treated as indicated and analyzed 48h post-treatment using CellTiter-Glo reagent (Promega) on an Applied Biosystems microplate luminometer.

3.5.6 Microtubule polymerization assay

Cells plated on poly-L-lysine coated coverslips were treated with 0.5 μM nocodazole for 30' at 37°C/5% CO_2. Coverslips were briefly washed with PBS and allowed to recover for the indicated periods of time in nocodazole-free media at room temperature. Coverslips were then fixed using ice-cold methanol (5 minutes, -20°C) and stored in 4% BSA, 0.1% Triton-X, 0.05% sodium azide for subsequent immunofluorescent detection of α- and γ-tubulin. Microtubule length measurements were performed on representative images (5 fields/sample) using OpenLab (Improvision) software.

Figure 1

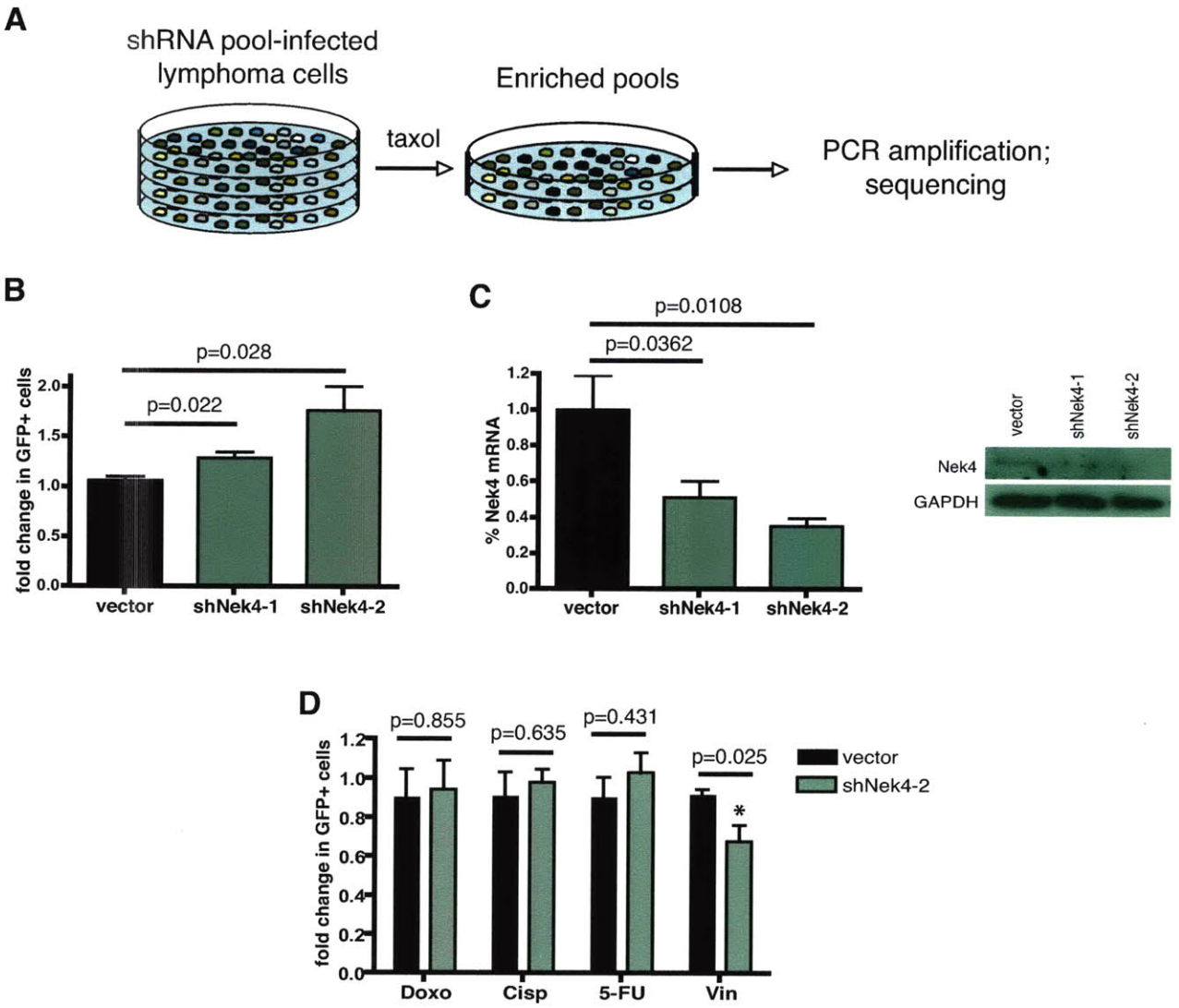

Figure 1 – RNAi screening identifies Nek4 as a regulator of microtubule poison-induced cell death.

(A) In vitro screening methodology. Lymphoma cells were partially infected with 48 pools of 48 distinct shRNAs, treated with taxol (4, 6, and 8μM) and monitored using GFP-based flow cytometry for changes in the relative percentage of shRNA-containing (GFP+) cells. Genomic DNA from enriched pools was subsequently subjected to shRNA-specific PCR and sequenced to determine relative shRNA abundance. (B) Two distinct shRNAs targeting Nek4 confer resistance to taxol (n=5 for all samples). (C) qRT-PCR (n≥3) and western blot confirmation of Nek4 suppression. (D) Partially-transduced lymphoma cells were separately treated with doxorubicin (10ng/ml), cisplatin (7.5ng/ml), 5-fluorouracil (40ng/ml) and vincristine (1.5nM) at similar levels of cytotoxicity (~90% cell death at 48h). The percentage of GFP+ cells was determined 48 hours post treatment (n=3 for doxorubicin, 5-FU, cisplatin, and n=5 for vincristine treatments). Values are shown with standard deviations (s.d.). P-values were determined using a Student's t-test.

Figure 2

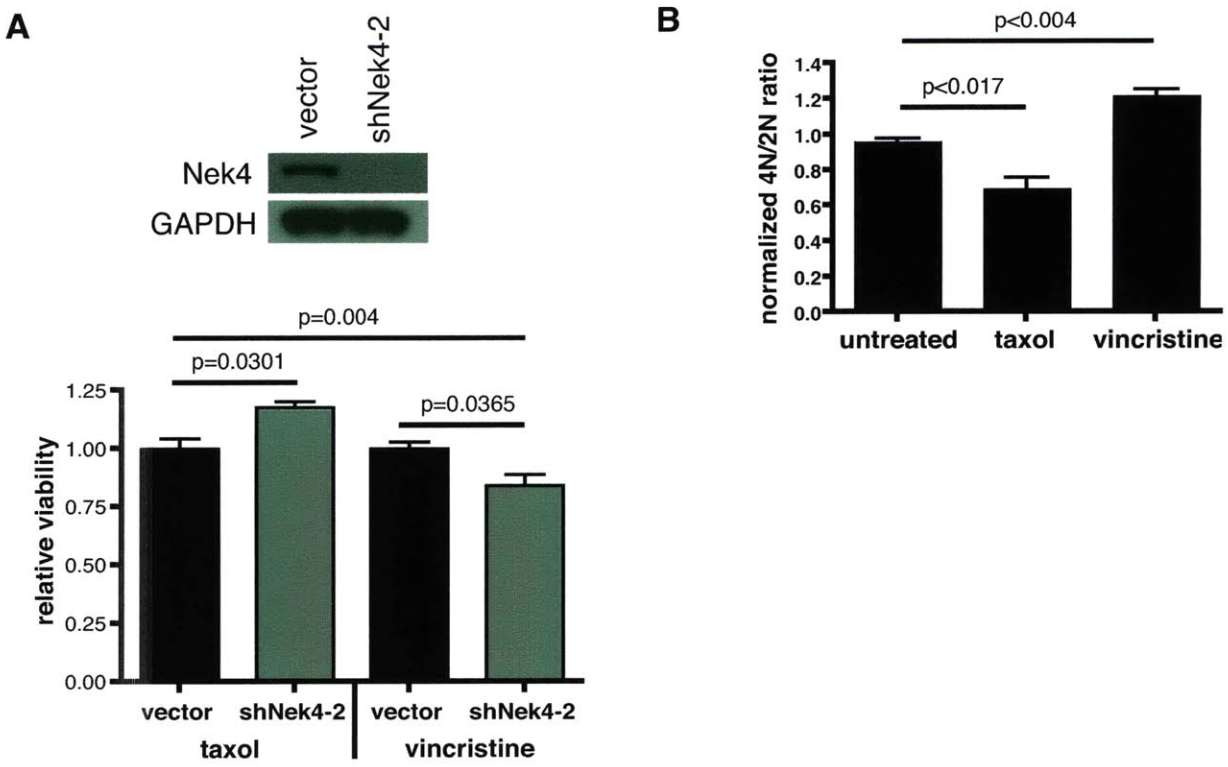

Figure 2 – Nek4 knockdown promotes resistance to taxol, while sensitizing cells to vincristine.

(A) (Above) A western blot showing Nek4 knockdown in lung adenocarcinoma cells expressing shNek4-2. (Below) shNek4-2 transduced cells were treated with taxol or vincristine and monitored for cell survival relative to cells expressing a vector control (n=3 independently treated samples for each drug, +/- s.d.). (B) G2/M arrest profiles in lung adenocarcinoma cells expressing shNek4-2. Knockdown cells were treated with 5μM taxol or 5μM vincristine for 8 hours and analyzed for DNA content by flow cytometry to determine the extent of the microtubule poison-induced G2/M arrest. Shown is the 4N/2N ratio (indicative of an arrest) normalized to matched vector control cells (n=3 for all samples +/- s.d.). P-values were determined using a Student's t-test.

Figure 3

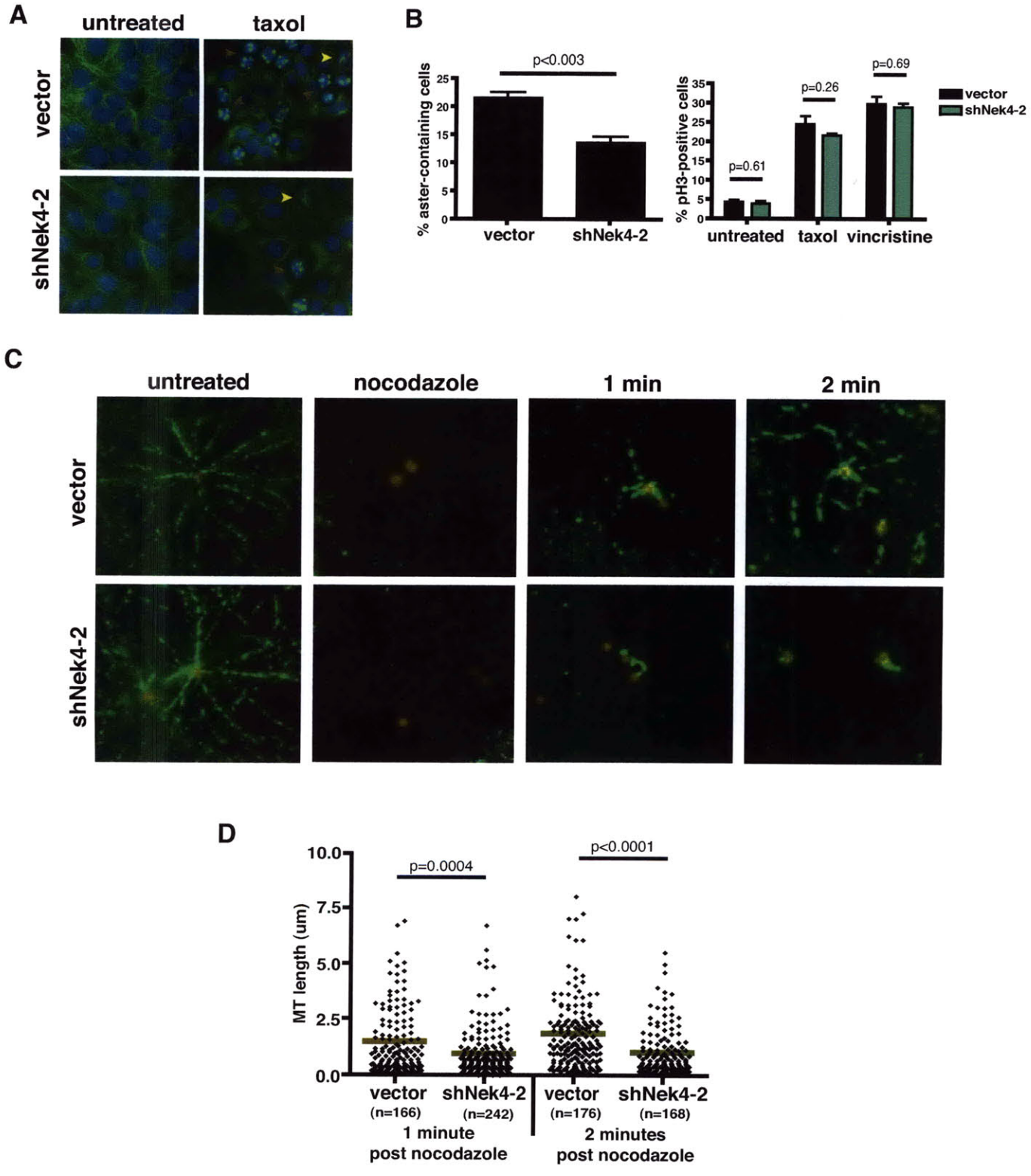
A
untreated
taxol
vector
shNek4-2
B
p<0.003
% aster-containing cells
vector
shNek4-2
p=0.61
p=0.26
p=0.69
% pH3-positive cells
untreated
taxol
vincristine
vector
shNek4-2
C
untreated
nocodazole
1 min
2 min
vector
shNek4-2
D
p=0.0004
p<0.0001
MT length (um)
vector (n=166)
shNek4-2 (n=242)
vector (n=176)
shNek4-2 (n=168)
1 minute post nocodazole
2 minutes post nocodazole

Figure 3 – Nek4 knockdown cells show altered microtubule phenotypes.
(A) LA cells expressing a Nek4 shRNA or a control vector were treated with 5μM taxol for 4h and then stained with anti-?-tubulin to visualize microtubules. Microtubule asters (red arrowheads) and bundles (yellow arrowheads) were observed under these conditions. (B) (Left graph) Quantification of the more abundant aster-containing cells revealed a significant decrease in aster number in Nek4 knockdown samples compared to matched controls (n=3 independently treated replicates, 6 averaged fields/sample). (Right) Phospho-histone H3 staining of drug treated LA cells failed to show any significant change in the mitotic index in the presence or absence of Nek4 (n=3 for all samples +/- s.d.). (C) In a microtubule repolymerization assay, lung adenocarcinoma cells were allowed to repolymerize microtubules following transient (0.5μM, 30 minutes) nocodazole treatment. Qualitative differences were apparent at one (third column) and two (fourth column) minutes post-nocodazole release. (D) Quantification of the repolymerization defect in shNek4-2 LA cells. Microtubule lengths are shown at the one and two-minute time points, respectively. The average microtubule length in each sample is indicated with a red bar. P-values were determined using a Student's t-test.

Figure 4

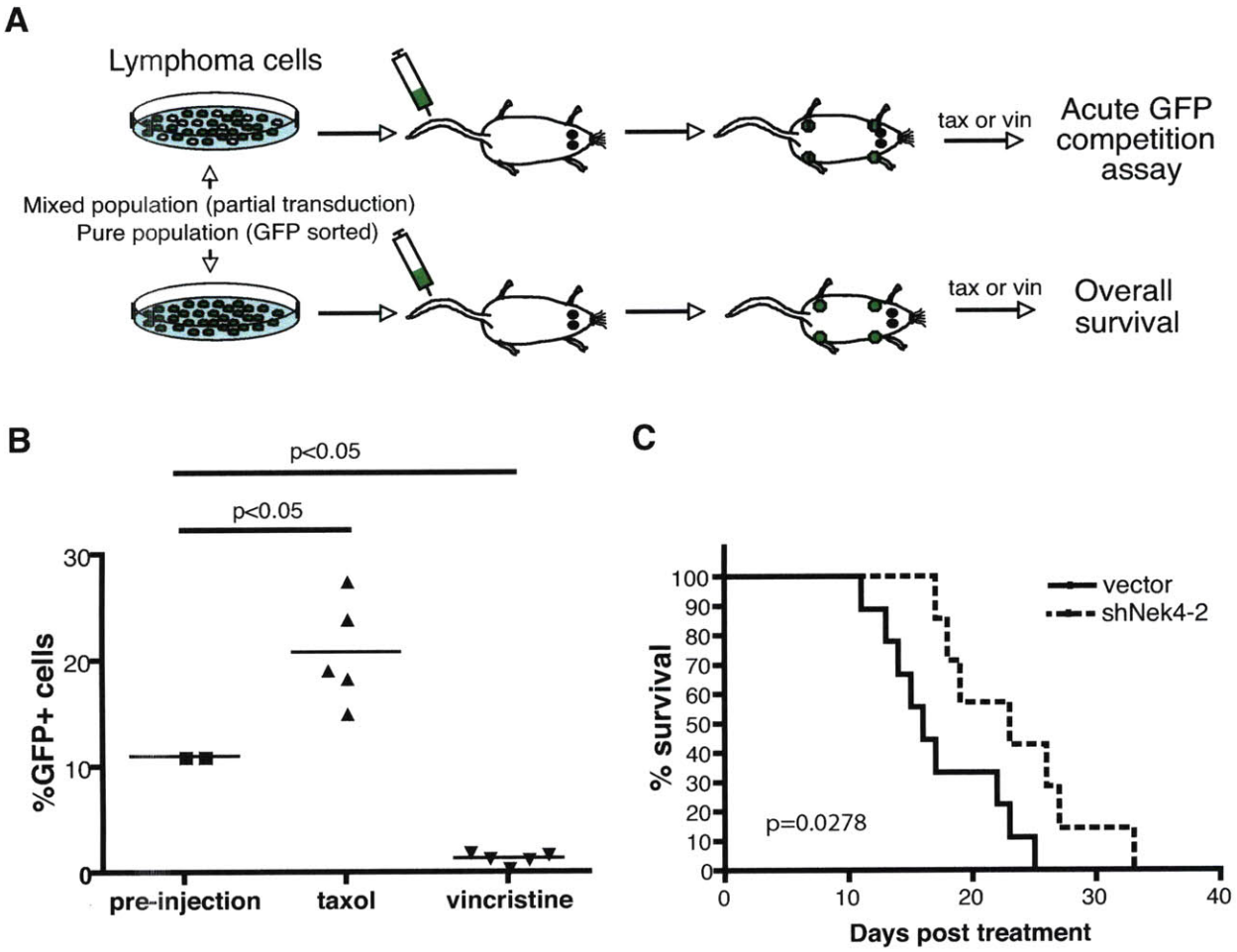

Figure 4 –Nek4 suppression alters the response to microtubule poisons in vivo. (A) Schematic depicting in vivo experimental approaches. Partially transduced (upper row) or GFP-sorted (lower row) lymphoma cells were injected into recipient mice and allowed to develop into palpable lymphomas. Resulting tumors were then treated with taxol or vincristine and then either harvested to examine the percentage of GFP+ cells or monitored for tumor-free and overall survival rates. (B) Partially transduced shNek4-2 lymphomas were harvested 24 hours post drug treatment and analyzed by flow cytometry for changes in GFP percentage. Taxol treatment resulted in an increase in the percentage of GFP+ cells (compared to pre-injection GFP levels), while vincristine-treated tumors displayed dramatic selection against Nek4 knockdown. P-values were determined using a Student's t-test (C) Mice bearing shNek4-2 expressing tumors lived significantly longer than mice with control tumors following treatment with vincristine (vector, n=13; shNek4-2, n=12). P-values were determined using a log rank test.

Figure 5

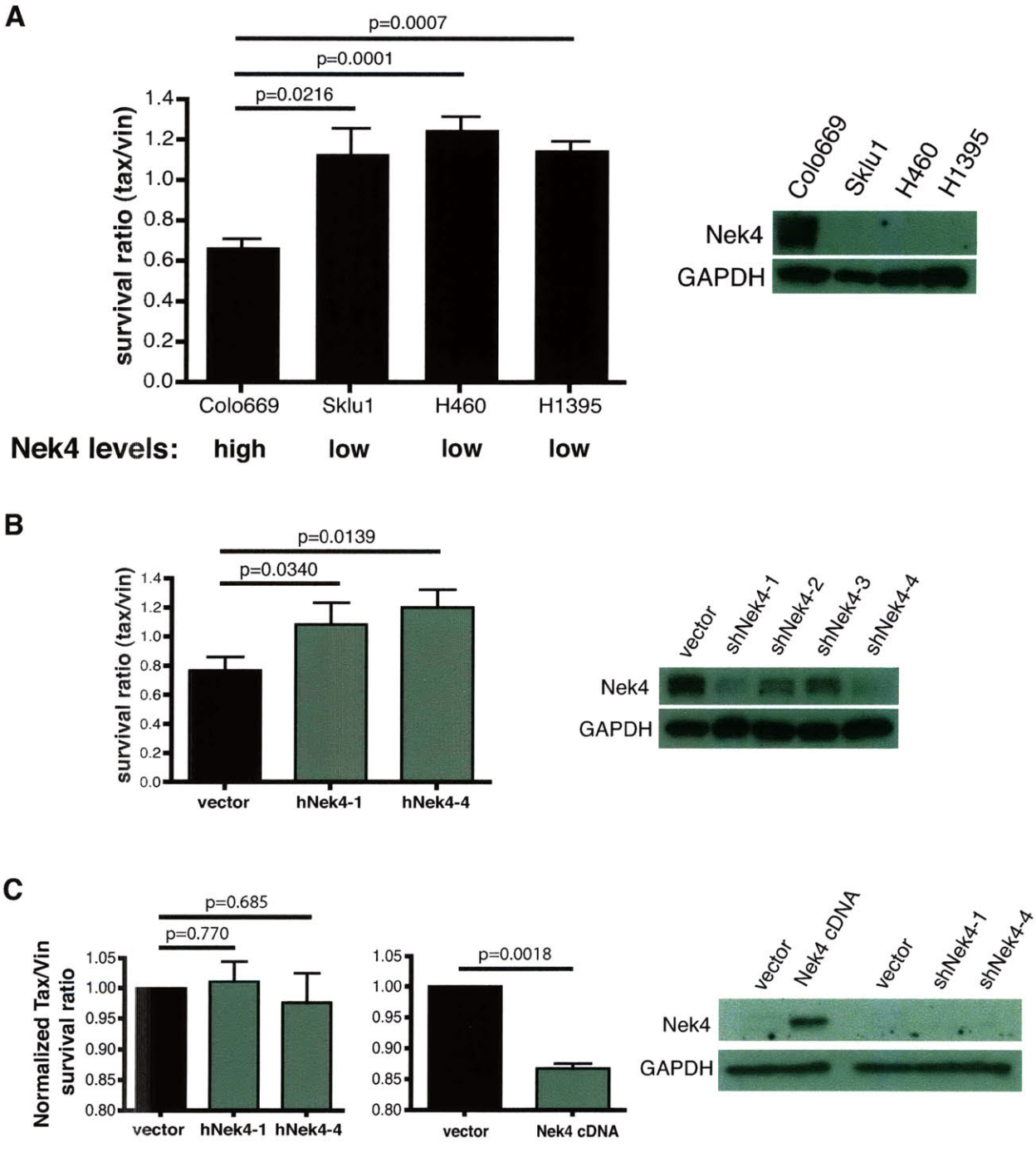
A
p=0.0007
p=0.0001
p=0.0216
survival ratio (tax/vin)
1.4
1.2
1.0
0.8
0.6
0.4
0.2
0.0
Colo669
Sklu1
H460
H1395
Nek4 levels: high low low low
Colo669
Sklu1
H460
H1395
Nek4
GAPDH
B
p=0.0139
p=0.0340
survival ratio (tax/vin)
vector
hNek4-1
hNek4-4
vector
shNek4-1
shNek4-2
shNek4-3
shNek4-4
Nek4
GAPDH
C
p=0.685
p=0.770
Normalized Tax/Vin survival ratio
1.05
1.00
0.95
0.90
0.85
0.80
vector
hNek4-1
hNek4-4
p=0.0018
vector
Nek4 cDNA
vector
Nek4 cDNA
vector
shNek4-1
shNek4-4
Nek4
GAPDH

Figure 5 – Nek4-dependent differential sensitivity to microtubule poisons in human lung adenocarinoma cells.
(A) Four human lung adenocarcinoma cell lines were separately treated with taxol and vincristine and examined for viability 48 hours after treatment. Viability comparisons (left, graph) at a fixed drug dose of 5μM taxol or vincristine revealed one cell line (colo669) with a significantly lower taxol/vincristine survival ratio. This cell line also had high baseline levels of Nek4 protein (right, western blot). (B) Colo669 cells were retrovirally infected with shRNAs targeting human Nek4 and subjected to in vitro survival assays. Knockdown cells with significant depletion of Nek4 protein (right, western blot) also demonstrated relative resistance to taxol and sensitivity to vincristine (left, shown as an upward shift in the taxol/vincristine survival ratio). (C) Transduction of Sklu1 cells with Nek4 shRNAs did not affect their relative sensitivity to taxol and vincristine (left graph). Stable overexpression of full-length human Nek4 cDNA in Sklu1 (low NEK4) cells results in increased sensitivity to taxol and resistance to vincristine (right graph). P-values were determined using a Student's t-test (n=3; all samples).

Table 1

	4N/2N ratio (PI)	Mit Index (pH3+)	doubling time (h)
vector	0.51+/-0.07	3.7+/-0.4	8.3+/-0.4
shNek4-1	0.46+/-0.5	3.5+/-1.2	8.4+/-0.8
shNek4-2	0.45+/-0.02	3.2+/-0.4	8.0+/-0.7
shNek4-3	0.5+/-0.06	3.9+/-0.6	8.7+/-1.0

Table 1. Cell cycle analysis of shNek4 infected *Eμ-myc* lymphoma cells. Actively cycling knockdown cell populations were fixed, stained with anti-phospho histone H3/propidium iodide, and analyzed by flow cytometry to determine the mitotic index (shown as % phospho histone H3 cells), and relative DNA content (shown as a ratio of 4N/2N cells). No significant differences were observed between control vs Nek4 knockdown cells (n=3 independently infected cell populations).

Supplemental Figure S1

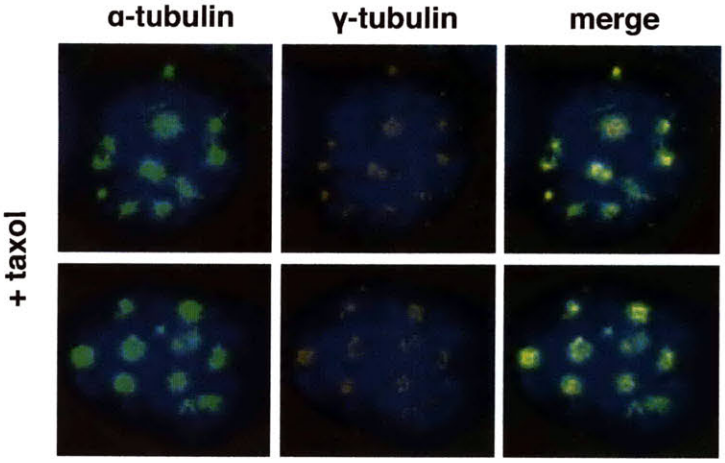

Supplemental Figure S1 – Taxol-induced asters contain centrosome-associated gamma-tubulin. Lung adenocarcinoma cells treated with taxol were fixed 4 hours after treatment and subjected to immunofluorescence detection for alpha and gamma-tubulin. Green aster structures (left column) co-stained with antibodies targeting gamma-tubulin. Two representative cells are shown.

Supplemental Figure S2

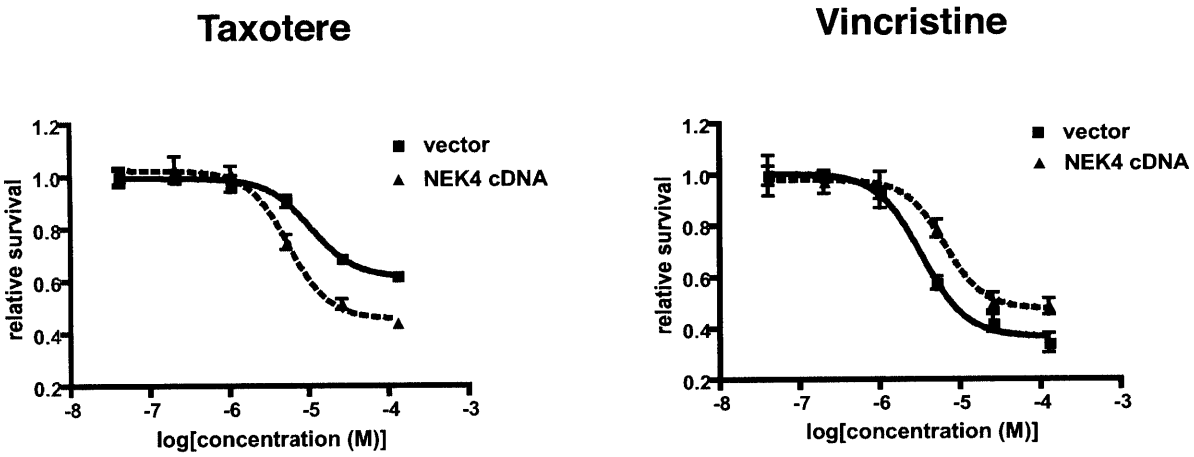

Supplemental Figure S2 - Differential dose response curves in 'low Nek4' lung adenocarcinoma cells overexpressing full-length Nek4 cDNA.
Sklu1 cells stably overexpressing full length Nek4 cDNA were treated with either taxotere or vincristine for 48h, at which time cell viability was assessed using CellTiterGlo reagents. Statistical comparison of EC50 values derived from best-fit non-linear regression curves revealed increased sensitivity (avg EC50 vector=10.5uM, NEK4=5.5uM, p=0.002) to taxotere and resistance to vincristine (avg EC50 vector=3.3uM, NEK4=6.4uM, p=0.002) in cells overexpressing Nek4.

Supplemental Table S1

GFP enrichment		no drug (%GFP+)	taxol 6nM (%GFP+)
rep #1	vector(1)	28.88	28.47
	shNek4-1(1)	18.16	25.54
	shNek4-2(1)	10.67	19.85
rep #2	vector(2)	29.45	29.46
	shNek4-1(2)	69.26	73.29
	shNek4-2(2)	43.33	47.58
rep #3	vector(3)	20.37	20.83
	shNek4-1(3)	18.76	24.46
	shNek4-2(3)	8.21	14.95
rep #4	vector(4)	42.62	50.08
	shNek4-1(4)	40.88	54.34
	shNek4-2(4)	27.51	62.56

Raw data from the GFP enrichment assay in lymphoma cells. Partially transduced lymphoma cells were treated with 6nM taxol and analyzed by FACS 48h post treatment. Shown are the raw percentages of GFP+ cells that either received drug or remained untreated for the same period of time. Data presented in this table represents four independently transduced and treated populations of cells.

Supplemental Table S2

Viability		rep #1	rep #2	rep #3
tax	vector	0.415	0.572	0.652
	shNek4-1	0.450	0.622	0.750
	shNek4-4	0.475	0.633	0.746
vin	vector	0.703	0.717	0.713
	shNek4-1	0.569	0.520	0.590
	shNek4-4	0.498	0.474	0.565

Raw data from viability assay in Colo669 cells. GFP-sorted (pure population) control, shNek4-1 and shNek4-4 cells were treated with either 5μM taxol (tax) or 5μM vincristine (vin) and analyzed 48 hours post treatment using the CellTiterGlo viability assay. Shown are the relative viability percentages of drug-treated colo669 cells, with or without shRNAs targeting endogenous Nek4. Data presented in this table represents three independently treated populations of cells.

3.8 Acknowledgements

I would like to thank William Hahn for generously providing us with the Nek4 antibody used in these studies. I would also like to thank Paul Chang for help with microtubule assays and members of the Hemann lab for helpful advice and discussions. At the time of publication in Cancer Research, M.T.H. was a Rita Allen Fellow and the Latham Family Career Development Assistant Professor of Biology and was supported by NIH RO1 CA128803-01. J.D. was supported by the MIT Department of Biology training grant.

3.9 References

1. Jordan MA, Wilson L. Microtubules and actin filaments: dynamic targets for cancer chemotherapy. Curr Opin Cell Biol 1998;10(1):123-30.

2. Bhalla K, Ibrado AM, Tourkina E, Tang C, Mahoney ME, Huang Y. Taxol induces internucleosomal DNA fragmentation associated with programmed cell death in human myeloid leukemia cells. Leukemia 1993;7(4):563-8.

3. Danesi R, Figg WD, Reed E, Myers CE. Paclitaxel (taxol) inhibits protein isoprenylation and induces apoptosis in PC-3 human prostate cancer cells. Mol Pharmacol 1995;47(6):1106-11.

4. Martin SJ, Cotter TG. Disruption of microtubules induces an endogenous suicide pathway in human leukaemia HL-60 cells. Cell Tissue Kinet 1990;23(6):545-59.

5. Woods CM, Zhu J, McQueney PA, Bollag D, Lazarides E. Taxol-induced mitotic block triggers rapid onset of a p53-independent apoptotic pathway. Mol Med 1995;1(5):506-26.

6. Morris PG, Fornier MN. Microtubule active agents: beyond the taxane frontier. Clin Cancer Res 2008;14(22):7167-72.

7. Kuppens IE. Current state of the art of new tubulin inhibitors in the clinic. Curr Clin Pharmacol 2006;1(1):57-70.

8. Mechetner E, Kyshtoobayeva A, Zonis S, et al. Levels of multidrug resistance (MDR1) P-glycoprotein expression by human breast cancer correlate with in vitro resistance to taxol and doxorubicin. Clin Cancer Res 1998;4(2):389-98.

9. Blade K, Menick DR, Cabral F. Overexpression of class I, II or IVb beta-tubulin isotypes in CHO cells is insufficient to confer resistance to paclitaxel. J Cell Sci 1999;112 (Pt 13):2213-21.

10. Fojo T, Menefee M. Mechanisms of multidrug resistance: the potential role of microtubule-stabilizing agents. Ann Oncol 2007;18 Suppl 5:v3-8.

11. Bhalla K, Huang Y, Tang C, et al. Characterization of a human myeloid leukemia cell line highly resistant to taxol. Leukemia 1994;8(3):465-75.

12. Orr GA, Verdier-Pinard P, McDaid H, Horwitz SB. Mechanisms of Taxol resistance related to microtubules. Oncogene 2003;22(47):7280-95.

13. Blagosklonny MV, Fojo T. Molecular effects of paclitaxel: myths and reality (a critical review). Int J Cancer 1999;83(2):151-6.

14. Strobel T, Swanson L, Korsmeyer S, Cannistra SA. BAX enhances paclitaxel-induced apoptosis through a p53-independent pathway. Proc Natl Acad Sci U S A 1996;93(24):14094-9.

15. Barboule N, Chadebech P, Baldin V, Vidal S, Valette A. Involvement of p21 in mitotic exit after paclitaxel treatment in MCF-7 breast adenocarcinoma cell line. Oncogene 1997;15(23):2867-75.

16. Hemann MT, Fridman JS, Zilfou JT, et al. An epi-allelic series of p53 hypomorphs created by stable RNAi produces distinct tumor phenotypes in vivo. Nat Genet 2003;33(3):396-400.

17. Dickins RA, Hemann MT, Zilfou JT, et al. Probing tumor phenotypes using stable and regulated synthetic microRNA precursors. Nat Genet 2005;37(11):1289-95.

18. Masuda A, Maeno K, Nakagawa T, Saito H, Takahashi T. Association between mitotic spindle checkpoint impairment and susceptibility to the induction of apoptosis by anti-microtubule agents in human lung cancers. Am J Pathol 2003;163(3):1109-16.

19. Sudo T, Nitta M, Saya H, Ueno NT. Dependence of paclitaxel sensitivity on a functional spindle assembly checkpoint. Cancer Res 2004;64(7):2502-8.

20. Wang X, Jin DY, Wong HL, Feng H, Wong YC, Tsao SW. MAD2-induced sensitization to vincristine is associated with mitotic arrest and Raf/Bcl-2 phosphorylation in nasopharyngeal carcinoma cells. Oncogene 2003;22(1):109-16.

21. Kim CF, Jackson EL, Kirsch DG, et al. Mouse models of human non-small-cell lung cancer: raising the bar. Cold Spring Harb Symp Quant Biol 2005;70:241-50.

22. Rowinsky EK, Donehower RC, Jones RJ, Tucker RW. Microtubule changes and cytotoxicity in leukemic cell lines treated with taxol. Cancer Res 1988;48(14):4093-100.

23. Schatten G, Schatten H, Bestor TH, Balczon R. Taxol inhibits the nuclear movements during fertilization and induces asters in unfertilized sea urchin eggs. J Cell Biol 1982;94(2):455-65.

24. Gascoigne KE, Taylor SS. Cancer cells display profound intra- and interline variation following prolonged exposure to antimitotic drugs. Cancer Cell 2008;14(2):111-22.

25. Goncalves A, Braguer D, Kamath K, et al. Resistance to Taxol in lung cancer cells associated with increased microtubule dynamics. Proc Natl Acad Sci U S A 2001;98(20):11737-42.

26. Schmitt CA, Rosenthal CT, Lowe SW. Genetic analysis of chemoresistance in primary murine lymphomas. Nat Med 2000;6(9):1029-35.

27. Morris NR. Mitotic mutants of Aspergillus nidulans. Genet Res 1975;26(3):237-54.

28. Osmani SA, May GS, Morris NR. Regulation of the mRNA levels of nimA, a gene required for the G2-M transition in Aspergillus nidulans. J Cell Biol 1987;104(6):1495-504.

29. O'Regan L, Blot J, Fry AM. Mitotic regulation by NIMA-related kinases. Cell Div 2007;2:25.

30. Quarmby LM, Mahjoub MR. Caught Nek-ing: cilia and centrioles. J Cell Sci 2005;118(Pt 22):5161-9.

31. Parker JD, Bradley BA, Mooers AO, Quarmby LM. Phylogenetic analysis of the Neks reveals early diversification of ciliary-cell cycle kinases. PLoS ONE 2007;2(10):e1076.

32. Ong V, Liem NL, Schmid MA, et al. A role for altered microtubule polymer levels in vincristine resistance of childhood acute lymphoblastic leukemia xenografts. J Pharmacol Exp Ther 2008;324(2):434-42.

33. Minotti AM, Barlow SB, Cabral F. Resistance to antimitotic drugs in Chinese hamster ovary cells correlates with changes in the level of polymerized tubulin. J Biol Chem 1991;266(6):3987-94.

34. Kavallaris M, Burkhart CA, Horwitz SB. Antisense oligonucleotides to class III beta-tubulin sensitize drug-resistant cells to Taxol. Br J Cancer 1999;80(7):1020-5.

35. Kavallaris M, Tait AS, Walsh BJ, et al. Multiple microtubule alterations are associated with Vinca alkaloid resistance in human leukemia cells. Cancer Res 2001;61(15):5803-9.

36. Ohta S, Nishio K, Kubota N, et al. Characterization of a taxol-resistant human small-cell lung cancer cell line. Jpn J Cancer Res 1994;85(3):290-7.

37. Burgess DJ, Doles J, Zender L, et al. Topoisomerase levels determine chemotherapy response in vitro and in vivo. Proc Natl Acad Sci U S A 2008;105(26):9053-8.

Chapter 4

Rev3 suppression sensitizes drug-resistant lung tumors to chemotherapy[1]

4.1 Abstract

Platinum-based chemotherapeutic drugs are front-line therapies for the treatment of non-small cell lung cancer. However, intrinsic drug resistance limits the clinical efficacy of these agents. Recent evidence suggests that loss of the translesion (TLS) polymerase, Polζ, can sensitize tumor cell lines to cisplatin, although the relevance of these findings to the treatment of chemoresistant tumors *in vivo* has remained unclear. Here, we describe a tumor transplantation approach that enables the rapid introduction of defined genetic lesions into a pre-clinical model of lung adenocarcinoma. Using this approach, we examined the effect of impaired translesion DNA synthesis on cisplatin response in aggressive late-stage lung cancers. In the presence of reduced levels of Rev3, an essential component of Polζ, tumors exhibited pronounced sensitivity to cisplatin, leading to a significant extension in overall survival of treated recipient mice. Additionally, treated Rev3-deficient cells exhibited reduced cisplatin-induced mutation – a process that has been implicated in the induction of secondary malignancies following chemotherapy. Taken together, our data illustrate the potential of Rev3 inhibition as an adjuvant therapy for the treatment of chemoresistant malignancies and highlight the utility of rapid transplantation

methodologies for evaluating mechanisms of chemotherapeutic resistance in pre-clinical settings.

[1]Significant sections of this chapter have been submitted for publication at *PNAS* as:

Doles J, Oliver TG, Hsu G, Jacks T, Walker GC, Hemann MT. Rev3 suppression sensitizes drug-resistant lung tumors to chemotherapy.

4.2 Introduction

Cisplatin and related compounds are widely used in the treatment of a variety of malignancies. While these agents have proven to be quite effective in treating certain tumor types, in others, such as ovarian and lung cancer, clinical success has been more variable. In particular, patients harboring advanced non-small cell lung cancer (NSCLC) generally respond poorly to aggressive chemotherapy, with median survival times commonly falling short of a year (1). In light of studies showing that nearly half of the patient population presents with advanced (stage IV) disease, it is not surprising that the 5-year survival rate for all NSCLC in the United States is less than 20%. Moreover, patients diagnosed with metastatic disease fare even worse (<4% 5-year survival) (2, 3). Therefore, a greater understanding of mechanisms of cisplatin resistance are essential to improve treatment of patients with advanced NSCLC and more broadly inform strategies to target highly drug resistant malignancies.

Like many cytotoxic chemotherapeutic agents, cisplatin targets DNA. Although only 5-10% of covalently bound cisplatin is bound to DNA, it is this DNA damage that is largely responsible for its cytotoxic properties (4-6). The predominant forms of cisplatin-induced damage are intrastrand crosslinks - 1,2-(GpG) (65%), 1,2 (ApG) (25%), and 1,3 (GpNpG) (5-10%) - with interstrand crosslinks and monoadducts accounting for 1-3% (4). Binding of HMGB proteins to 1,2-intrastrand crosslinks can contribute to cytotoxicity by shielding them from DNA repair (4, 5), while interstrand crosslinks are a particularly cytotoxic form of

DNA damage (7, 8). Numerous mechanisms of cisplatin resistance have been identified, including decreasing drug uptake (e.g. by downregulation of the copper transporter CTR1) increased efflux, and increased glutathione-based detoxification (6, 9). In addition, resistance can also arise from changes that increase a cell's capacity to either repair or tolerate DNA damage (10-12). It is this latter group of DNA repair and tolerance based mechanisms that have come under recent scrutiny as potential contributors to clinical cisplatin resistance.

REV3L, the catalytic subunit of the DNA Polζ, which plays a key role in the DNA damage tolerance mechanism of translesion synthesis (TLS) (13, 14), is of unusual interest because of its critical role in preventing cisplatin cytotoxicity. Notably, human cells expressing reduced levels of REV3L are more sensitive to killing by cisplatin (14, 15). Additionally, in an siRNA-based screen, a reduction in REV3L sensitized human cells to killing by cisplatin to an extent equal or greater to a reduction of BRCA1 (16). Finally, chicken DT40 cells deficient in Rev3 showed the highest sensitivity to cisplatin of any the DNA repair or checkpoint mutants tested (17). In *S. cerevisiae*, Polζ (Rev3 and its auxiliary subunit Rev7), functions together with Rev1 in the mutagenic branch of TLS that is responsible for most mutations induced by ultraviolet (UV) light and many chemical mutagens (18). The mammalian Rev3 orthologs, human *REV3L* and mouse *Rev3L*, are nearly twice the size of *S. cerevisiae Rev3*, mostly due to one large intron (14).

In mammalian cells, as in yeast, REV1, REV3L and REV7 are required for most of the mutagenesis induced by UV light and chemical mutagens such as benzo[a]pyrene diol epoxide (19, 20). REV3L function has also been implicated in homologous recombination, somatic hypermutation, cell-cycle control, and genome stability (14, 21). Notably, in response to DNA damaging agents such as UV light and benzo[a]pyrene diol epoxide, loss of Rev3 function has a greater effect on mutagenesis than cell survival (14). It seems likely that the striking sensitization to cisplatin killing caused by a reduction in REV3L levels is due to REV3L's roles in the specific repair of both cisplatin-induced intra- and interstrand crosslinks (22). Consistent with this idea, inhibition of REV7 (MAD2B) or REV1, which are also involved in the repair of both intra- and interstrand crosslinks (22), similarly sensitizes mammalian cells to cisplatin (22, 23).

Little is known, however about the effects of REV3L suppression on chemotherapeutic response in relevant pre-clinical settings. In this study, we examined the impact of Rev3l depletion on cisplatin response in a highly chemoresistant mouse model of late-stage lung adenocarcinoma. Given the striking similarities between lung tumors occurring in this Kras-driven mouse model and human NSCLC (24), our data suggest a rationale for targeting TLS as an adjuvant therapy in the treatment of advanced lung cancer.

4.3 Results

4.3.1 Rev3 deficiency sensitizes *LSL-Kras^{G12D}; p53$^{-/-}$* lung adenocarcinoma cells to cisplatin

To begin to examine the effects of Rev3L suppression on cisplatin response in a clinically-relevant mouse model system, we chose to use lung adenocarcinoma cell lines derived from previously described *LSL-Kras^{G12D}; p53$^{fl/fl}$* mice. Tumors generated in this context are thought to mirror human NSCLC with respect to overt clinical phenotype, as well as to core molecular mechanisms governing adenocarcinoma development (24, 25). Interestingly, recent work has shown that autochthonous *LSL-Kras^{G12D}; p53$^{-/-}$* lung tumors, like human NSCLC, also show intrinsic resistance to front-line chemotherapy (26). Most notably, these tumors proved to be refractory to cisplatin therapy, providing a system in which we could evaluate candidate drug-sensitizing genetic alterations. To this end, we designed and retrovirally expressed three unique short hairpin RNAs (shRNAs) targeting REV3L, and subsequently verified suppression of REV3L transcript by quantitative PCR (Q-PCR) in virally transduced target cells (Figure 1A). As impairment of translesion synthesis might have deleterious effects on cell growth or viability, we first sought to determine if our REV3L shRNAs impaired cell cycle progression. DNA content analysis did not reveal any change in population doubling time, nor was there any cell cycle defect, suggesting that our level of REV3L inhibition was not grossly affecting normal growth kinetics (Figure 1B, C). We then tested the effect of REV3L-depletion on cisplatin response and found all three shREV3L-expressing cell

populations to be markedly sensitized to drug relative to vector control-infected cells (Figure 1D). Additionally, when treated with a high dose of cisplatin and evaluated for long-term survival, cells lacking REV3L demonstrated a diminished capacity to recover from such an insult and consequently formed fewer colonies compared to treated control cells (Figure 1E, F).

REV3L deficiency in human and mouse cell lines has been associated with double strand breaks and chromosome instability (27, 28). Consistent with these prior observations, we saw a relative increase in the number and intensity of γ-H2AX foci, a surrogate marker for DNA double-strand breaks, following cisplatin treatment of REV3L knock-down cells (Figure 2A). Additionally, when examined over time by flow cytometry, REV3L-deficient cells failed to show a significant decrease in either the overall percentage of γ-H2AX-positive cells or in mean cellular γ-H2AX immunofluorescence intensity (Figure 2B). Coincident with the increase in cell death associated with this enhanced level of unrepaired DNA damage, we observed a pronounced cell cycle arrest phenotype within the surviving cell population. Specifically, cisplatin treated REV3L-deficient cells exhibited characteristics of DNA-damage induced senescence, including the appearance of a flattened, vacuolized cell morphology (Figure 2C) as well as the induction of senescence-associated β-galactosidase activity (Figure 2C, D). Thus REV3L suppression impairs the repair of cisplatin-induced DNA damage, leading to both cell death and irreversible cell cycle arrest.

Polζ is an error-prone DNA polymerase that is essential, not only for much of the mutagenesis that is caused by agents such as UV light, but for cisplatin-induced mutagenesis in human colon carcinoma cells and immortal human fibroblasts as well (15, 29). To evaluate the effect of REV3L knockdown on cisplatin-induced mutagenesis in our *LSL-Kras*^{G12D}*; p53*$^{-/-}$ cells, we performed a hypoxanthine phosphoribosyl-transferase (*hprt*) mutation assay where control and REV3L were treated with cisplatin, allowed to recover, and then selected in the presence of the toxic nucleoside analog 6-thioguanine (6-TG). As *hprt* function is required for 6-TG-mediated toxicity, this assay allows for the quantitation of cisplatin-induced *hprt* mutation. Cells expressing shREV3L-1 and shREV3L-2 shRNAs showed a dramatic reduction in 6-TG resistant colonies (4.7-6.6 fold) relative to control cells (Figure 2E). While shREV3L-3 transduced cells also showed a decrease in colony number, this decrease was not statistically significant. Notably, this shRNA also produces less cisplatin sensitization than shREV3L-1 and shREV3L-2 in colony outgrowth assays. Taken together, these cell-based assays suggest that reducing the level of REV3L not only sensitizes a highly resistant lung cancer cells to cisplatin, but also prevents cisplatin-induced mutation in surviving cells.

4.3.2 Development of a genetically tractable lung adenocarcinoma transplant system

While cell-based treatment studies may yield important insight into potential tumor responses to therapy, achieving durable therapeutic responses in

malignancies in their native microenvironment has proven considerably more difficult (30). Thus, we decided to evaluate the potential of REV3L inhibition as a strategy to improve upon existing cisplatin-based chemotherapeutic regimens in an established preclinical model of NSCLC. To this end, we adapted methodologies previously used for tumor transplantation in hematopoietic malignancies for use in our lung adenocarcinoma cell line (31). Such an approach allows for rapid manipulation of *in vivo* tumor cell genetics, without the requirement for generating stable genetically engineered mouse models. Lung adenocarcinoma cells (~$5x10^4$) were intravenously injected via tail vein into syngeneic immuno-competent recipient mice. As early as 20 days post-transplantation, highly proliferative tumor foci were detectable in the lung (Figure 3A), with nearly every recipient mouse exhibiting a disseminated disease within 30-35 days (Figure 3B). Notably, tumor presentation was specific to the lung, suggesting that either the route of cell delivery or the lung microenvironment restricts the development of transplanted malignancies to the appropriate target organ.

To assess the ability of these transplanted cells to recapitulate the original disease, we examined overall tumor histology. Transplanted tumors exhibited features reminiscent of their epithelial origin in the lung – namely, alveolar and sheet-like structures (Figure 3B). Interestingly, we found that the transplants displayed a markedly aggressive morphology, consistent with hallmark features of late-stage carcinomas. In some cases, the transplanted tumors breached the

visceral pleura, penetrating the pleural space proximal to the chest cavity (Figure 3B, bottom right panel). Immunohistochemical staining of tumor specimens with antibodies targeting Nkx2.1 and HMGA2, two markers of lung adenocarcinoma progression (Winslow and Jacks, personal communication), further suggested that these transplants represent a highly aggressive version of the disease suitable for modeling the treatment of late-stage lung cancer (Figure 3C).

4.3.3 REV3L depletion sensitizes lung adenocarcinoma transplants to cisplatin *in vivo*

Using the most potent shRNA targeting REV3L, we transplanted pure populations of retrovirally-infected lung adenocarcinoma cells into syngeneic recipient mice and allowed tumors to form (~3-4 weeks). Mice were subsequently sacrificed 48h following cisplatin treatment to analyze the effects of cisplatin on tumor cell proliferation rate and survival. Histopathological evaluation of harvested tumors corroborated our *in vitro* observations, as we noted both a decrease in mitotic index (Figure 4A) as well as an increase in apoptosis (Figure 4B) in treated REV3L-deficient transplants.

In order to more carefully examine the effect of REV3L suppression on lung adenocarcinoma response to cisplatin, we took an *in vivo* imaging-based approach that allowed us to study individual tumor dynamics over a course of therapy. Using a microcomputed tomography (microCT) imaging platform, we were able to image the lung and surrounding tissues at regular intervals to identify and subsequently track disease progression in individual tumor-bearing

mice over the course of cisplatin treatment. As illustrated in reconstructed 3D isosurface and 2D axial images taken ten days following the initiation of therapy (10mg/kg cisplatin on day 0), Rev3-deficient transplants exhibited an enhanced response to cisplatin relative to controls (Figure 5). This was evidenced at the level of individual tumors (Figure 5A-C) as well as in the broader context of the entire lung (Figure 5D, E). Indeed, quantitative evidence of overall tumor regression or at a minimum, growth stasis, was observed in cisplatin-treated REV3L-knockdown transplants, whereas most control transplants continued to grow and displace healthy lung volume (Figure 5E). Importantly, Kaplan-Meier analysis of overall survival supported these imaging-based observations, with mice harboring Rev3-deficient transplants surviving nearly twice as long compared to the control cohort (Figure 5F).

4.4 Discussion

Our experiments provide a striking illustration of how reducing the activity of a key translesion DNA polymerase can make an intractable lung cancer model of NSCLC susceptible to cisplatin-based chemotherapy. Thus, REV3L represents a *bona fide* lung cancer drug target. Inhibiting REV3L activity or expression may be particularly effective in this context, since cisplatin treatment, itself, increases REV3L mRNA levels (15) and elevated REV3L has been shown to promote cisplatin resistance (12). Notably, similar therapies that exploit DNA repair deficiencies, including the use of PARP inhibitors in BRCA1/2 deficient tumor cells (32, 33), have emerged as promising approaches targeting highly chemoresistant malignancies. While it is unclear whether advanced malignancies acquire a similar dependence upon REV3L function, cell based studies examining gliomas – a highly chemoresistant malignancy - have documented elevated levels of REV3L in this setting and shown that downregulation of REV3L sensitizes these cells to cisplatin (12). Interestingly, mismatch repair (MMR) deficient tumor cells also show up to 20X increases in REV3L levels (34), suggesting that malignancies driven by mutagenesis in the absence of MMR may be particularly reliant upon REV3L function.

The striking cisplatin sensitization seen in the absence of REV3L may result from the dual requirement for REV3L function in the repair of both intrastrand crosslinks, which constitute the majority of the lesions, as well as highly toxic interstrand crosslinks, which are much less frequent. The functions of

Polζ (REV3L/REV7), REV1, Polη, and RAD18 are all required for replicative bypass of cisplatin intrastrand crosslinks (22). Polζ has been shown to cooperate wih Polη and Polκ in error-free and error-prone TLS, respectively over a 1,2-GpG cisplatin adduct (35). In addition, Polζ and REV1 have been hypothesized to facilitate repair of interstrand crosslinks independently of PCNA monoubiquitination (22). Furthermore, biochemical analyses of replication-dependent interstrand crosslink repair using Xenopus extracts have implicated Polζ in the translesion synthesis across from the crosslink during the repair process (36).

A potential benefit to a chemotherapeutic strategy that relies on combining a reduction in REV3L activity/expression with a DNA damaging chemotherapeutic agent is that cisplatin-induced mutagenesis might also be reduced. *In vitro* studies of immortal human fibroblasts have shown that reduced levels of REV3L lowers cisplatin-induced mutation, including mutation that leads to cisplatin resistance (15). Additionally (as shown in the following chapter), we use another clinically relevant mouse model to illustrate how interfering with REV1/REV3L/REV7 pathway of mutagenic TLS can reduce the frequency of acquired drug resistance following tumor relapse.

While specific TLS inhibitors have not been developed, improvements to *in vivo* RNAi delivery methodologies suggest that adjuvant siRNA therapies may be achievable in accessible tumor sites (37). Additionally, the development of

specific inhibitors targeting critical protein interactions in TLS polymerase complexes holds significant therapeutic promise. While it is reasonable to believe that rapidly growing tumor cells have a greater requirement for TLS function, future work will be required to determine whether TLS inhibition can be achieved in tumors without enhancing cisplatin-related normal cell toxicity.

Genetically engineered mouse models of cancer provide the opportunity to validate candidate drug targets in relevant pathophysiologic settings (30, 38). While autochthonous tumor models represent the ideal context for such studies, efficient mechanisms to introduce diverse genetic alterations into such models are currently lacking. This is particularly true for drug sensitization experiments, where all tumor cells may need to be modified to see a therapeutic effect. Here, we have developed a tumor transplant approach that allows for rapid *ex vivo* modification of lung adenocarcinoma cells. Importantly, transplanted tumors develop in the appropriate organ system, in the presence of an adaptive immune system, and are pathologically similar to aggressive autochthonous tumors. While this does not supplant the subsequent value of autochthonous tumor models, it may inform their development. Additionally, we have recently shown that large-scale RNAi-based screening approaches can be performed *in vivo* (39). Thus, robust transplantation of cell lines derived from Kras-driven lung tumor models may not only serve as an attractive setting in which to evaluate putative mediators of chemotherapeutic response, but may also function as a

platform from which to screen for and identify novel genetic factors capable of sensitizing aggressive NSCLC to existing chemotherapies.

4.5 Materials and methods

4.5.1 Cell culture, retroviral vectors, and chemicals

Mouse lung adenocarcinoma cells were cultured in standard DMEM/10% FBS media. shRNA constructs were designed and cloned as previously described (31). Sequences (5'-3') targeted by shRNAs are as follows: shRev3-1: TTTACTACAGATACCATGCTG, shRev3-2: TATCTTTATAAGCTGCTCCTG, shRev3-3: TACAGTTATACAAATATCCTA. Cloning strategies and primer sequences are available from the authors on request. Retrovirally-infected cells were then selected with puromycin. Cisplatin was purchased from Calbiochem and used at the indicated concentrations (0-15uM). For *in vivo* studies, cisplatin was dissolved in a 0.9% NaCl solution, protected from light, and immediately injected intraperitoneally into tumor-bearing mice. X-gal for senescent cell identification was purchased from USB Corporation.

4.5.2 RT-qPCR, Immunohistochemistry, and Immunofluorescence

For real-time quantitative PCR, total RNA was isolated after retroviral infection and puromycin selection. RT-qPCR was performed using SYBR green on a BioRad thermal cycler. GAPDH and Rev3 primer sequences are available upon request. For immunohistochemistry assays, mice were sacrificed by CO_2 asphyxiation and lungs were fixed overnight in 10% neutral-buffered formalin. Lung lobes were separated and embedded in paraffin according to standard procedures. Lungs were sectioned at 4μm and stained with hematoxylin and eosin for tumor pathology. For detection of cleaved caspase 3 (CC3, Cell

Signaling, 1:500) and phospho-histone-H3 (pH3, Cell Signaling, 1:200), TTF-1 (Nkx2.1, Epitomics, 1:200), HMGA2 (Biocheck, 1:500), tissue sections were subjected to antigen retrieval in citrate buffer, blocked in 3% H202 for 10 min, blocked for 1 hr in 5% serum/PBS-T, and stained overnight at 4°C. Secondary antibodies were used according to Vectastain ABC kits (Vector Laboratories). Cells for immunofluorescence were grown and treated on poly-L-lysine coated coverslips, fixed with 100% methanol for 5 minutes at -20°C and stored for later use. Anti-gamma-H2AX (Upstate, 1:500) was used along with an Alexa secondary (568) antibody (Molecular Probes) to visualize gH2AX foci. Stained coverslips were imaged and analyzed using Applied Precision DeltaVision instruments and deconvolution software.

4.5.3 *In vitro* viability assays and FACS

For short-term viability assays, cells were seeded in triplicate (6×10^3 per well) in 96-well plates and treated as indicated with cisplatin. After 48 h treatment, cell viability was measured using Cell-Titer-Glo (Promega) on an Applied Biosystems microplate luminometer. Long-term viability assays were performed by initially treating $4x10^5$ lung adenocarcinoma cells with 15uM cisplatin for 24h. Four days following treatment, cells were split 1:20 onto a fresh 10cm plate and allowed to form colonies for ~10d. To visualize colonies, plates were washed with 0.05% ethidium bromide (in 50%EtOH) for 10-15 seconds and imaged using a UV-gel box/camera. Images were processed and colonies counted using ImageJ software. All flow cytometry was performed using Becton-

Dickinson FACScan or MoFlo flow cytometers. Cell death was detected by propidium iodide (PI) incorporation (0.05 mg/mL), and dead cells were excluded from GFP analysis. Live cell sorting was performed using GFP co-expression as a marker of cell transduction. For γ-H2AX assays, cells were fixed in 70% EtOH, then stained using an anti-gH2AX antibody (Upstate, 1:2500) followed by an Alexa (488) secondary antibody. Stained cells were then co-stained in a sodium citrate/PI buffer prior to FACS analysis and subsequently analyzed using FloJo software.

4.5.4 Mutagenesis *(hprt)* assay

Retrovirally transduced cells were initially cultured for a minimum of two weeks in media containing hypoxanthine, aminopterin, and thymidine (HAT) to remove any pre-existing *hprt*- variants from the population. Cells were then split into fresh media (-HAT) 24h prior to treatment with cisplatin. Target cells were then mutagenized with 15μM cisplatin for 1hr, allowed to recover, and passaged for an additional 10 days (in the absence of HAT) to stabilize any induced mutations. Mutagenized cells were then split onto fresh 10cm plates in media containing 6-thioguanine (6-TG) to select for variants with impaired hprt function. Resultant colonies were visualized using 0.05% ethidium bromide (see above) and imaged using a UV-gel box/camera. Images were processed and colonies counted using ImageJ software.

4.5.5 *In vivo* transplantation and imaging

Lung adenocarcinoma cells (~$5x10^4$) were intravenously injected into the tail vein of syngeneic C57BL6/Jx129-JAE male recipient mice and monitored weekly using a GE Healthcare microCT imaging device (45-μm resolution, 80 kV, with 450-μA current) beginning 3 weeks following injection. Images were acquired and processed using GE eXplore software.

Figure 1

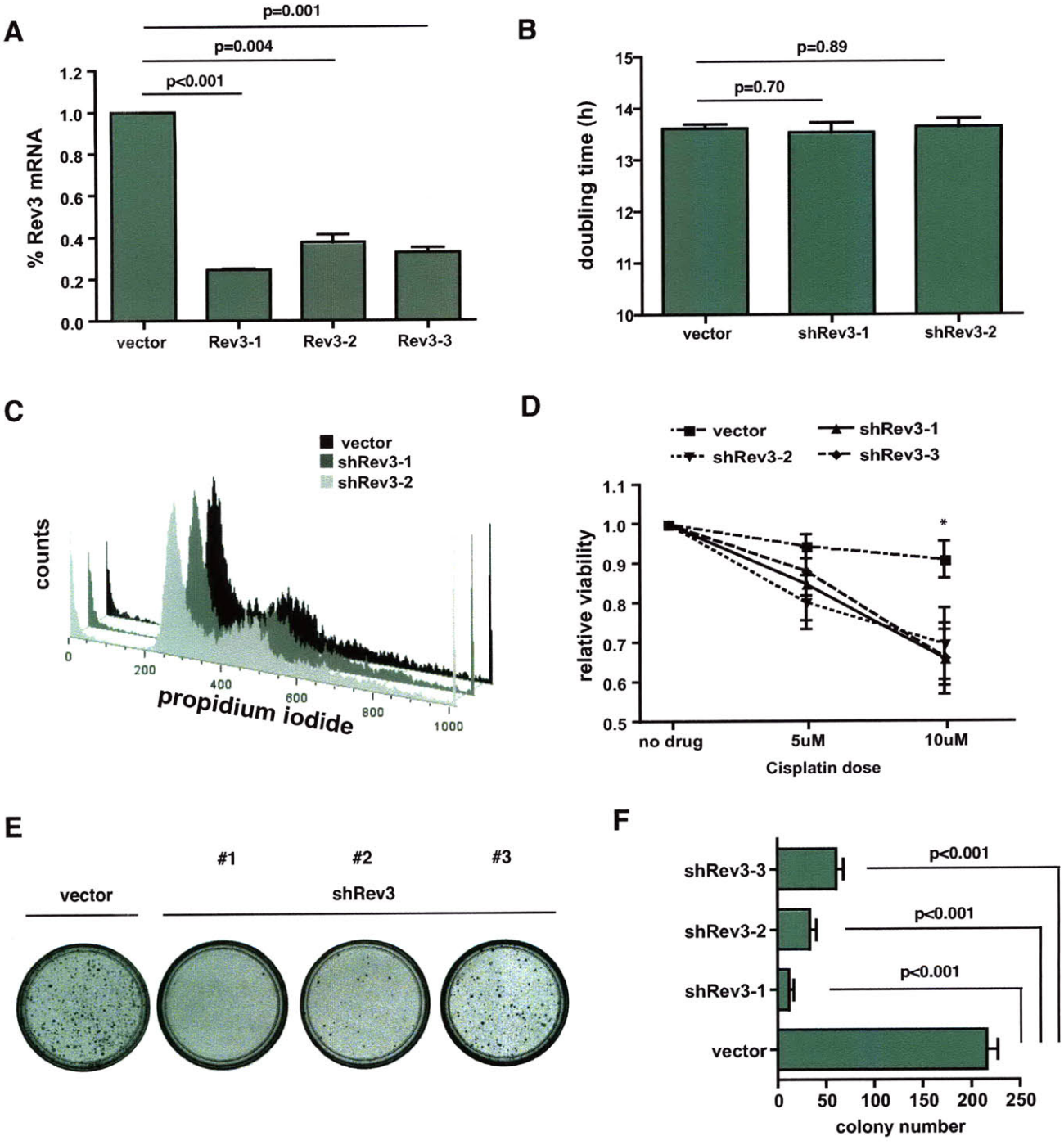
A
p=0.001
p=0.004
p<0.001
% Rev3 mRNA
1.2
1.0
0.8
0.6
0.4
0.2
0.0
vector
Rev3-1
Rev3-2
Rev3-3
B
p=0.89
p=0.70
doubling time (h)
15
14
13
12
11
10
vector
shRev3-1
shRev3-2
C
vector
shRev3-1
shRev3-2
counts
0
200
400
600
800
1000
propidium iodide
D
vector
shRev3-1
shRev3-2
shRev3-3
relative viability
1.1
1.0
0.9
0.8
0.7
0.6
0.5
*
no drug
5uM
10uM
Cisplatin dose
E
#1
#2
#3
vector
shRev3
F
shRev3-3
shRev3-2
shRev3-1
vector
p<0.001
p<0.001
p<0.001
0
50
100
150
200
250
colony number

Figure 1 – Rev3-deficiency sensitizes LSL-KrasG12D; p53-/- lung adenocarcinoma cells to cisplatin.

(A) qRT-PCR (n≥3) confirmation of Rev3 mRNA suppression in transduced cell populations. Untreated control and Rev3 knock down cells were counted and analyzed by flow cytometry to determine (B) overall population doubling times, and (C) cell cycle distribution profiles (DNA content histogram). (D) Overall cell survival following cisplatin treatment was compared for adenocarcinoma cells transduced with a Rev3 shRNA or a control Cells were then treated with cisplatin and monitored for cell survival (Cell-Titer-Glo) reagents relative to treated vector control cells (n=3 independently treated samples for each construct, +/- s.d. The asterisk represents a statistical significance of $p<0.05$ for all three shRev3 constructs at this dose). (E) A long-term (14d) colony-outgrowth assay comparing shRev3 and vector control transduced lung adenocarcinoma cells treated with 15μM cisplatin. The images shown depict representative 10cm plates stained with propidium iodide (PI) to visualize colonies. (F) Quantification of images collected from three independently treated populations of cells. Data represents the mean colony number +/- s.d.

Figure 2

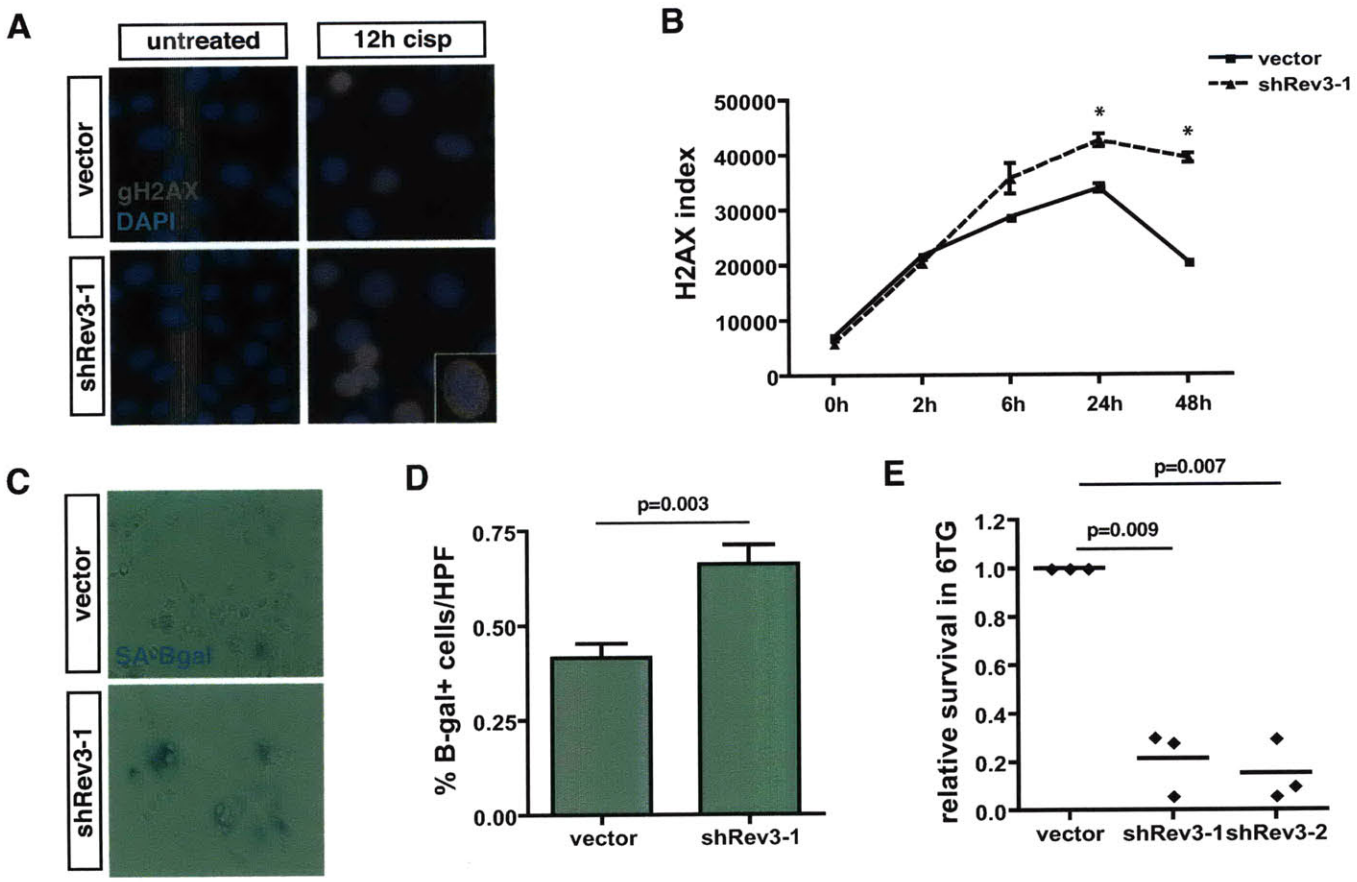

Figure 2 – Rev3 depletion promotes cisplatin-induced DNA damage while limiting associated mutagenesis.

(A) Immunofluorescence images of control and shRev3 expressing lung adenocarcinoma cells treated with 10μM cisplatin and incubated with an anti-?-H2AX antibody. (B) Flow-cytometric analysis of ?-H2AX immunofluorescence in cisplatin treated cells. The ?-H2AX index was calculated by multiplying the number of ?-H2AX-positive cells by the mean intensity of the ?-H2AX population (n=3 independently treated samples at each timepoint). (C) ?-galactosidase staining of control and Rev3 knock down cells seven days after treatment with 2.5μM cisplatin. (D) Senescent cells were identified using a standard X-gal staining protocol and manually quantified from representative microscope images. Data represents the mean of six 40x high power fields (HPF) from two independent samples for each experimental condition. (E) A cisplatin in vitro mutagenesis assay. Shown is the relative colony forming ability of control and Rev3-deficient cells treated with 15μM cisplatin and then selected for 6-thioguanine resistance. Each data point represents an independently treated and selected experimental replicate.

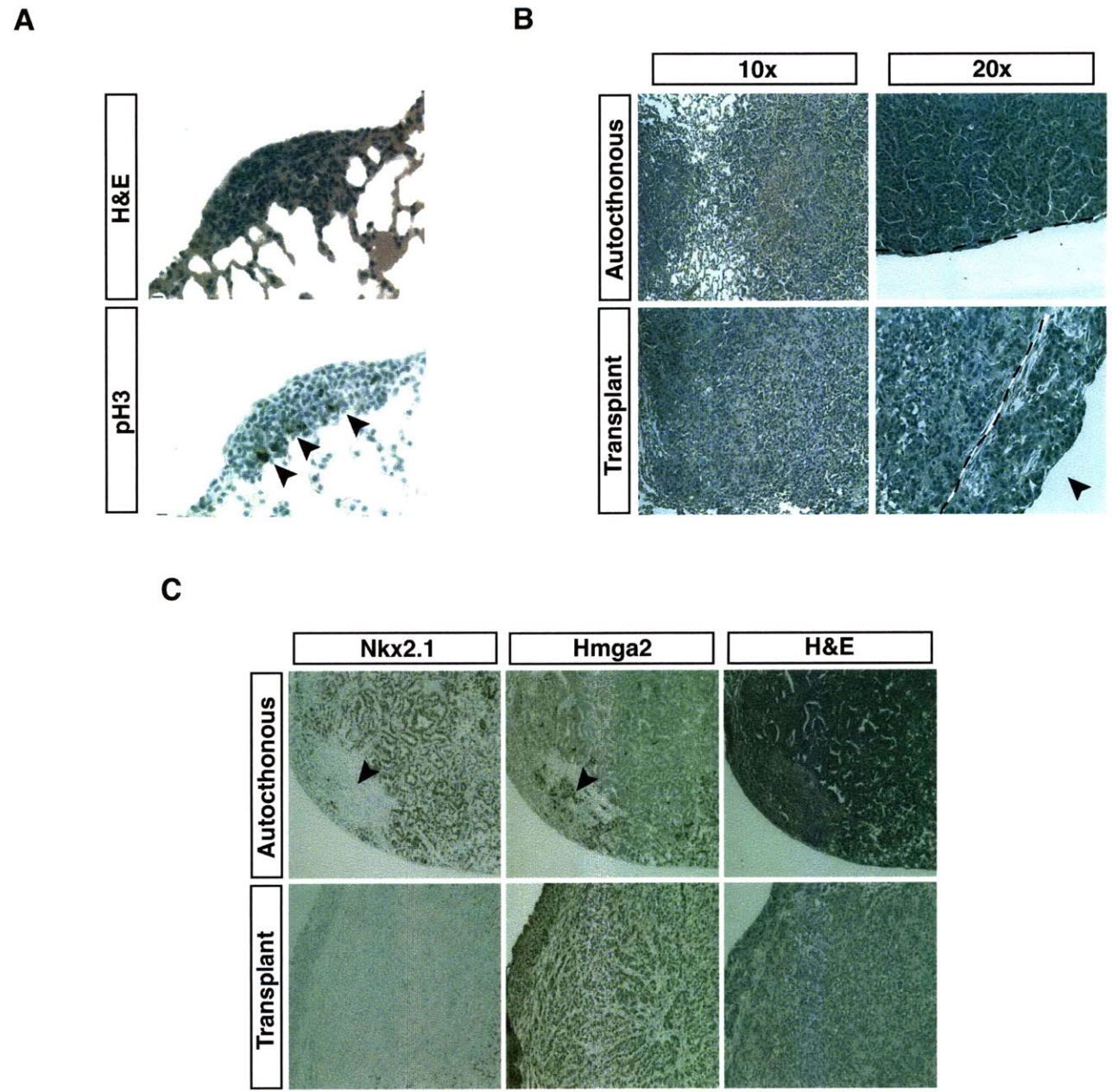
A
H&E
pH3
B
10x
20x
Autocthonous
Transplant
C
Nkx2.1
Hmga2
H&E
Autocthonous
Transplant

Figure 3 – Histological analysis of LSL-KrasG12D; p53-/- adenocarcinoma transplants. (A) H&E (top) and anti-phospho histone H3 (pH3) immunohistochemical (bottom) staining of lung adenocarcinoma transplants harvested at 18 days post injection. Arrows demarcate pH3-positive cells. (B) H&E staining of tumor transplants harvested at 30 days post injection, as well as representative images of an autocthonous LSL-KrasG12D; p53-/- lung adenocarcinoma. The dotted line represents the visceral pleural boundary, with an arrow highlighting the tumor mass extending into the pleural space. (C) Anti-Nkx2.1 and anti-HMGA2 immunostaining of early and late stage lung adenocarcinomas, respectively. The arrows indicate a region in the autocthonous tumor with high expression of the late-stage marker HMGA2 and corresponding down-regulation of the early-stage marker Nkx2.1.

Figure 4

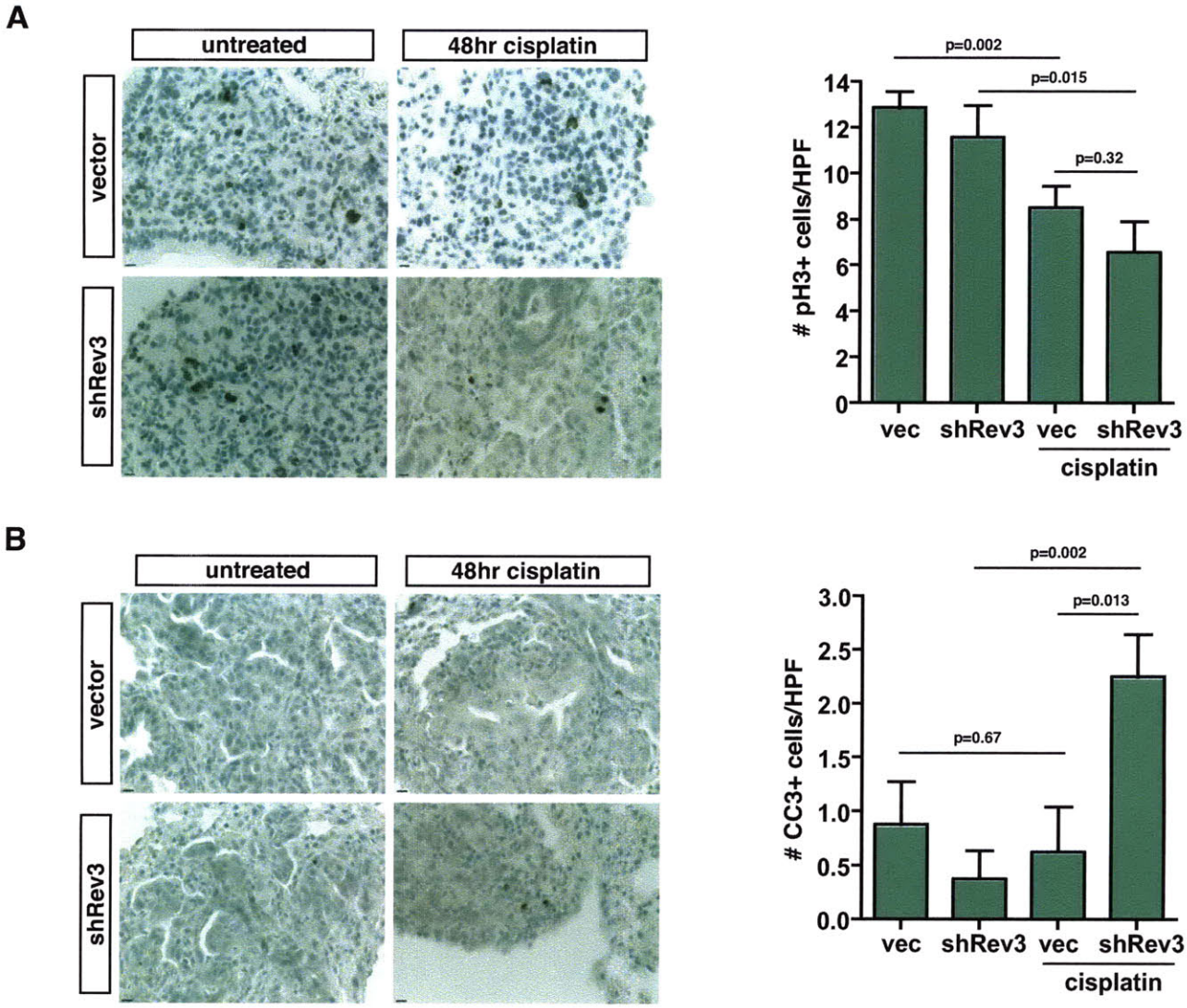

Figure 4 – Rev3 depletion sensitizes transplanted lung adenocarcinoma to cisplatin.

(A) anti-phosphoH3 and (B) cleaved caspase 3 staining of control and shRev3 transduced tumor transplants 48 hours following treatment with 10mg/kg cisplatin. Tumors were treated upon detection of tumor mass by microCT. P-values were determined using two-tailed Student's t-tests.

Figure 5

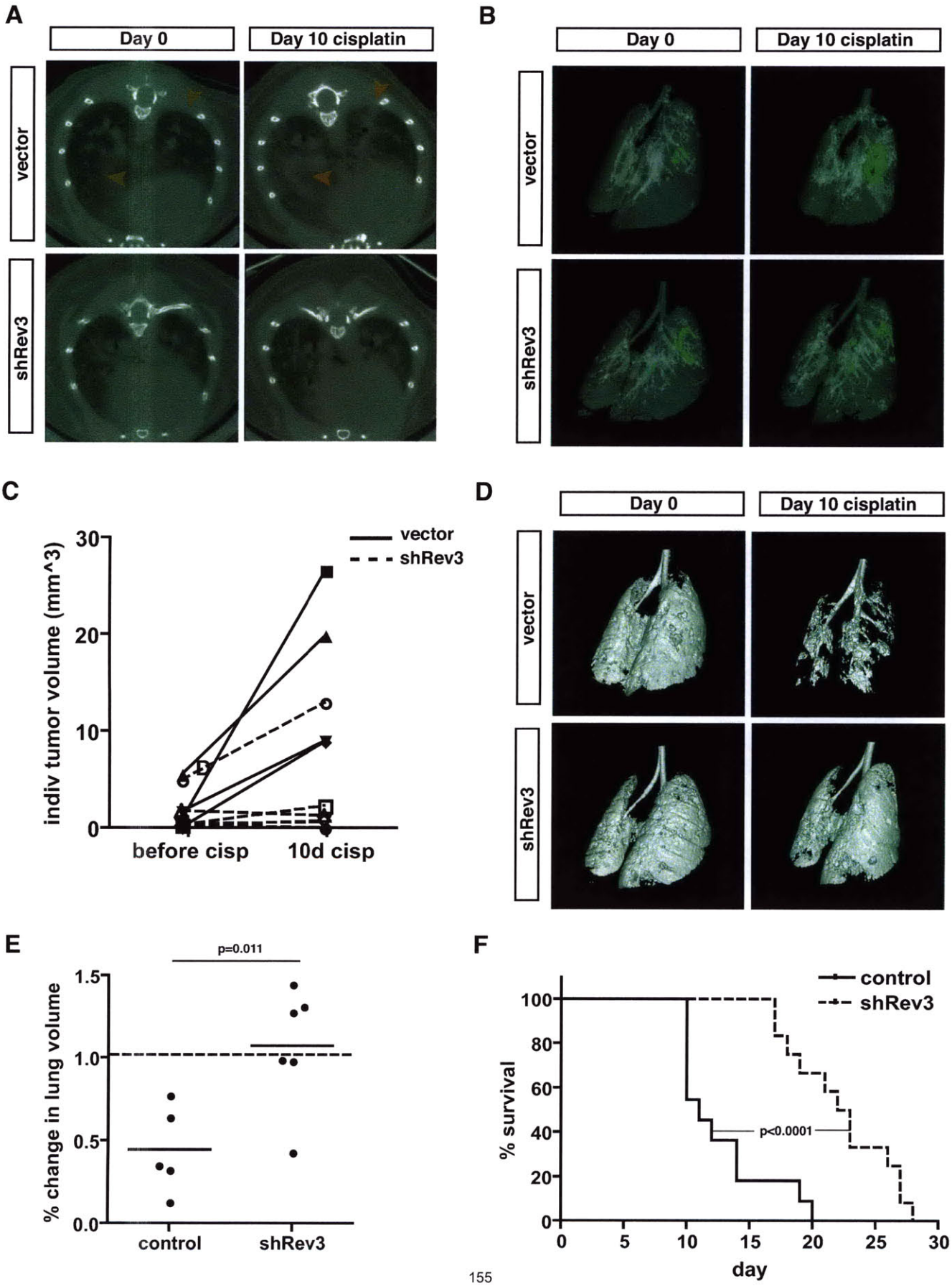
A
Day 0
Day 10 cisplatin
vector
shRev3
B
Day 0
Day 10 cisplatin
vector
shRev3
C
indiv tumor volume (mm^3)
30
20
10
0
vector
shRev3
before cisp
10d cisp
D
Day 0
Day 10 cisplatin
vector
shRev3
E
p=0.011
% change in lung volume
1.5
1.0
0.5
0.0
control
shRev3
F
control
shRev3
% survival
100
80
60
40
20
0
p<0.0001
0
5
10
15
20
25
30
day

Figure 5 – Rev3 depletion promotes cisplatin efficacy in vivo.
(A) Representative axial images of mouse lungs harboring transplanted lung adenocarcinoma cells. The darker areas represent healthy, air-filled lung space, whereas the lighter shades highlight denser tissues, including areas populated by tumor cells. Red arrowheads demarcate individual tumors in treated control mice that respond poorly to cisplatin treatment. (B) 3-D isosurface projections of selected lung regions. Green staining indicates lung adenocarcinoma mass. (C) Individual tumor volume calculations for several control and shRev3 transplants. (D) Inverse 3-D isosurface projections of healthy lung volume before and after cisplatin treatment. White/gray surfaces indicate disease-free, healthy lung space whereas hollowed-out voids indicate the presence of tumor material. (E) Quantification of healthy lung volumes from (D). P-values were determined using a Student's t-test. (F) A Kaplan-Meier curve comparing survival of mice bearing shRev3-infected transplants versus mice bearing control tumors following treatment with cisplatin (vector, n=11; shRev3, n=12; median survival time = 11 and 22.5 days, respectively). P-values were determined using a log rank test.

Supplemental Figure S1

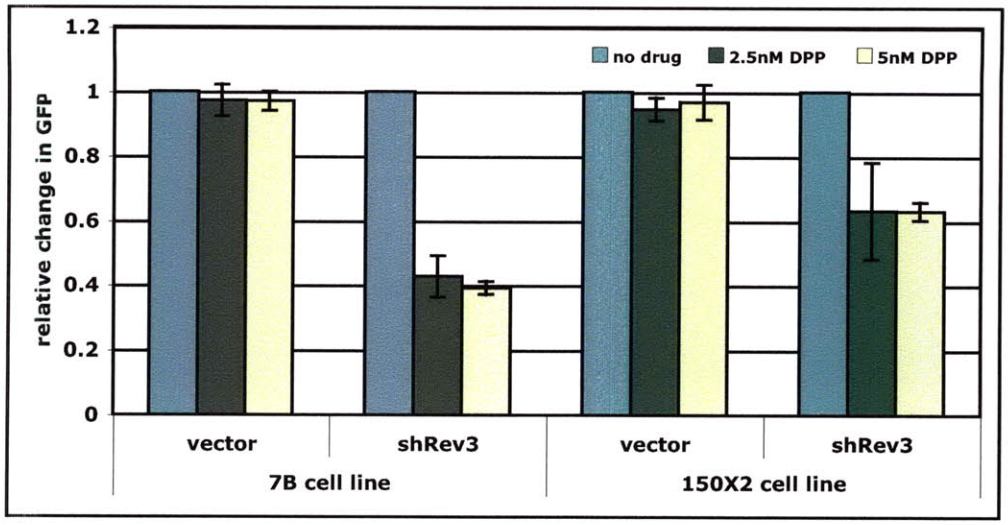

Supplemental Figure S1- Rev3 knockdown sensitizes additional Kras;p53 lung adenocarcinoma cell lines to cisplatin

Shown is a graph of relative GFP percentage obtained from a 72h in vitro GFP competition assay. The '7B' cell line was used extensively throughout this thesis. The 150X2 cell line was independently derived by Trudy Oliver (Tyler Jacks lab).

Supplemental Figure S2

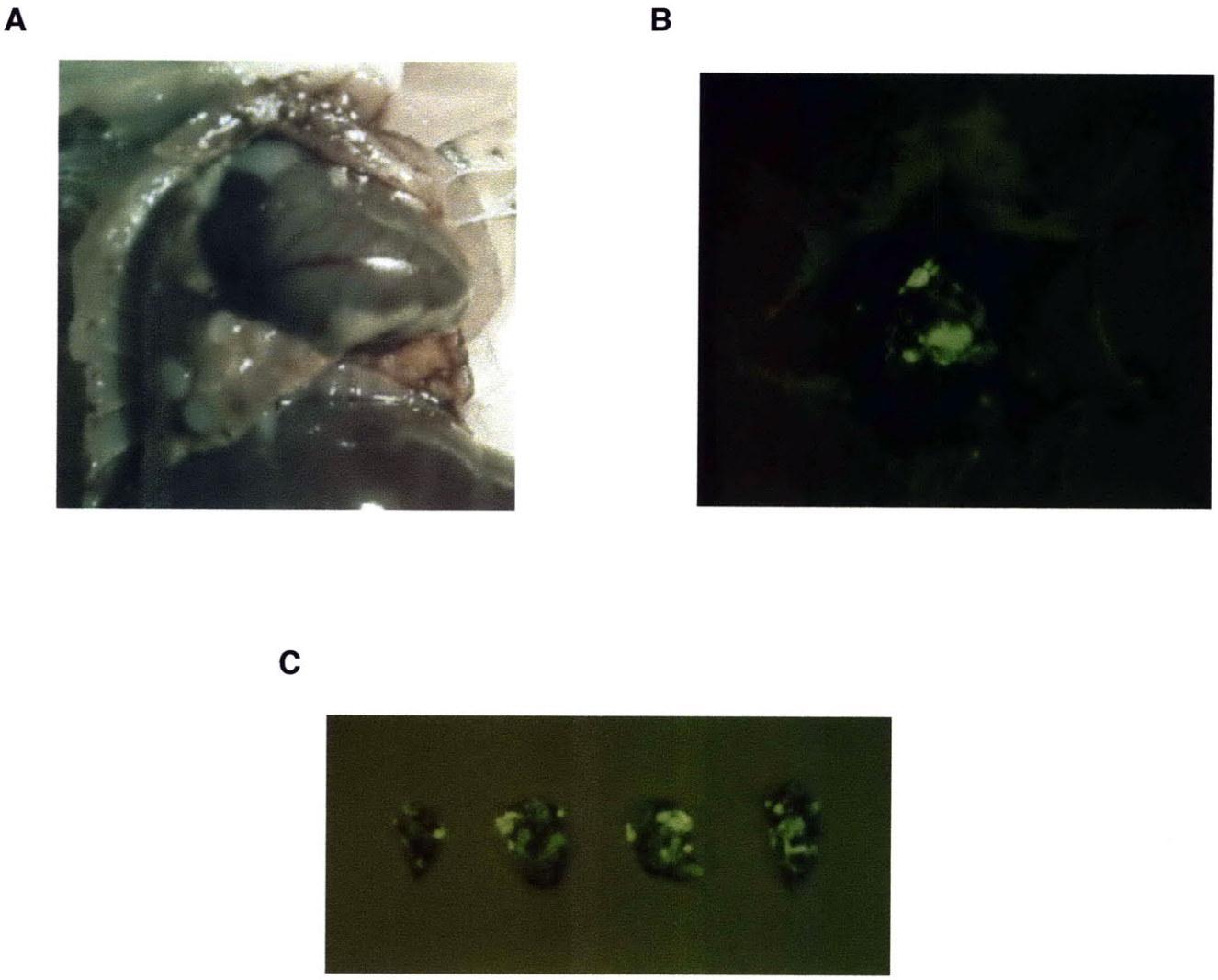

Supplemental Figure S2- Lung adenocarcinoma transplant images
(A) Gross morphological depiction of lung adenocarcinoma transplants 30d post injection. (B and C) GFP images of lungs harboring control GFP-transduced transplants.

4.8 Acknowledgements

I would like to thanks members of the Hemann and Walker labs for helpful advice and discussions. M.T.H. is a Rita Allen Fellow and the Latham Family Career Development Assistant Professor of Biology and is supported by NIH RO1 CA128803. T.J. is a Howard Hughes Medical Institute Investigator and a Daniel K. Ludwig Scholar. G.C.W. is an American Cancer Society Research Professor and is supported by NIEHS ES015818 and grant P30 ES002109 from the Center of Environmental Health Sciences (MIT). J.D. is supported by the MIT Department of Biology training grant and a Ludwig Center Graduate Fellowship.

4.9 References

1. Goss GD, Arnold A, Shepherd FA, et al. Randomized, Double-Blind Trial of Carboplatin and Paclitaxel With Either Daily Oral Cediranib or Placebo in Advanced Non-Small-Cell Lung Cancer: NCIC Clinical Trials Group BR24 Study. J Clin Oncol 2009.

2. Finlay GA, Joseph B, Rodrigues CR, Griffith J, White AC. Advanced presentation of lung cancer in Asian immigrants: a case-control study. Chest 2002;122(6):1938-43.

3. U.S. National Institutes of Heath NCI. Surveillance Epidemiology and End Results (SEER) Cancer Statistics Review. 1999-2005 [cited; Available from:

4. Ahmad S. Platinum-DNA interactions and subsequent cellular processes controlling sensitivity to anticancer platinum complexes. Chem Biodivers;7(3):543-66.

5. Jung Y, Lippard SJ. Direct cellular responses to platinum-induced DNA damage. Chem Rev 2007;107(5):1387-407.

6. Fuertes MA, Castilla J, Alonso C, Perez JM. Cisplatin biochemical mechanism of action: from cytotoxicity to induction of cell death through interconnections between apoptotic and necrotic pathways. Curr Med Chem 2003;10(3):257-66.

7. McVey M. Strategies for DNA interstrand crosslink repair: Insights from worms, flies, frogs, and slime molds. Environ Mol Mutagen.

8. Scharer OD. DNA interstrand crosslinks: natural and drug-induced DNA adducts that induce unique cellular responses. Chembiochem 2005;6(1):27-32.

9. Brozovic A, Ambriovic-Ristov A, Osmak M. The relationship between cisplatin-induced reactive oxygen species, glutathione, and BCL-2 and resistance to cisplatin. Crit Rev Toxicol;40(4):347-59.

10. Li J, Li ZN, Du YJ, Li XQ, Bao QL, Chen P. Expression of MRP1, BCRP, LRP, and ERCC1 in advanced non-small-cell lung cancer: correlation with response to chemotherapy and survival. Clin Lung Cancer 2009;10(6):414-21.

11. Larminat F, Bohr VA. Role of the human ERCC-1 gene in gene-specific repair of cisplatin-induced DNA damage. Nucleic Acids Res 1994;22(15):3005-10.

12. Wang H, Zhang SY, Wang S, et al. REV3L confers chemoresistance to cisplatin in human gliomas: the potential of its RNAi for synergistic therapy. Neuro Oncol 2009;11(6):790-802.

13. Errol Friedberg GW, Wolfram Siede, Richard Wood, Roger Shultz, Tom Ellenberger. DNA Repair and Mutagenesis. 2 ed: ASM Press; 2005.

14. Gan GN, Wittschieben JP, Wittschieben BO, Wood RD. DNA polymerase zeta (pol zeta) in higher eukaryotes. Cell Res 2008;18(1):174-83.

15. Wu F, Lin X, Okuda T, Howell SB. DNA polymerase zeta regulates cisplatin cytotoxicity, mutagenicity, and the rate of development of cisplatin resistance. Cancer Res 2004;64(21):8029-35.

16. Bartz SR, Zhang Z, Burchard J, et al. Small interfering RNA screens reveal enhanced cisplatin cytotoxicity in tumor cells having both BRCA network and TP53 disruptions. Mol Cell Biol 2006;26(24):9377-86.

17. Nojima K, Hochegger H, Saberi A, et al. Multiple repair pathways mediate tolerance to chemotherapeutic cross-linking agents in vertebrate cells. Cancer Res 2005;65(24):11704-11.

18. Waters LS, Minesinger BK, Wiltrout ME, D'Souza S, Woodruff RV, Walker GC. Eukaryotic translesion polymerases and their roles and regulation in DNA damage tolerance. Microbiol Mol Biol Rev 2009;73(1):134-54.

19. Li Z, Zhang H, McManus TP, McCormick JJ, Lawrence CW, Maher VM. hREV3 is essential for error-prone translesion synthesis past UV or benzo[a]pyrene diol epoxide-induced DNA lesions in human fibroblasts. Mutat Res 2002;510(1-2):71-80.

20. Diaz M, Watson NB, Turkington G, Verkoczy LK, Klinman NR, McGregor WG. Decreased frequency and highly aberrant spectrum of ultraviolet-induced mutations in the hprt gene of mouse fibroblasts expressing antisense RNA to DNA polymerase zeta. Mol Cancer Res 2003;1(11):836-47.

21. Schenten D, Kracker S, Esposito G, et al. Pol zeta ablation in B cells impairs the germinal center reaction, class switch recombination, DNA break repair, and genome stability. J Exp Med 2009;206(2):477-90.

22. Hicks JK, Chute CL, Paulsen MT, et al. Differential roles for DNA polymerases eta, zeta, and REV1 in lesion bypass of intrastrand versus interstrand DNA cross-links. Mol Cell Biol;30(5):1217-30.

23. Okuda T, Lin X, Trang J, Howell SB. Suppression of hREV1 expression reduces the rate at which human ovarian carcinoma cells acquire resistance to cisplatin. Mol Pharmacol 2005;67(6):1852-60.

24. Sweet-Cordero A, Mukherjee S, Subramanian A, et al. An oncogenic KRAS2 expression signature identified by cross-species gene-expression analysis. Nat Genet 2005;37(1):48-55.

25. Kim CF, Jackson EL, Kirsch DG, et al. Mouse models of human non-small-cell lung cancer: raising the bar. Cold Spring Harb Symp Quant Biol 2005;70:241-50.

26. Oliver TG, Mercer KL, Sayles LC, et al. Chronic cisplatin treatment promotes enhanced damage repair and tumor progression in a mouse model of lung cancer. Genes Dev;24(8):837-52.

27. Brondello JM, Pillaire MJ, Rodriguez C, et al. Novel evidences for a tumor suppressor role of Rev3, the catalytic subunit of Pol zeta. Oncogene 2008;27(47):6093-101.

28. Wittschieben JP, Reshmi SC, Gollin SM, Wood RD. Loss of DNA polymerase zeta causes chromosomal instability in mammalian cells. Cancer Res 2006;66(1):134-42.

29. Lin X, Okuda T, Trang J, Howell SB. Human REV1 modulates the cytotoxicity and mutagenicity of cisplatin in human ovarian carcinoma cells. Mol Pharmacol 2006;69(5):1748-54.

30. Sharpless NE, Depinho RA. The mighty mouse: genetically engineered mouse models in cancer drug development. Nat Rev Drug Discov 2006;5(9):741-54.

31. Burgess DJ, Doles J, Zender L, et al. Topoisomerase levels determine chemotherapy response in vitro and in vivo. Proc Natl Acad Sci U S A 2008;105(26):9053-8.

32. Farmer H, McCabe N, Lord CJ, et al. Targeting the DNA repair defect in BRCA mutant cells as a therapeutic strategy. Nature 2005;434(7035):917-21.

33. Bryant HE, Schultz N, Thomas HD, et al. Specific killing of BRCA2-deficient tumours with inhibitors of poly(ADP-ribose) polymerase. Nature 2005;434(7035):913-7.

34. Lin X, Howell SB. DNA mismatch repair and p53 function are major determinants of the rate of development of cisplatin resistance. Mol Cancer Ther 2006;5(5):1239-47.

35. Shachar S, Ziv O, Avkin S, et al. Two-polymerase mechanisms dictate error-free and error-prone translesion DNA synthesis in mammals. Embo J 2009;28(4):383-93.

36. Raschle M, Knipscheer P, Enoiu M, et al. Mechanism of replication-coupled DNA interstrand crosslink repair. Cell 2008;134(6):969-80.

37. Wullner U, Neef I, Tur MK, Barth S. Targeted delivery of short interfering RNAs--strategies for in vivo delivery. Recent Pat Anticancer Drug Discov 2009;4(1):1-8.

38. Van Dyke T, Jacks T. Cancer modeling in the modern era: progress and challenges. Cell 2002;108(2):135-44.

39. Meacham CE, Ho EE, Dubrovsky E, Gertler FB, Hemann MT. In vivo RNAi screening identifies regulators of actin dynamics as key determinants of lymphoma progression. Nat Genet 2009;41(10):1133-7.

Chapter 5

Error-prone translesion synthesis mediates acquired chemoresistance[1]

5.1 Abstract

The development of cancer drug resistance is a persistent clinical problem limiting the successful treatment of disseminated malignancies. However, the molecular mechanisms by which initially chemoresponsive tumors develop therapeutic resistance remain poorly understood. Error-prone translesional DNA synthesis (TLS) is known to underlie the mutagenic effects of numerous anti-cancer agents, yet little is known as to whether mutation induced by this process is ultimately relevant to tumor drug resistance. Here, we use a tractable mouse model of B cell lymphoma to interrogate the role of error prone translesional DNA synthesis in chemotherapy-induced mutation and resistance to front-line chemotherapy. We find that suppression of Rev1, an essential TLS scaffold protein, inhibits both cisplatin and cyclophosphamide induced mutagenesis. Additionally, by performing repeated cycles of tumor engraftment and treatment, we show that Rev1 plays a critical role in the development of acquired cyclophosphamide resistance. Thus, chemotherapy not only selects for drug resistant tumor populations, but also directly promotes the TLS-mediated acquisition of resistance causing mutations. As TLS also represents a critical mechanism of DNA synthesis in tumor cells following chemotherapy, these data

suggest that TLS inhibition may have dual anti-cancer effects – sensitizing tumors to therapy, as well as preventing the emergence of tumor chemoresistance.

Contributions:

Drs. Hemann, Walker and Xie, as well as myself, designed experiments and wrote the manuscript as it was submitted to the *Proceedings of the National Academy of Sciences*. I, along with Dr. Xie, performed experiments and analyzed data. Figures and data that were collaborative efforts between Dr. Xie and myself will be clearly noted within the text.

[1]Significant sections of this chapter have been submitted for publication at *PNAS* as:

Xie K*, Doles J*, Hemann MT, Walker GW. Error-prone translesion synthesis mediates acquired chemoresistance.
*Equal Contributors

5.2 Introduction

The development of acquired chemoresistance is a persistent clinical problem limiting the successful treatment of disseminated malignancies. Tumors that relapse following initial treatment are frequently refractory to subsequent administration of the initial drug regimen, and are often unresponsive to other distinct chemotherapeutics as well. While a number of key pathways have been implicated in resistance to conventional chemotherapeutics, including enhanced drug efflux, increased drug metabolism, drug inactivation, enhanced DNA repair, and defects in apoptosis programs (1), the mechanisms by which tumors develop drug resistance-causing mutations remains unclear.

At its core, acquired chemoresistance represents the emergence of sub-populations of drug resistant tumor cells, a phenomenon rooted in the inherent genetic heterogeneity of the tumor itself. This heterogeneity may occur as a consequence of tumor genetic instability – a process known to underlie tumor development in numerous malignancies. Alternatively, cancer therapy, itself, may promote mutation and subsequent chemoresistance in relapsed tumors. Support for the latter hypothesis comes from several observations. First, conventional chemotherapeutics can be highly mutagenic (2). In fact, considerable work has gone into highlighting the mutagenic properties of platinum-based and other DNA-adduct forming chemotherapeutics as well as the genes that act in the cellular response to these toxins (3, 4). Second, patients treated with conventional chemotherapies show significantly increased

incidences of secondary malignancies – a phenomenon specifically tied to the mutagenic potential of genotoxic agents (5). Finally, recent tumor genome sequencing studies have shown exceptional high mutation frequency in relapsed malignancies (6). However, there is little evidence to directly implicate therapy-induced mutation, as opposed to the outgrowth of cells with rare pre-existing mutations, as a major contributor to drug resistance.

A fundamental principle of mutagenesis is that most mutations induced by DNA damaging agents result from the action of specialized DNA polymerases carrying out translesion synthesis (TLS) across from DNA lesions (2, 7). In eukaryotes, three genes whose products play a critical role in mutagenesis were first identified in a screen for *S. cerevisiae* mutants that displayed a "*reversionless*" phenotype, i.e. exhibited a reduced frequency of mutations after UV-irradiation (8, 9). The products of the REV1, REV3, and REV7 genes act together in a mutagenic branch of TLS that is responsible for most mutations induced by ultraviolet (UV) light and chemical mutagens (2, 7). The human orthologs of these same genes, REV1, REV3L, and REV7 (MAD2B) are similarly required for most of the mutagenesis induced by exposure to DNA damaging agents such as UV light, as well as chemical mutagens such as benzo[a]pyrene diol epoxide and cisplatin (10-14). Rev1, a member of the Y family of TLS DNA polymerases, has both a dCMP transferase activity that contributes to the bypass of certain lesions and a second important role as a scaffolding protein that associates with several translesion DNA polymerases, including Polζ (2, 15, 16).

Rev3 is the catalytic subunit of Polζ, a member of the B family of DNA polymerases, while Rev7 is the auxiliary subunit.

In this study, we present *in vivo* evidence showing that acquired resistance to the front-line chemotherapeutic cyclophosphamide in a mouse model of B-cell lymphoma arises as consequence of the mutagenic TLS DNA polymerases copying over drug-induced lesions. In doing so, we provide a link between drug induced mutation and resistance to the mutagenic drug in a relevant physiological setting. Given the widespread use of cyclophosphamide and related compounds in the clinic, our results, combined with results showing drug sensitization to lung adenocarcinomas by TLS inhibition (Chapter 4), suggest a rationale for TLS inhibition as an adjuvant therapy for DNA adduct forming chemotherapeutics.

5.3 Results

5.3.1 Suppression of translesion DNA synthesis (TLS) sensitizes B-cell lymphomas to cisplatin *in vivo*

Using a well-established pre-clinical model of Burkitt's lymphoma, the *Eμ-myc* mouse (17), we sought to determine if Rev3L depletion could further sensitize chemoresponsive tumors to cisplatin-based chemotherapy. Three distinct short hairpin RNAs (shRNAs) targeting Rev3L were expressed from retroviral vectors, and the level of Rev3L transcript was assessed by quantitative PCR (Q-PCR) following transduction of target lymphoma cells (Figure 1A). As an initial *in vitro* validation step, Rev3L shRNAs were tested for their ability to promote cisplatin sensitivity in a highly sensitive GFP competition assay. In this assay, GFP is used as a surrogate marker for the presence of an shRNA, and the impact of gene suppression is determined by the relative change in the percent of GFP positive cells following treatment. In this context, all Rev3L shRNA-infected cells showed significantly depleted GFP percentages relative to cells transduced with a control vector (Figure 1B).

We then injected pure populations of GFP-sorted control and Rev3L-deficient lymphoma cells into syngeneic recipient mice and allowed palpable tumors to form (~2 weeks). Upon tumor presentation, mice were treated with a single 10mg/kg dose of cisplatin and monitored using *in vivo* GFP imaging. Independently treated mice bearing Rev3L-deficient tumors exhibited a marked reduction in GFP positive tumor cells twenty-four hours post-treatment compared

to treated control mice (Figures 1C and D). Thus, Rev3L suppression can acutely sensitize cells to the cytotoxic effects of cisplatin *in vivo* in a lymphoma model as well as in a model of an intrinsically chemoresistant model of non small cell lung cancer (discussed in Chapter 5).

Since Rev1 also plays a key role in preventing cisplatin cytotoxicity and DNA damage induced mutagenesis, we extended our analysis by similarly designing and testing three unique shRNA vectors targeting Rev1 and observed suppressed Rev1 protein expression in transduced cell populations by western blot (Figure 2A). We then subjected these cells to rigorous dose response experiments to examine the effect of Rev1 suppression in the context of cisplatin treatment. Comparison of best-fit regression curves revealed significantly lower EC50 values in all three Rev1 shRNA populations with respect to vector control cells (Figure 2B; shRev1-1: $p=0.0039$, shRev1-2: $p=0.0076$, shRev1-3: $p=0.0035$). Importantly, when examined using a GFP competition assay *in vivo*, partially transduced cells expressing the most potent Rev1 shRNA exhibited a markedly robust negative selection in response to cisplatin, as opposed to vector control cells, which displayed a similar percentage of GFP-positive cells before and after treatment (Figure 2C).

5.3.2 Rev1 suppression limits cyclophosphamide-induced mutagenesis and acquired drug resistance *in vitro*

Whereas cisplatin serves as a front-line therapy for numerous malignancies, including testicular, ovarian and lung cancer, the standard of care for many hematopoietic malignancies typically features alkylating, rather than platinum-based, chemotherapeutic agents. In particular, cyclophosphamide (CTX) is the front-line treatment for a wide range of lymphoma subtypes, either as a single agent or in combination with other chemotherapeutics. CTX is a nitrogen mustard alkylating agent that, like cisplatin, forms highly toxic intrastrand crosslinks between guanine nucleotides that impede normal DNA replication (18-20). We chose to evaluate the role of Rev1 in mediating the response of our lymphoma cells to CTX because of: i) its central role in mutagenesis (2, 7), ii) its key role in interacting with Polζ and other TLS DNA polymerases (2, 15, 16) and iii) because it has been implicated in the replication-dependent repair of a nitrogen-mustard-like interstrand crosslink in a Xenopus cell-free system (21). Using the same set of three Rev1-targeting shRNAs described in the context of cisplatin therapy, we examined the effect of Rev1 depletion on the acute response to increasing doses of CTX. While statistical comparison of the resulting data revealed a slight but significant difference for two of three Rev1-deficient survival curves compared to the control curve (Figure 3a; shRev1-1: $p=0.035$, shRev1-2: $p=0.121$, shRev1-3: $p=0.009$), we observed no meaningful shifts in either the calculated EC50 (shRev1-1: $p=0.2555$, shRev1-2: $p=0.2209$, shRev1-3: $p=0.1062$) or the hillslope (shRev1-1: $p=0.6663$, shRev1-2: $p=0.7827$, shRev1-3: $p=0.2187$) values. Thus, Rev1 suppression promotes only limited sensitization of cultured lymphoma cells to CTX. This finding is reminiscent of

prior observations which showed that the loss of mutagenic TLS function has little effect on cell survival in response to agents such as UV light and benzo[a]pyrene diol epoxide (16). Notably, however, the same studies also documented a significant decrease in drug-induced mutation in response to DNA damaging agents in TLS-deficient cells.

To examine the role of Rev1-dependent TLS in CTX-induced mutations, we performed two complementary and classically defined mutagenesis assays in the presence and absence of Rev1 suppression. Notably, these assays were carried out in liquid culture, as hematopoietic malignancies are not amenable to more conventional colony-based assays. In the first setting, we used CTX-induced mutagenesis at the *hprt* locus to serve as a readout of relative mutagenic burden. Briefly, cells were exposed to 4μg/ml CTX for one hour, cultured for two weeks, then challenged with 6-thioguanine (6TG) to select for mutants with impaired *hprt* gene function. As *hprt* function is required for 6-TG-mediated toxicity, this assay allows for the quantitation of CTX-induced *hprt* mutation. As shown in Figure 3B, Rev1 deficiency reduced the frequency of 6TG-resistant variants by 3.2-4.1 fold compared to control-infected cells. To confirm this observation in a related context, we made use of a mouse lymphoma cell line (L5178Y) that is heterozygous at the thymidine kinase (*TK*) locus. As TK activity is necessary for the cytotoxic effects of the thymidine analog triflorothymidine, these cells provide a highly sensitized setting for selection of CTX-induced mutations at the *TK* locus. Using the same set of three Rev1

shRNA vectors described above, we generated three Rev1 knock down L5178Y lymphoma cell populations and tested their relative mutagenicities in response to cyclophosphamide. In agreement with the *hprt* experiments performed in our *Eμ-myc* lymphoma cells, Rev1 suppression in L5178Y cells reduced the mutagenic burden 2.4-3.3 fold relative to control cells (Figure 3C). Thus, the effects of Rev1 on survival and mutagenesis are largely separable in this context, as Rev1 shRNAs fail to significantly sensitize lymphoma cells to CTX treatment but potently inhibit CTX-induced mutagenesis.

A fundamental question in cancer chemotherapy is whether genotoxic drugs can induce mutations that promote tumor chemoresistance. Given the importance of Rev1 in CTX-induced mutagenesis, we sought to determine whether Rev1 depletion could inhibit the development of CTX resistance in treated tumor cells. To test this, we treated a fixed number of control or shRev1-expressing *Eμ-myc* lymphoma cells ($1x10^6$ cells/ml) with a fixed dose (~EC70 in control samples) of cyclophosphamide, assayed for cell survival at 48 hours, and allowed the cells to recover for an additional five days, at which point we initiated a subsequent round of chemotherapy. To chart the evolution of drug resistance in a given cell population over time, we normalized survival data recorded during each round of therapy to the initial values collected during the first round of treatment. As expected, control cell populations became progressively resistant to repeated CTX exposure (Figure 3D, left). In contrast, Rev1-deficient cells

displayed a significantly diminished resistance profile by the fourth round of treatment (Figure 3D, right).

5.3.3 Rev1 deficiency inhibits the acquisition of cyclophosphamide resistance *in vivo*

The preceding experiments strongly suggest that, in cultured cells, Rev1-dependent mutagenesis can actively promote chemotherapeutic resistance. However, the relevance of this mutagenesis to tumor relapse and drug resistance has not been investigated. To examine whether Rev1 deficiency could similarly delay the development of chemoresistant tumors *in vivo*, we injected GFP-sorted, control and Rev1-deficient *Eμ-myc* lymphoma cells into syngeneic recipient mice and allowed palpable tumors to form. We then treated tumor-bearing mice with 30mg/kg CTX and monitored tumor burden using *in vivo* GFP imaging. At this dose, we failed to observe any difference between control and Rev1-deficient transplants with respect to both acute tumor regression as well as time to tumor relapse (Figure 4A). Thus, consistent with our cell culture data, Rev1 deficiency fails to promote CTX sensitivity *in vivo*.

To examine the role of Rev1 in the evolution of tumor chemoresistance, we harvested tumors from individual mice at relapse, re-sorted tumors for GFP positive lymphoma cells, and re-injected sorted tumor cells into syngeneic recipient mice for a second round of therapy. Following tumor transplantation, a subset of control tumors showed acute chemoresistance upon retreatment with

CTX (Figure 4B). Mice bearing these tumors showed a complete lack of tumor-free survival, with continued lymphoma progression following treatment. Strikingly, we observed a complete absence of this class of acutely chemoresistant tumors following suppression of Rev1, with all recipient mice showing sustained periods of tumor regression and enhanced overall survival. To further extend these findings, we subjected control and Rev1 knock down tumors to a third round of treatment. In this setting, 3 out of 4 Rev1-deficient tumors still retained a pronounced sensitivity to CTX treatment, while all control tumor recipients showed little or no tumor free survival (Figure 4 C-E). Of note, drug resistant control tumors were also significantly more aggressive than their Rev1-deficient counterparts, showing perivascular infiltration into non-hematopoietic organs like the liver and lung (Figure 4F). Thus, the emergence of tumor drug resistance is coincident with the acquisition of additional tumor growth characteristics – likely due to the high mutational load present in treated TLS proficient cells.

5.4 Discussion

Chemotherapeutic intervention rarely results in complete tumor eradication. More frequently, tumors exhibit varying degrees of response and ultimately relapse with more aggressive, drug resistant phenotypes. It has been postulated that tumor mutation rate is one of a few critical determinants of clinical resistance to a variety of human cancers (22). To this end, mathematical models have been proposed to suggest that evolving drug resistant tumor subpopulations emerge under the selective pressure of drug exposure (23). However, an added layer of complexity is introduced when one considers the intrinsically mutagenic properties of the therapy itself – an effect that greatly compounds any pre-existing mutagenic tendencies inherent in a given tumor. Using a genetically tractable and highly dynamic model of B-lymphoma, we show that by impairing mutagenic translesion DNA repair, tumors are not only sensitized to relevant chemotherapies, but are also partially protected from the consequences of mutagenic chemotherapies that do not succeed in killing target cells.

A treatment strategy based on pairing a DNA damaging chemotherapeutic agent such as cisplatin with a drug that inhibited the mutagenic TLS pathway could be very powerful as it could significantly reduce the rate at which cells acquire chemoresistance. *In vitro* studies of cultured human cell lines have shown that suppressing either Rev1 or Rev3L reduces the rate of emergence of cisplatin resistance (12, 13), so there is reason to think that similar effects would

be seen for cisplatin and other DNA damaging chemotherapeutics in clinically relevant contexts. Such a strategy might be additionally effective because DNA damaging agents such as cisplatin and the alkylating agent *N*-methyl-*N'*-nitro-*N*-nitrosoguanidine not only introduce lesions into DNA, but also induce the expression of Rev3L (12, 24). Since increased REV3L expression has been shown to promote resistance to cisplatin (25), a drug that inhibited the Rev1/3/7-dependent mutagenic TLS pathway would suppress the acquisition of drug resistance mutations.

It is possible that mutagenic TLS polymerases may play a role in cancer causation as well as in acquired resistance. Recent sequencing of the genomes of cancer cell lines and of a lung cancer has shown the presence of 20,000 – 50,000 mutations (26-28). The majority of the mutations are inferred to have been caused by lesions in DNA, and the nature of the mutations, predominantly base pair substitutions and small insertions and deletions, resemble those known to be introduced during mutagenic TLS (2, 7). Rev1 has also been implicated in the development of carcinogen-induced lung cancer (29). Normal levels of TLS DNA polymerases, together with the large amounts of DNA damage from exogenous agents such as smoking or sunlight, might be sufficient to account for the many mutations observed in tumors. However, the rate of mutagenesis might also be increased by elevated expression of TLS DNA polymerases as cancer progresses. This has been reported for advanced stage gliomas (25) or colorectal adenocarinoma, for which loss of both mismatch repair and p53

increases the levels of expression of Rev1 and REV3L by 10 fold and 20 fold respectively (30). Furthermore, mutations or conditions that alter the complex web of protein-protein interaction that control the access of TLS DNA polymerases to primer termini (31, 32) could also increase the rate of both spontaneous and induced mutagenesis. For example, the Rev1-257Ser single nucleotide polymorphism has been suggested as a risk factor for lung adenocarcinoma and squamous cell carcinoma and homozygous Rev1-373Ser status is associated with an increased risk for cervical carconoma (33).

Tumors that do have higher levels of mutagenic TLS activity, such as later stage gliomas (25) or mismatch repair defective, $p53^{-/-}$ colorectal adenocarcinomas (30) might be particularly susceptible to the sensitizing and antimutagenic effects of a drug targeting the mutagenic TLS pathway. It worth noting that components of the mutagenic TLS system can also be tumor suppressors since their loss results in increased chromosome instability in cells that can tolerate TLS deficiency (34, 35). A tumor lacking a component of the TLS system would not benefit from the chemotherapeutic strategy we are proposing, but might be susceptible to drugs that inhibit other DNA repair or tolerance pathways. In fact, combination therapies that exploit similar DNA repair deficiencies, including the use of PARP inhibitors in BRCA1/2 deficient tumor cells or DNA-PKcs inhibitors in ATM deficient cells (36-38), have gained increasing traction as synthetic lethal strategies for cancer treatment.

5.5 Materials and Methods

5.5.1 Cell culture, retroviral vectors, and chemicals

Eμ-myc B-cell lymphoma and L5178Y/TK-/- lymphoma cells were cultured in B-cell medium (45% DMEM/45% IMDM/10% FBS, supplemented with 2mM L-glutamine and 5μM β-mercaptoethanol). shRNA constructs were designed and cloned as previously described. Sequences (5'-3') targeted by shRNAs are as follows: shRev3-1: TTTACTACAGATACCATGCTG, shRev3-2: TATCTTTATAAGCTGCTCCTG, shRev3-3: TACAGTTATACAAATATCCTA, shRev1-1: GCGGAGGAATTGAGAAATCTA, shRev1-2: AAACAGTGTTGCTAGCAGGCTA, shRev1-3: CCTCCGGGAACAAATAGAACAA. Cloning strategies and primer sequences are available from the authors on request. Cisplatin (Calbiochem) and 4-OH-cyclophosphamide (Toronto Research Chemicals) were dissolved in DMSO to make 1000-2000x stock solutions and were diluted (0-15μM, 0-8μg/ml final concentration, respectively) in fresh media containing cells at the time of treatment. For *in vivo* studies, cisplatin (8-10mg/kg) and cyclophosphamide (300mg/kg) were dissolved in a 0.9% NaCl solution, protected from light, and immediately injected intraperitoneally into tumor-bearing mice.

5.5.2 qRT-PCR and western blotting

For real-time quantitative PCR, total RNA was isolated after retroviral infection and puromycin selection. RT-qPCR was performed using SYBR green on a BioRad thermal cycler. Primer sequences are available upon request. For

western blotting, cell lysates were prepared in lysis buffer (1% sodium deoxycholine, 0.1% SDS, 1% triton-X, 10 mM Tris-HCl, pH 8.0, 140 mM NaCl) for 10 minutes, cleared for 15 minutes at 14,000 rpm, then mixed with 5x SDS sample buffer. Proteins were then run on a 10% SDS-PAGE gel, transferred to PVDF (Millipore) and detected with the following antibodies: anti-Rev1 (Niels De Wind Lab, 1:50) and anti-GAPDH (Santa Cruz, 1:10000).

5.5.3 Mutagenesis assays

Retrovirally transduced cells were initially cultured for a minimum of two weeks in media containing hypoxanthine, aminopterin, and thymidine (HAT) to remove pre-existing *hprt*- and *tk*- mutants from the experimental population. Cells were then split into fresh media (-HAT) 24h prior to treatment with cisplatin. Target cells were then mutagenized with 8μg/ml 4-OH-cyclophosphamide for 1hr, allowed to recover, and passaged for an additional 10 days (in the absence of HAT) to stabilize any induced mutations. Mutagenized cells were then split onto fresh 10cm feeder plates in media containing either 6-thioguanine (6-TG; *Eμ-myc* lymphoma) or triflorothymidine (TFT, L5178Y lymphoma) to select for variants with impaired *hprt* or *tk* function, respectively. Cell viability was determined by flow cytometry after one week of selection.

5.5.4 *In vitro* viability assays and FACS

For short-term viability assays, cells were seeded in triplicate (6×10^3 per well) in 96-well plates and treated as indicated with cisplatin. After 48 h of

treatment, cell viability was measured using Cell-Titer-Glo (Promega) on an Applied Biosystems microplate luminometer. Long-term viability assays were performed by initially treating $4x10^5$ lung adenocarcinoma cells with 15uM cisplatin for 24h. Four days following treatment, cells were split 1:20 onto a fresh 10cm plate and allowed to form colonies for ~10d. To visualize colonies, plates were washed with 0.05% ethidium bromide (in 50%EtOH) for 10-15 seconds and imaged using a UV-gel box/camera. Images were processed and colonies counted using freely available ImageJ software. All flow cytometry was performed using Becton-Dickinson FACScan or MoFlo flow cytometers. Cell death was detected by propidium iodide (PI) incorporation (0.05 mg/mL), and dead cells were excluded from GFP analysis. Live cell sorting was performed using GFP co-expression as a marker of cell transduction.

5.5.5 *In vivo* transplantation and imaging

Syngeneic C57BL6/J female recipient mice were intravenously injected (via tail vein) with 4 million lymphoma cells and monitored until palpable tumors formed (~14 days). Upon tumor presentation, mice were administered either 8-10mg/kg cisplatin or 300mg/kg cyclophosphamide and monitored until the indicated timepoints, at which time mice were sacrificed and tumor material collected, if necessary. Mice subjected to live *in vivo* GFP imaging were immobilized using isoflurane anesthesia and imaged/analyzed using a NightOwl (Berthold Technologies) imaging platform.

Figure 1

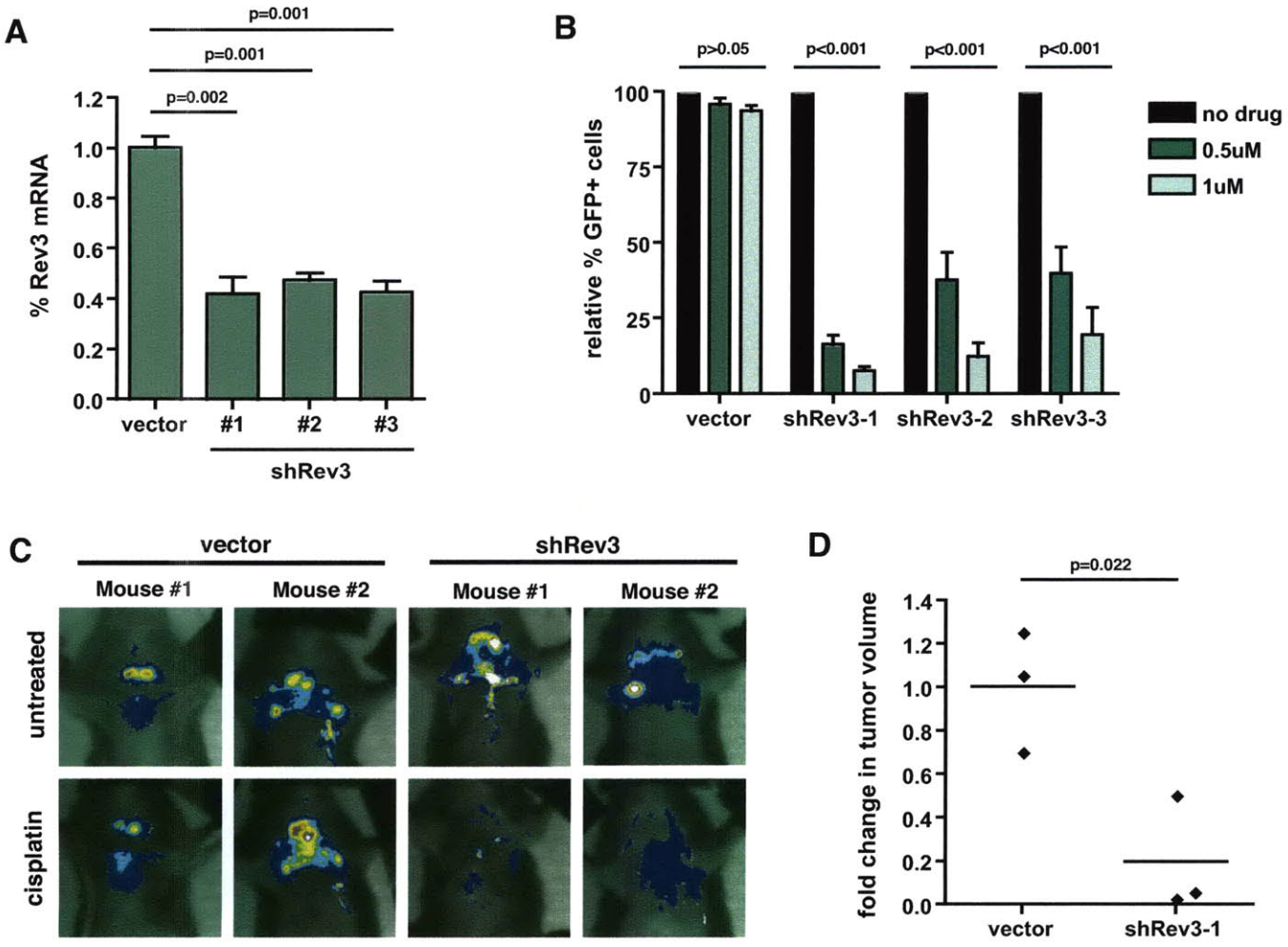

Figure 1 – Rev3 depletion sensitizes B-cell lymphomas to cisplatin in vitro and in vivo. (A) Quantitative RT-PCR (n≥3) confirmation of target mRNA suppression using three distinct shRNAs targeting Rev3 in transduced Eμ-myc; p19arf-/- lymphoma cells. (B) Naïve lymphoma cell populations were partially infected with Rev3 shRNAs, treated with cisplatin (0.5 and 1.0μM) and monitored using GFP-based flow cytometry for changes in the relative percentage of shRNA-containing (GFP-positive) cells. n≥3 for all samples. (C) Representative pseudo-colored images showing the tumor burden in four individual mice (two control and two Rev3 knockdown mice) treated with cisplatin for 24hr. (D) Quantification of relative changes in tumor volume before and after cisplatin treatment (24hr). n=3 individual mice in each group. All quantified data shown represents the mean +/- s.d. P-values were determined using Student's t-tests.

Figure 2

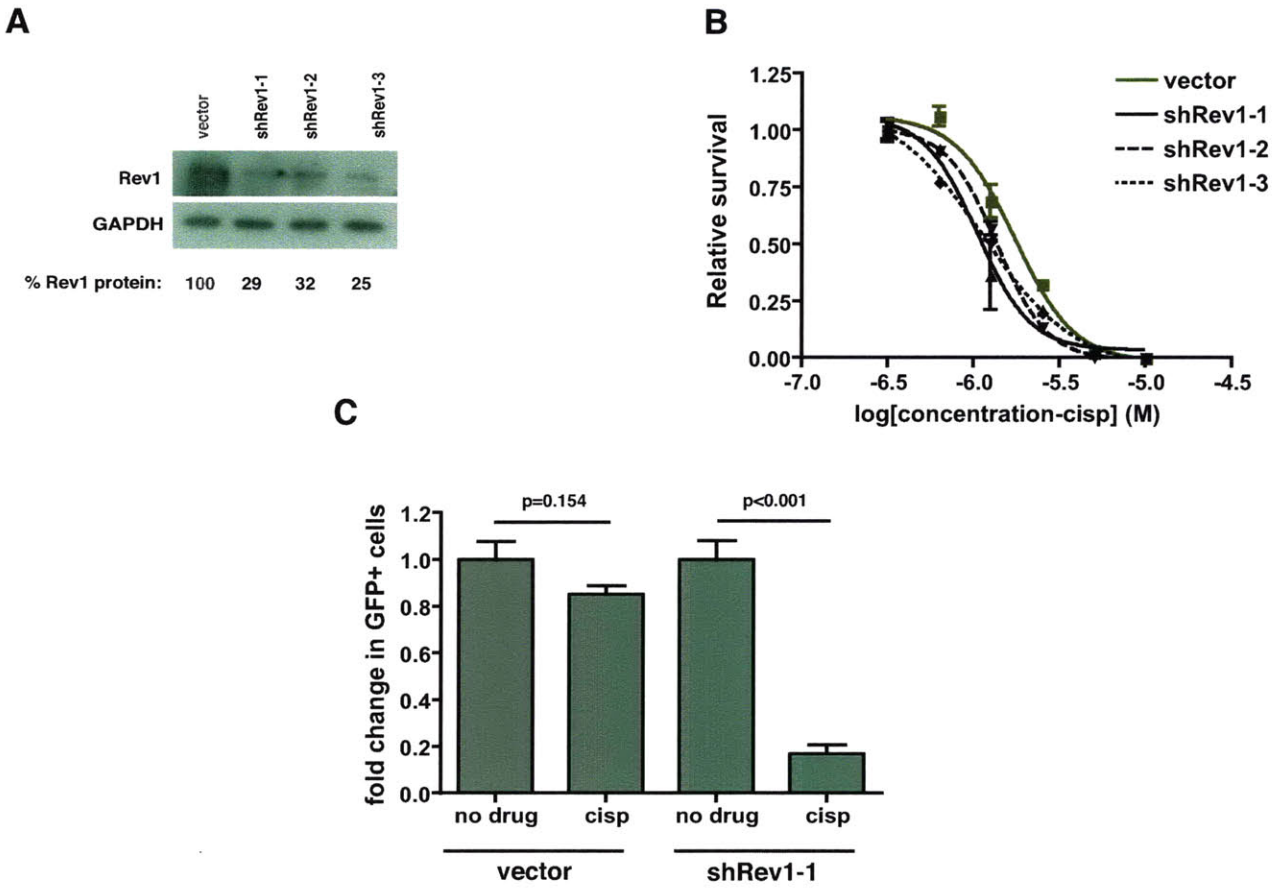

Figure 2 – Rev1 depletion sensitizes B-cell lymphoma to cisplatin in vivo.
(A) Western blot confirmation of Rev1 suppression in Rev1 shRNA-expressing lymphoma cell populations. (B) Cisplatin dose-response curves in cells expressing normal (vector, red) or impaired (shRev1, black) levels of Rev1 protein (shRev1-1: p=0.0039, shRev1-2: p=0.0076, shRev1-3: p=0.0035). n=3 replicates/dose/sample. P-values were determined using an F-test comparison of EC50 values derived from best-fit non-linear regression curves. (C) Mice harboring partially transduced lymphoma cell transplants were treated with 8mg/kg cisplatin for 24h. Shown is the percentage of GFP-positive cells in mice treated with either cisplatin or vehicle (PBS) alone. P-values were determined using a Student's t-tests.

Figure 3

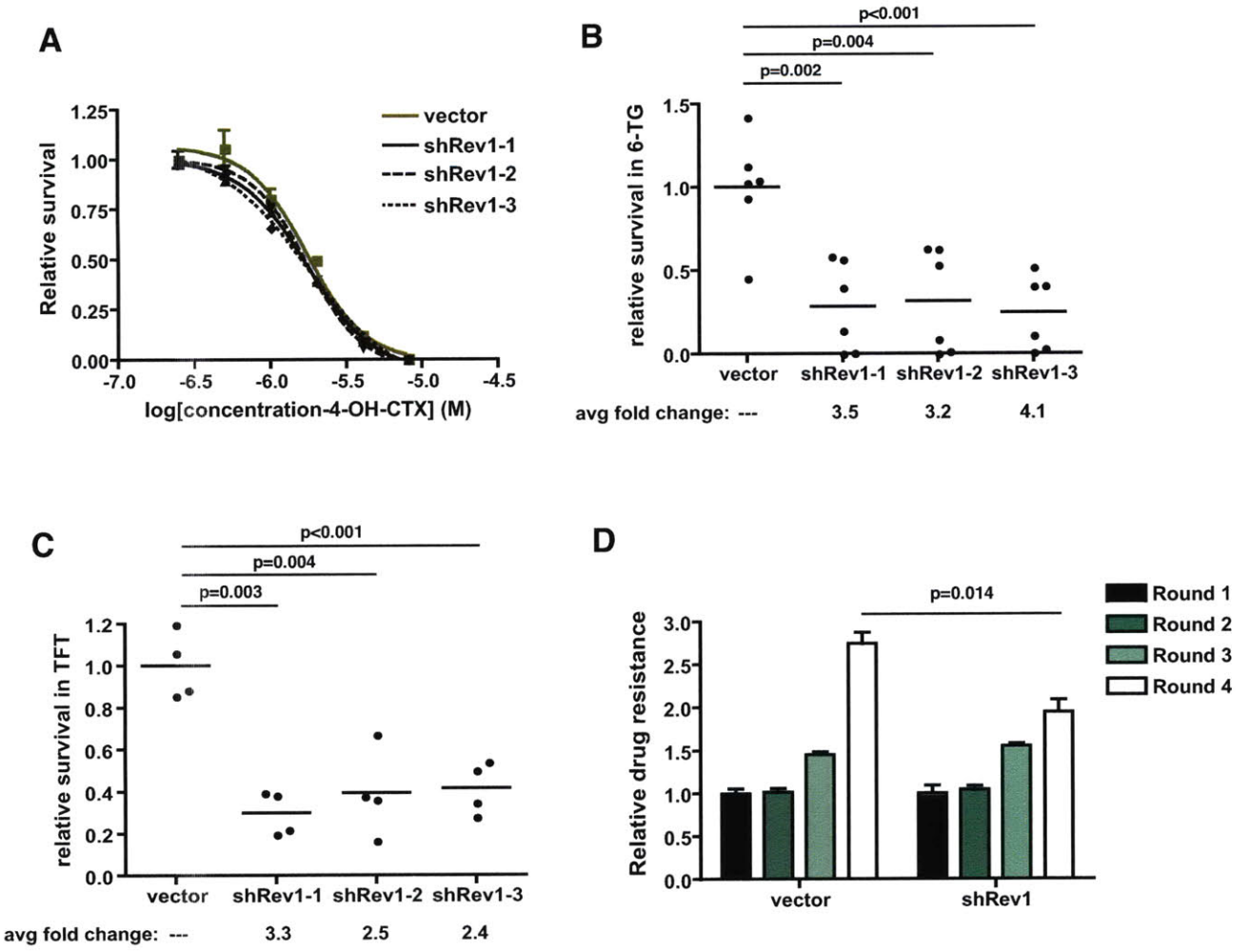

Figure 3 – Rev1 suppression inhibits cyclophosphamide-induced mutagenesis.
(A) Cyclophosphamide dose-response curves in control and Rev1 knockdown cells (shRev1-1: p=0.2555, shRev1-2: p=0.2209, shRev1-3: p=0.1062). N=3 replicates/dose/sample. P-values were determined using an F-test comparison of EC50 values derived from best-fit non-linear regression curves. (B) A graph showing the relative survival of CTX-treated (4μg/ml 4-OH-cyclophosphamide for one hour) control and Rev1 knock down Eμ-myc lymphoma cells following exposure to 1μM 6-thioguanine for 1 week. (C) A graph showing the relative survival of CTX-treated (4μg/ml 4-OH-cyclophosphamide for one hour) control and Rev1 knock down L5178Y-TK+/- mouse lymphoma following exposure to10μM triflorothymidine (TFT). (D) A graph showing the relative response of control and Rev1 knock down Eμ-myc lymphoma cells to multiple rounds of cyclophosphamide treatment in vitro. In each case lymphoma cell viability was determined 48 hours following exposure to 1.3μg/ml 4-OH-cylophosphamide. Relative drug resistance was determined by normalizing viability measurements to those observed in round 1. P-values shown in (B) – (D) were determined using Student's t-tests.

***Data in Figure 4D generated by Dr. Xie

Figure 4

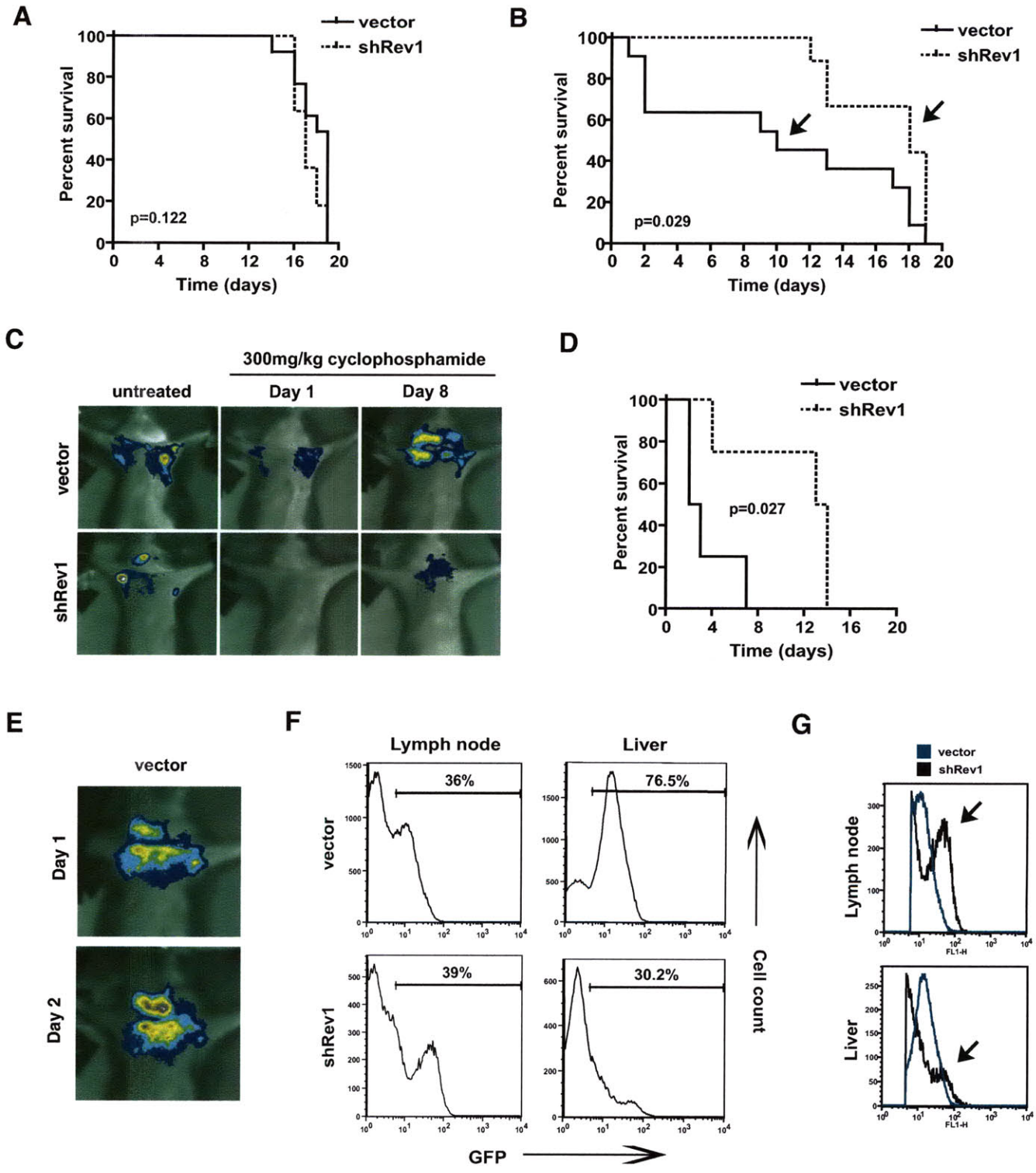
A
vector
shRev1
Percent survival
p=0.122
Time (days)
B
vector
shRev1
Percent survival
p=0.029
Time (days)
C
300mg/kg cyclophosphamide
untreated
Day 1
Day 8
vector
shRev1
D
vector
shRev1
Percent survival
p=0.027
Time (days)
E
vector
Day 1
Day 2
F
Lymph node
Liver
vector
shRev1
36%
76.5%
39%
30.2%
Cell count
GFP
G
vector
shRev1
Lymph node
Liver
FL1-H

Figure 4 – Rev1 depletion improves cyclophosphamide-based chemotherapy in vivo. (A) Kaplan-Meier survival curves of tumor-bearing mice treated with a single dose of cyclophosphamide (300mg/kg; n=13 vector control, n=11 shRev1). Day 0 represents the day of drug administration. At disease relapse, individual tumors were harvested and re-injected into new recipient mice for additional drug treatment. (B) Kaplan-Meier survival curves of control and shRev1 transplant-bearing mice challenged with a second round of cyclophosphamide chemotherapy (n=11 vector control, n=9 shRev1). As in (A), tumors were harvested at relapse and re-injected into naive recipient mice. (C) In vivo GFP imaging showing representative mice from each experimental group (indicated with arrows in (B)). (D) Round 3 Kaplan-Meier survival data (n=4 vector control, n=4 shRev1). P-values for all survival studies were determined using logrank curve comparison tests. (E) GFP imaging of a highly drug-resistant vector control tumor treated with cyclophosphamide. (F) GFP histograms of dissociated whole tissue harvested from tumor bearing mice. The percentages represent the proportion of control vector or shRev1 lymphoma cells present in the indicated tissue.

*** Data in this figure was generated in collaboration with Dr. Xie.

5.7 Acknowledgements

We would like to thanks members of the Hemann and Walker labs for helpful advice and discussions. K.X. and G.C.W. are supported by NIEHS ES015818 and grant P30 ES002109 from the Center of Environmental Health Sciences (MIT). G.C.W. is an American Cancer Society Research Professor. M.T.H. is a Rita Allen Fellow and the Latham Family Career Development Assistant Professor of Biology and is supported by NIH RO1 CA128803. J.D. is supported by the MIT Department of Biology training grant and a Ludwig Center Graduate Fellowship.

5.8 References

1. Johnstone RW, Ruefli AA, Lowe SW. Apoptosis: a link between cancer genetics and chemotherapy. Cell 2002;108(2):153-64.

2. Friedberg E, G. W, W. S, Wood R, Schultz R, Ellenberger T. DNA repair and mutagenesis, 2nd ed. Washington, DC; 2005.

3. Beck DJ, Brubaker RR. Mutagenic properties of cis-plantinum(II)diammino-dichloride in Escherichia coli. Mutat Res 1975;27(2):181-9.

4. Zwelling LA, Bradley MO, Sharkey NA, Anderson T, Kohn KW. Mutagenicity, cytotoxicity and DNA crosslinking in V79 Chinese hamster cells treated with cis- and trans-Pt(II) diamminedichloride. Mutat Res 1979;67(3):271-80.

5. Feig SA. Second malignant neoplasms after successful treatment of childhood cancers. Blood Cells Mol Dis 2001;27(3):662-6.

6. Parsons DW, Jones S, Zhang X, et al. An integrated genomic analysis of human glioblastoma multiforme. Science 2008;321(5897):1807-12.

7. Waters LS, Minesinger BK, Wiltrout ME, D'Souza S, Woodruff RV, Walker GC. Eukaryotic translesion polymerases and their roles and regulation in DNA damage tolerance. Microbiol Mol Biol Rev 2009;73(1):134-54.

8. Lemontt JF. Mutants of yeast defective in mutation induced by ultraviolet light. Genetics 1971;68(1):21-33.

9. Lawrence CW, Das G, Christensen RB. REV7, a new gene concerned with UV mutagenesis in yeast. Mol Gen Genet 1985;200(1):80-5.

10. Gibbs PE, Wang XD, Li Z, et al. The function of the human homolog of Saccharomyces cerevisiae REV1 is required for mutagenesis induced by UV light. Proc Natl Acad Sci U S A 2000;97(8):4186-91.

11. Li Z, Zhang H, McManus TP, McCormick JJ, Lawrence CW, Maher VM. hREV3 is essential for error-prone translesion synthesis past UV or benzo[a]pyrene diol epoxide-induced DNA lesions in human fibroblasts. Mutat Res 2002;510(1-2):71-80.

12. Wu F, Lin X, Okuda T, Howell SB. DNA polymerase zeta regulates cisplatin cytotoxicity, mutagenicity, and the rate of development of cisplatin resistance. Cancer Res 2004;64(21):8029-35.

13. Okuda T, Lin X, Trang J, Howell SB. Suppression of hREV1 expression reduces the rate at which human ovarian carcinoma cells acquire resistance to cisplatin. Mol Pharmacol 2005;67(6):1852-60.

14. Cheung HW, Chun AC, Wang Q, et al. Inactivation of human MAD2B in nasopharyngeal carcinoma cells leads to chemosensitization to DNA-damaging agents. Cancer Res 2006;66(8):4357-67.

15. Washington MT, Carlson KD, Freudenthal BD, Pryor JM. Variations on a theme: eukaryotic Y-family DNA polymerases. Biochim Biophys Acta;1804(5):1113-23.

16. Gan GN, Wittschieben JP, Wittschieben BO, Wood RD. DNA polymerase zeta (pol zeta) in higher eukaryotes. Cell Res 2008;18(1):174-83.

17. Adams JM, Cory S. Oncogene co-operation in leukaemogenesis. Cancer Surv 1992;15:119-41.

18. Scharer OD. DNA interstrand crosslinks: natural and drug-induced DNA adducts that induce unique cellular responses. Chembiochem 2005;6(1):27-32.

19. Lawley PD, Phillips DH. DNA adducts from chemotherapeutic agents. Mutat Res 1996;355(1-2):13-40.

20. Noll DM, Mason TM, Miller PS. Formation and repair of interstrand cross-links in DNA. Chem Rev 2006;106(2):277-301.

21. Raschle M, Knipscheer P, Enoiu M, et al. Mechanism of replication-coupled DNA interstrand crosslink repair. Cell 2008;134(6):969-80.

22. Sawyers CL. Calculated resistance in cancer. Nat Med 2005;11(8):824-5.

23. Komarova NL, Wodarz D. Drug resistance in cancer: principles of emergence and prevention. Proc Natl Acad Sci U S A 2005;102(27):9714-9.

24. Yu Y, Yang J, Zhu F, Xu F. Response of REV3 promoter to N-methyl-N'-nitro-N-nitrosoguanidine. Mutat Res 2004;550(1-2):49-58.

25. Wang H, Zhang SY, Wang S, et al. REV3L confers chemoresistance to cisplatin in human gliomas: the potential of its RNAi for synergistic therapy. Neuro Oncol 2009;11(6):790-802.

26. Pleasance ED, Stephens PJ, O'Meara S, et al. A small-cell lung cancer genome with complex signatures of tobacco exposure. Nature;463(7278):184-90.

27. Pleasance ED, Cheetham RK, Stephens PJ, et al. A comprehensive catalogue of somatic mutations from a human cancer genome. Nature;463(7278):191-6.

28. Lee W, Jiang Z, Liu J, et al. The mutation spectrum revealed by paired genome sequences from a lung cancer patient. Nature;465(7297):473-7.

29. Dumstorf CA, Mukhopadhyay S, Krishnan E, Haribabu B, McGregor WG. REV1 is implicated in the development of carcinogen-induced lung cancer. Mol Cancer Res 2009;7(2):247-54.

30. Lin X, Howell SB. DNA mismatch repair and p53 function are major determinants of the rate of development of cisplatin resistance. Mol Cancer Ther 2006;5(5):1239-47.

31. Lehmann AR, Niimi A, Ogi T, et al. Translesion synthesis: Y-family polymerases and the polymerase switch. DNA Repair (Amst) 2007;6(7):891-9.

32. Chun AC, Jin DY. Ubiquitin-dependent regulation of translesion polymerases. Biochem Soc Trans;38(Pt 1):110-5.

33. He X, Ye F, Zhang J, Cheng Q, Shen J, Chen H. REV1 genetic variants associated with the risk of cervical carcinoma. Eur J Epidemiol 2008;23(6):403-9.

34. Wittschieben JP, Patil V, Glushets V, Robinson LJ, Kusewitt DF, Wood RD. Loss of DNA polymerase zeta enhances spontaneous tumorigenesis. Cancer Res;70(7):2770-8.

35. Wittschieben JP, Reshmi SC, Gollin SM, Wood RD. Loss of DNA polymerase zeta causes chromosomal instability in mammalian cells. Cancer Res 2006;66(1):134-42.

36. Farmer H, McCabe N, Lord CJ, et al. Targeting the DNA repair defect in BRCA mutant cells as a therapeutic strategy. Nature 2005;434(7035):917-21.

37. Bryant HE, Schultz N, Thomas HD, et al. Specific killing of BRCA2-deficient tumours with inhibitors of poly(ADP-ribose) polymerase. Nature 2005;434(7035):913-7.

38. Jiang H, Reinhardt HC, Bartkova J, et al. The combined status of ATM and p53 link tumor development with therapeutic response. Genes Dev 2009;23(16):1895-909.

Chapter 6

Conclusions and future directions

6.1 Overview

While indeed much insight into drug action has been gained in the past several decades, there remain significant gaps in our mechanistic understanding of even the most commonly used chemotherapeutic agents. Powerful new technologies such as RNAi-based gene knockdown and high-throughput sequencing represent a new generation of experimental tools promising to deconvolute this complex cellular response and improve patient quality of care. The work presented in this thesis features previously unappreciated mechanistic insight into chemotherapeutic response identified using these new technologies and builds upon these in an effort to improve future use of RNAi-based screening. First, this work demonstrates the utility of shRNA-mediated gene knockdown and pool-based screening to yield critical mechanistic insight into the cellular response to topoisomerase poisons. Second, these data show that RNAi-based methodologies are capable of identifying and characterizing novel genetic mediators of chemotherapeutic response. Finally, concurrent with screening-heavy efforts, this work shows that a targeted shRNA knockdown approach is useful for probing *in vivo* chemotherapeutic response in a well-established model of B-lymphoma as well as in a newer setting, murine lung adenocarcinoma. Together, these results underscore the importance of both large-scale, unbiased gene discovery and target-based interrogation of genetic determinants of chemotherapeutic response.

6.2 shRNA screening for mediators of chemotherapeutic response in hematopoietic malignancies

In Chapters 2 and 3, I discussed my work using pool-based, shRNA screening methodologies to identify mediators of chemotherapeutic response to the topoisomerase poison doxorubicin and the microtubule poison taxol, respectively. In the former screen, shRNAs targeting p53, chk2 and top2A were identified as being 'resistance-conferring' in Eμ-myc, p19arf-/- lymphoma cells treated with doxorubicin. While these genes have been previously implicated in doxorubicin response, our methodologies allowed us to evaluate the *in vivo* significance of these drug mediators in the context of a tumor-bearing host. In the end, we uncovered an intriguing relationship between Top2A and Top1 levels – an observation that has significant clinical implications given the frequency of abnormal topoisomerase expression levels in cancer patients as well as the widespread therapeutic use of topoisomerase poisons (discussed in greater detail in Chapter 2). Interestingly, several groups have linked alterations in the Her2-proximal *Top2A* locus to anthrycycline response in breast cancer (1-3). While the significance of these findings remains unclear (2, 4-6), our work suggests a rationale for including *Top2A* status as an important consideration when designing topoisomerase poison-based chemotherapeutic regimens.

Additionally, the analysis of Nek4 in Chapter 3 highlighted the ease with which one could move between *in vitro* and *in vivo* experimental settings to identify and subsequently characterize novel mediators of chemotherapeutic

response. Importantly, the work described in Chapter 3 underscored the potential relevance of using genetically informed, personalized chemotherapy regimens to maximize therapeutic outcome. As Nek4 is located in a genomic region that is commonly mutated in lung cancer, our data would suggest that combination therapies tailored towards this deficiency (ie. vincristine/cisplatin) may be more effective than current front-line therapies (ie. taxol/cisplatin) in patients with 3p/Nek4 deletions.

6.2.1 Next steps: *in vivo* shRNA screening

Years of genetic screening in mice have led to the identification of many novel and cooperating cancer genes. In particular, retroviral insertional mutagenesis screens in the mouse hematopoietic system, such as those pioneered by Berns and collegues over 20 years ago, have proven to be effective in identifying cancer-associated genetic loci (7, 8). Additionally, more recent screening approaches using transposon-mediated insertional mutagenesis in mice have similarly facilitated the identification of genes and pathways involved in cancer progression (9, 10).

The ability to manipulate gene expression using RNAi has recently evolved as an efficient tool with which to conduct reverse-genetic screens in mice. Indeed several groups have described large-scale screens in mice that have led to the identification of novel cancer genes that may not otherwise have been discovered using standard *in vitro* RNAi screening methodologies (11-13).

To date, however, large-scale shRNA-mediated screening for mediators of chemotherapeutic response has not been performed *in vivo*. This is of particular importance when considering the relevance of the local microenvironment to chemotherapeutic drug response programs (14-16).

A recent paper from our lab (12) underscores the importance of conducting shRNA screens in physiologically-relevant contexts and raises the possibility of using *in vivo* screening technology to screen for genetic mediators of chemotherapeutic response. In fact, several colleagues are currently working to adapt pool-based approaches described in this thesis to screen for shRNAs capable of sensitizing lymphoma and leukemia lines to a variety of front-line and targeted chemotherapeutics *in vivo* (Jennifer Ricks, Corbin Meacham; personal communication).

Looking beyond these initial *in vivo* screening efforts, several important considerations need to be addressed. First, to what extent can we realistically interrogate diverse gene sets in the context of a single mouse? To that end, work from the above mentioned study suggests that nearly 1000 unique shRNA constructs can be identified in shRNA library infected *Eμ-myc; p19*$^{arf-/-}$ lymphoma cells following transplantation (12). This is certainly encouraging if one were to screen smaller, targeted shRNA libraries such as those targeting 'druggable' kinases and phosphatases (17). However, significant obstacles remain – namely mouse requirements for a saturating screen – if one were to attempt this on a

genome-wide scale. In particular, sensitization studies would be challenging, as low-abundance shRNAs (before treatment) that are negatively selected as a consequence of therapy may be difficult to call with accuracy. Interestingly, recent work using transplantation of Bcr-Abl-driven acute lymphoblastic leukemia cells (18) suggests that up to 7000 shRNA constructs can be screened in a single mouse (Corbin Meacham, personal communication). Thus, as it relates to large library screening *in vivo*, selection of an experimental model with robust transplantability appears to be a critical variable.

An additional layer of complexity exists when considering the appropriate therapeutic drug dose for screening purposes. Specifically, drug doses that are too effective at killing tumor cells will have the unintended consequence of skewing the heterogeneity of the starting library to the point where shRNAs at the end of the experiment represent those that survived the 'bottle-necking' effects of the drug rather than true mediators of chemotherapeutic response. For example, although p53 loss is known to mediate drug resistance (19-21), a significant fraction of p53-deficient cells still die following chemotherapy. Thus, in the context of treated lymphoma cells infected with a diverse shRNA library (which includes shp53), a sufficient number of cells expressing p53 shRNAs would need survive the therapeutic bottle-neck such that enrichment (relative to the rest of the library) would be detectable. To address this issue, one should test drug dosing schedules using dilution-based experiments prior to screening. Specifically, lymphoma cells infected with a positive control shRNA (one known

to mediate resistance to therapy, such as shp53) could be diluted down with uninfected cells and injected into recipient mice. Choosing a proper drug dose would therefore be limited to those where enrichment or depletion of a positive control could be readily visualized.

6.2.2 Next steps: Improving experimental tools

Performing a successful *in vivo* genome wide shRNA screen for mediators of chemotherapeutic response is not without its challenges. While selection of an appropriate model system is certainly a contributing factor (ALL seems to be an early front-runner), improvements to existing tools and reagents would also go a long way towards accomplishing this goal. For example, a major concern with our current approach is the amount of 'pre-selection' that our shRNA library is subjected to prior to therapeutic challenge. As it stands, lymphoma cells remain in culture for several days (up to a week) post infection, a period that includes FACS-based GFP-sorting and subsequent recovery. Subsequently, cells are injected into mice where tumors are allowed to form, a process that can take up to two weeks. This means that up to the point of therapy, shRNA-infected cells have had up to three weeks worth of selection time – not only growth selection, but also selection associated with *in vitro* culture stress as well as *in vivo* lymphoma establishment. In effect, much library diversity may already be lost prior to the intended 'time zero' of the experiment.

Strategies for circumventing 'pre-selection' often involve the use of regulatable expression systems. For example, tetracycline-based control over shRNA expression would be one way in which to limit expression of our shRNA library to a defined period of experimental time. Indeed such an approach has been shown to work in the context of shRNA-mediated suppression/rexpression of p53 in cultured mouse fibroblasts (22). As an initial first step in translating these methodologies to our system, it would be important to verify the effective and toxicity-limiting doses of the chemical inducer (doxycycline, in the case of 'tet-on'-mediated control of our shRNA expression vectors) using positive-control GFP competition and standard viability assays, respectively. Looking beyond common technical issues along the way, with improved control over shRNA expression *in vivo*, we can not only expect a more faithful representation of shRNA diversity at the onset of treatment, but also a greater sense of confidence in hits arising as a consequence of drug treatment.

On a related note, and one that applies to shRNA-mediated RNAi in general, strategies that may contribute to more effective screening include improvements to shRNA construct as well as to expression vector design. Improved average shRNA potency (23-25) would certainly go a long way towards helping to keep library size down, while maintaining or even improving the reliable hit rate. Nevertheless, these improvements will never entirely supplant the need for multiple shRNA constructs per gene, as this numerical redundancy is an excellent internal screening control for off-target RNAi effects.

6.3 shRNA screening for mediators of chemotherapeutic response in mouse models of solid cancer

6.3.1 Transplant-based approaches

Screening studies using the mouse hematopoietic system have a number of experimental advantages. Most notably, robust transplantability makes the prospect of large-scale shRNA-based screening particularly appealing. In Chapter 5, I described a transplantation approach that allowed us to evaluate chemotherapeutic response in a clinically relevant model of human lung adenocarcinoma. In this setting we were able to retrovirally transduce a lung adenocarcinoma cell line with shRNAs targeting the translesion repair gene Rev3, transplant genetically-modified cells into immunocompetent syngeneic recipient mice, and monitor established transplant tumors treated *in vivo* with cisplatin using microCT-based imaging. While that study focused on the evaluation of a single gene on chemotherapeutic response, future studies are by no means limited to that paradigm. In order to assess the practicality of screening in this model, however, several key issues must first be addressed. Many of the experiments described in Chapter 5 relied on pre-selection of GFP+ cells to establish sorted Rev3 knockdown cell populations. These cells in turn were compared to control infected cells (GFP only) also subjected to identical sorting protocols. Thus, it is difficult to assert, a priori, that significant numbers of injected cells contribute to the resulting disease. A useful initial control experiment would be to inject mice with a known mixed percentage of GFP+ cells and check at disease onset for maintenance of that diversity. Assuming that

transplants can faithfully maintain GFP percentage of a mixed control cell population, one could then transduce cells with pools of shRNA constructs and test resulting tumor transplants (using high-throughput sequencing for example (12)) for preservation of library diversity in transplanted tumors. Though I have not, to date, performed any of these experiments, one important piece of evidence suggests that a reasonable heterogeneity is maintained in these tumor transplants: cells harvested both before and after treatment display similar GFP histogram plots when analyzed by FACS. In other words, evidence of clonal selection, or in this case extreme bottle-necking at the point of transplant establishment, would result in a tighter GFP distribution relative to input (ie. one or more sharp spikes) – a phenomenon that did not occur in any of my FACS-analyzed transplants (unpublished observations).

Assuming a reasonable number of cells contribute to the transplanted disease, an important next step would be to define the experimental parameters relating to pool size with respect to drug dose. To that end, control dilution experiments using known mediators of cisplatin response in this setting (ie. Rev3) could be helpful in establishing an appropriate therapeutic window for maintaining reasonable tumor cell numbers in response to therapy.

6.3.2 shRNA screening in an autocthonous tumor setting

Despite the advantages of screening using transplant-based systems, an argument can still be made as to the biological relevance of the rapidly forming

transplant. This is particularly true in the context of *KrasG12D; p53-/-* lung adenocarcinoma, as autocthonous disease progression typically occurs over a period of months rather than the few weeks injected cells take to form transplants. Interestingly, recent reports from the laboratory of Tyler Jacks outline the use of lentiviral Cre-recombinase constructs to initiate tumor formation in *KrasG12D; p53-/-* mice (26, 27). In one study, Kumar and colleagues co-expressed a let-7a microRNA along with Cre-recombinase to evaluate the contribution of enforced let-7a expression on Kras/p53 lung tumor formation. Using this approach, one could generate a library of lenti-cre-shRNA constructs, infect mice with virus and treat with appropriate chemotherapies (ie. cisplatin or paclitaxel) at defined time intervals to screen for shRNAs that mediate *in vivo* chemotherapeutic response in a Kras+/p53- background. Additionally, temporal control over shRNA expression using tetracycline-based genetic tools would allow for precise studies into stage-specific mediators of chemotherapeutic response. Specifically, the shRNA in the lenti-cre-shRNA vector described above could first be engineered to be under the control of a tet-inducible promotor. Second, the resulting virus could be used to infect *KrasG12D; p53fl/fl; Rosa26*^{rtTA} compound mutant mice to allow expression of shRNAs at defined points during tumor development using *in vivo* doxycycline administration. While this approach certainly has its challenges, it would be interesting to adapt screening-based methodologies to address issues of tumor stage-specific chemotherapeutic response.

6.4 The problem of acquired resistance

As I discussed in Chapter 4, tumors exhibit varying degrees of response to chemotherapy. Furthermore, those that do display initial drug sensitivity often relapse with more aggressive, drug resistant phenotypes. This acquired resistance to repeated drug exposure has been hypothesized to evolve from tumor mutations – a consequence of intrinsic mutability, or alternatively, exposure to exogenous mutagens (ie. chemotherapy) (28, 29). Using our initially chemoresponsive model of B-lymphoma – the *Eμ-myc* mouse – we show [in Chapter 4] that by impairing mutagenic translesion DNA repair, tumors are partially protected from the consequences of the mutagenic chemotherapies cisplatin and cyclophosphamide. Specifically, we show that chemotherapy directly promotes TLS-mediated mutation acquisition and that TLS impairment attenuates resistance acquisition over time.

6.4.1 High-throughput sequencing as a strategy for interrogating mechanisms of acquired resistance

Importantly, we do not directly show selection of drug-induced mutations as the underlying cause of acquired resistance. Commonly used techniques to evaluate mutagenic burden, while invaluable, are limited by the fact that they are frequently reporter-based (ie. plasmid reactivation, 6-thioguanine/triflorothymidine resistance, etc.). Thus, while insights into global mutagenic burden may be extrapolated from the data, patterns of mutagenesis that may exist and that may contribute to the evolution of increasingly drug-resistant tumors remain obscured.

In a preliminary effort to investigate whether or not drug-induced mutations were causal with respect to acquired resistance, we employed a high-throughput sequencing approach to gain insight into precise sequence alterations associated with drug treatment. Such an experimental strategy would not be entirely unprecedented as similar methodologies characterizing somatic mutations in several cancer cell lines have recently been described (30-32).

Our initial analysis involved comparing the sequenced transcriptomes of cisplatin treated control vs. Rev3 knockdown lung adenocarcinoma transplants (Figure 1). Sequencing data from the parental cell line was also included in the analysis as a reference for cell-line specific sequence variation (ie. SNPs). Although still a work in progress, preliminary bioinformatics analyses of the data sets revealed a consistent increase in the number of 'mutations' in control treated compared to control untreated tumors. Further, we observed a consistent (~2-3 fold) decrease in relative mutational burden in Rev3-deficent treated tumors compared to treated controls (Figure 2). Importantly, this is in agreement with our cisplatin mutagenesis data shown in Chapter 5, suggesting that, at a bare-minimum, high-throughput sequencing can be a reliable way of detecting relative mutation burden in matched samples.

Perhaps a more rigorous analysis of a smaller data set would be required to fully determine the future applicability of this approach for studying drug-induced mutations and resistance. Specifically, one could simply compare naïve

transplants before and several weeks after cisplatin treatment. Mutations identified specifically in the drug-treated sample (and further expected to result in gene expression impairment) could then be validated using an shRNA-based approach similar to the one described using lymphoma cells in Chapter 4.

Figure 1

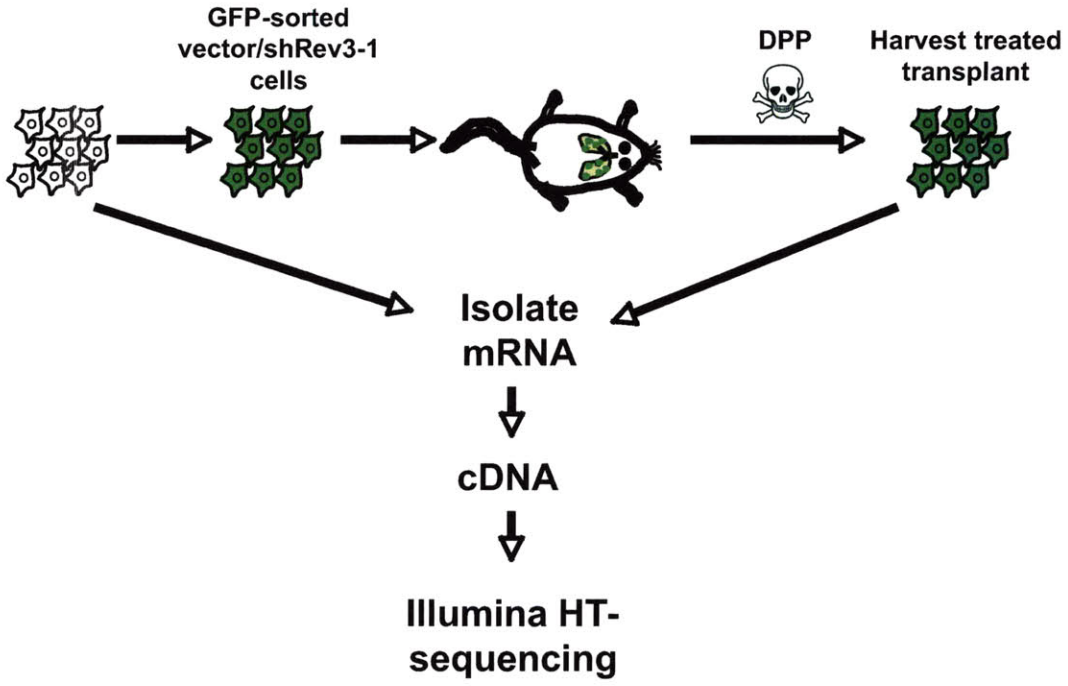

Figure 1- Experimental flowchart for RNA-seq analysis of cisplatin treated lung adeno-carcinoma transplants.
Naive KrasG12D; p53-/- lung adenocarcinoma cells are retrovirally trasduced with control or Rev3 shRNA constructs, injected into syngeneic recipient mice (~25,000 cells) and treated upon tumor presentation (~3-4 weeks). Tumors are allowed to recover in vivo for 10 days at which time they are harvested for Illumina sequencing preparation.

Figure 2

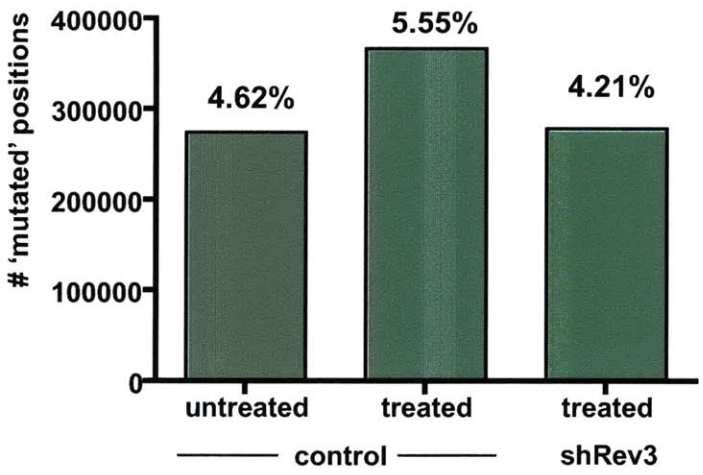

Figure 2- Rev3 knockdown limits cisplatin-induced mutation accumulation.
A graph showing the raw number of mutated (multi-allelic) bases in lung adenocarcinoma transplants treated with cisplatin as determined using high-throughput RNA-seq. The percentage of mutated bases is relative to the total number of bases covered at a sequencing depth of five or greater.

***Bioinformatics processing of raw sequencing data performed by Dr. Vincent Butty (Burge Lab)

6.6 References

1. O'Malley FP, Chia S, Tu D, et al. Topoisomerase II alpha and responsiveness of breast cancer to adjuvant chemotherapy. J Natl Cancer Inst 2009;101(9):644-50.

2. Slamon DJ, Press MF. Alterations in the TOP2A and HER2 genes: association with adjuvant anthracycline sensitivity in human breast cancers. J Natl Cancer Inst 2009;101(9):615-8.

3. Usha L, Tabesh B, Morrison LE, et al. Topoisomerase II alpha gene copy loss has adverse prognostic significance in ERBB2-amplified breast cancer: a retrospective study of paraffin-embedded tumor specimens and medical charts. J Hematol Oncol 2008;1:12.

4. Bartlett JM, Munro AF, Dunn JA, et al. Predictive markers of anthracycline benefit: a prospectively planned analysis of the UK National Epirubicin Adjuvant Trial (NEAT/BR9601). Lancet Oncol;11(3):266-74.

5. Harris LN, Broadwater G, Abu-Khalaf M, et al. Topoisomerase II{alpha} amplification does not predict benefit from dose-intense cyclophosphamide, doxorubicin, and fluorouracil therapy in HER2-amplified early breast cancer: results of CALGB 8541/150013. J Clin Oncol 2009;27(21):3430-6.

6. Tubbs R, Barlow WE, Budd GT, et al. Outcome of patients with early-stage breast cancer treated with doxorubicin-based adjuvant chemotherapy as a function of HER2 and TOP2A status. J Clin Oncol 2009;27(24):3881-6.

7. Jonkers J, Berns A. Retroviral insertional mutagenesis as a strategy to identify cancer genes. Biochim Biophys Acta 1996;1287(1):29-57.

8. van Lohuizen M, Verbeek S, Scheijen B, Wientjens E, van der Gulden H, Berns A. Identification of cooperating oncogenes in E mu-myc transgenic mice by provirus tagging. Cell 1991;65(5):737-52.

9. Collier LS, Carlson CM, Ravimohan S, Dupuy AJ, Largaespada DA. Cancer gene discovery in solid tumours using transposon-based somatic mutagenesis in the mouse. Nature 2005;436(7048):272-6.

10. Dupuy AJ, Akagi K, Largaespada DA, Copeland NG, Jenkins NA. Mammalian mutagenesis using a highly mobile somatic Sleeping Beauty transposon system. Nature 2005;436(7048):221-6.

11. Bric A, Miething C, Bialucha CU, et al. Functional identification of tumor-suppressor genes through an in vivo RNA interference screen in a mouse lymphoma model. Cancer Cell 2009;16(4):324-35.

12. Meacham CE, Ho EE, Dubrovsky E, Gertler FB, Hemann MT. In vivo RNAi screening identifies regulators of actin dynamics as key determinants of lymphoma progression. Nat Genet 2009;41(10):1133-7.

13. Zender L, Xue W, Zuber J, et al. An oncogenomics-based in vivo RNAi screen identifies tumor suppressors in liver cancer. Cell 2008;135(5):852-64.

14. Adjei AA, Rowinsky EK. Novel anticancer agents in clinical development. Cancer Biol Ther 2003;2(4 Suppl 1):S5-15.

15. Henning T, Kraus M, Brischwein M, Otto AM, Wolf B. Relevance of tumor microenvironment for progression, therapy and drug development. Anticancer Drugs 2004;15(1):7-14.

16. Massague J. TGFbeta in Cancer. Cell 2008;134(2):215-30.

17. Draviam VM, Stegmeier F, Nalepa G, et al. A functional genomic screen identifies a role for TAO1 kinase in spindle-checkpoint signalling. Nat Cell Biol 2007;9(5):556-64.

18. Williams RT, Roussel MF, Sherr CJ. Arf gene loss enhances oncogenicity and limits imatinib response in mouse models of Bcr-Abl-induced acute lymphoblastic leukemia. Proc Natl Acad Sci U S A 2006;103(17):6688-93.

19. el Rouby S, Thomas A, Costin D, et al. p53 gene mutation in B-cell chronic lymphocytic leukemia is associated with drug resistance and is independent of MDR1/MDR3 gene expression. Blood 1993;82(11):3452-9.

20. Fan S, el-Deiry WS, Bae I, et al. p53 gene mutations are associated with decreased sensitivity of human lymphoma cells to DNA damaging agents. Cancer Res 1994;54(22):5824-30.

21. Lowe SW, Bodis S, McClatchey A, et al. p53 status and the efficacy of cancer therapy in vivo. Science 1994;266(5186):807-10.

22. Dickins RA, Hemann MT, Zilfou JT, et al. Probing tumor phenotypes using stable and regulated synthetic microRNA precursors. Nat Genet 2005;37(11):1289-95.

23. Matveeva OV, Kang Y, Spiridonov AN, et al. Optimization of duplex stability and terminal asymmetry for shRNA design. PLoS One;5(4):e10180.

24. Schopman NC, Liu YP, Konstantinova P, ter Brake O, Berkhout B. Optimization of shRNA inhibitors by variation of the terminal loop sequence. Antiviral Res;86(2):204-11.

25. Weiwei M, Zhenhua X, Feng L, Hang N, Yuyang J. A significant increase of RNAi efficiency in human cells by the CMV enhancer with a tRNAlys promoter. J Biomed Biotechnol 2009;2009:514287.

26. DuPage M, Dooley AL, Jacks T. Conditional mouse lung cancer models using adenoviral or lentiviral delivery of Cre recombinase. Nat Protoc 2009;4(7):1064-72.

27. Kumar MS, Erkeland SJ, Pester RE, et al. Suppression of non-small cell lung tumor development by the let-7 microRNA family. Proc Natl Acad Sci U S A 2008;105(10):3903-8.

28. Komarova NL, Wodarz D. Drug resistance in cancer: principles of emergence and prevention. Proc Natl Acad Sci U S A 2005;102(27):9714-9.

29. Sawyers CL. Calculated resistance in cancer. Nat Med 2005;11(8):824-5.

30. Ley TJ, Mardis ER, Ding L, et al. DNA sequencing of a cytogenetically normal acute myeloid leukaemia genome. Nature 2008;456(7218):66-72.

31. Mardis ER, Ding L, Dooling DJ, et al. Recurring mutations found by sequencing an acute myeloid leukemia genome. N Engl J Med 2009;361(11):1058-66.

32. Pleasance ED, Cheetham RK, Stephens PJ, et al. A comprehensive catalogue of somatic mutations from a human cancer genome. Nature;463(7278):191-6.